NORSAR

NORSAR Scientific Report No. 1-1999/2000

Semiannual Technical Summary

1 April - 30 September 1999

Kjeller, November 1999

20000204 059

DTIC QUALITY INSPECTED 2

REPORT DOCUMENTATION PAGE

Form Approved
OMB No. 0704-0188

1a. REPORT SECURITY CLASSIFICATION Unclassified	1b. RESTRICTIVE MARKINGS Not applicable		
2a. SECURITY CLASSIFICATION AUTHORITY Not Applicable	3. DISTRIBUTION/AVAILABILITY OF REPORT Approved for public release; distribution unlimited		
2b. DECLASSIFICATION/DOWNGRADING SCHEDULE			

4. PERFORMING ORGANIZATION REPORT NUMBER(S) Scientific Rep.1-1999/200	5. MONITORING ORGANIZATION REPORT NUMBER(S) Scientific Rep. 1-1999/2000

6a. NAME OF PERFORMING ORGANIZATION NORSAR	6b. OFFICE SYMBOL (If applicable)	7a. NAME OF MONITORING ORGANIZATION HQ/AFTAC/TTS
6c. ADDRESS (City, State, and ZIP Code) Post Box 51 N-2027 Kjeller, Norway		7b. ADDRESS (City, State, and ZIP Code) Patrick AFB, FL 32925-6001

8a. NAME OF FUNDING/SPONSORING ORGANIZATION Advanced Research Projects Agency/NTPO	8b. OFFICE SYMBOL (If applicable) NMRO/NTPO	9. PROCUREMENT INSTRUMENT IDENTIFICATION NUMBER Contract No. F08650-96-C-0001		
8c. ADDRESS (City, State, and ZIP Code) 1901 N. Moore St., Suite 609 Arlington, VA 22209		10. SOURCE OF FUNDING NUMBERS		

10. SOURCE OF FUNDING NUMBERS			
PROGRAM ELEMENT NO. R&D	PROJECT NO. NORSAR Phase 3	TASK NO. SOW Task 5.0	WORK UNIT ACCESSION NO. Sequence No. 004A2

11. TITLE (Include Security Classification)

Semiannual Technical Summary, 1 April - 30 September 1999

12. PERSONAL AUTHOR(S)

13a. TYPE OF REPORT Scientific Summary	13b. TIME COVERED FROM 1 Apr 99 TO 30 Sep 99	14. DATE OF REPORT (Year, Month, Day) 1999 November	15. PAGE COUNT 121

16. SUPPLEMENTARY NOTATION

17. COSATI CODES			18. SUBJECT TERMS (Continue on reverse if necessary and identify by block number)
FIELD	GROUP	SUB-GROUP	NORSAR, Norwegian Seismic Array
8	11		

19. ABSTRACT (Continue on reverse if necessary and identify by block number)

This Semiannual Technical Summary describes the operation, maintenance and research activities at the Norwegian Seismic Array (NORSAR), the Norwegian Regional Seismic Array (NORES), the Arctic Regional Seismic Array (ARCES) and the Spitsbergen Regional Array for the period 1 April - 30 September 1999. Statistics are also presented for additional seismic stations, which through cooperative agreements with institutions in the host countries provide continuous data to the NORSAR Data processing Center (NDPC). These stations comprise the Finnish Regional Seismic Array (FINES), the German Regional Seismic Array (GERESS), the Hagfors array in Sweden and the regional seismic array in Apatity, Russia.

(cont.)

20. DISTRIBUTION/AVAILABILITY OF ABSTRACT ☐ UNCLASSIFIED/UNLIMITED ☐ SAME AS RPT. ☐ DTIC USERS	21. ABSTRACT SECURITY CLASSIFICATION	
22a. NAME OF RESPONSIBLE INDIVIDUAL Mr. Michael C. Baker	22b. TELEPHONE (Include Area Code) (407) 494-7985	22c. OFFICE SYMBOL AFTAC/TTS

DD Form 1473, JUN 86   Previous editions are obsolete.   SECURITY CLASSIFICATION OF THIS PAGE

Abstract (cont.)

Beginning 1 January 1999, the responsibility for funding the operational activities of the seismic field systems and the Norwegian National Data Center (NDC) has been taken over by the Norwegian Government, with the understanding that the funding of IMS-related activities will gradually be arranged through the CTBTO/PTS. Research activities described in this report, as well as transmission of selected data to the United States NDC, are continuing to be funded by the United States Department of Defense.

The NOA Detection Processing system has been operated throughout the period with an average uptime of 99.93%. A total of 2244 seismic events have been reported in the NOA monthly seismic bulletin for April through September 1999. The performance of the continuous alarm system and the data transfer to AFTAC has been satisfactory. Processing of requests for full NOA and regional array data on magnetic tapes has progressed according to established schedules.

This Semiannual Report also presents statistics from operation of the Regional Monitoring System (RMS). The RMS has been operated in a limited capacity, with continuous automatic detection and location and with analyst review of selected events of interest for GSETT-3. Data sources for the RMS have comprised all the regional arrays processed at NORSAR. The Generalized Beamforming (GBF) program continues to be used as a pre-processor to RMS.

On-line detection processing and data recording at the NORSAR Data Processing Center (NDPC) of NORES, ARCES, FINES and GERES data have been conducted throughout the period. Data from two small-aperture arrays at sites in Spitsbergen and Apatity, Kola Peninsula, as well as the Hagfors array in Sweden, have also been recorded and processed. Processing statistics for the arrays as well as results of the RMS analysis for the reporting period are given.

The operation of the regional arrays has proceeded normally in the period. Maintenance activities in the period comprise preventive/corrective maintenance in connection with all of the NOA subarrays. The ARCES array has been completely refurbished, under a contract with the CTBTO/PTS. Other activities have involved repair of defective electronic equipment, cable splicing and work in connection with the small-aperture array in Spitsbergen. Work is also progressing in making the modifications required for formal station certification of the NOA array.

A summary of the activities related to the GSETT-3 experiment and experience gained at the Norwegian NDC during the reporting period is provided in Section 4. Norway has been contributing primary station data from three arrays: ARCES, NORES and NOA and one auxiliary array (Spitsbergen). Norway's NDC is also acting as a regional data center, forwarding data to the IDC from GSETT-3 primary and auxiliary stations in several countries. The work at the Norwegian NDC has continued to focus on operational aspects, like stable forwarding of data using the Alpha protocol, proper handling of outgoing and incoming messages, improvement to routines for dealing with failure of critical components, as well as implementation of other measures to ensure maximum reliability and robustness in providing data to the IDC. The NDC will continue the efforts towards improvements and hardening of all critical data acquisition and data forwarding hardware and software components, so as to meet future requirements related to operation of IMS stations to the maximum extent possible.

The PrepCom has tasked its Working Group B with overseeing, coordinating and evaluating the GSETT-3 experiment until the end of 1999. The PrepCom has also encouraged states that

operate IMS-designated stations to continue to do so on a voluntary basis and in the framework of the GSETT-experiment until such time that the stations have been certified for formal inclusion in IMS. In line with this, we envisage continuing the provision of data from Norwegian IMS-designated stations without interruption to the PIDC, and later on, following certification, to the IDC in Vienna, via the new global communications infrastructure.

Summaries of six scientific and technical contributions are presented in Chapter 6 of this report.

Section 6.1 is entitled "Earthquake location accuracies in Norway based on a comparison between local and regional networks". Detailed studies of the low to intermediate seismicity in two coastal regions of Norway have been used in a comparison between earthquake locations from local high-precision networks on the one side and locations using a sparse regional array network on the other side. To this end, a reference set of 32 low-magnitude earthquakes have been located using two local temporary networks in northern and western Norway, with estimated epicenter accuracies better than 5 and 10 km, respectively.

Comparisons are made between the local network solutions and the NORSAR Generalized Beamforming (GBF) system, which provides automatic phase association and location estimates using the Fennoscandian regional array network. The median automatic GBF location error is of the order of 20-30 km when four or more arrays detect the event, increasing to about 80-100 km when only two arrays are available, and the automatic GBF bulletin is essentially complete down to magnitude M_L=2.0. Most of the mislocation vectors of the NORSAR GBF solutions are oriented perpendicular to the Norwegian coast, and with a tendency to pull the location in a southeasternly direction. The GBF performance is clearly better, both in terms of accuracy and completeness, than the performance of the automatic bulletin of the Prototype International Data Center (pIDC) which uses data from essentially the same network.

The analyst reviewed NORSAR and pIDC bulletins show, not unexpectedly, an improvement in location accuracy compared to the automatic solutions and appear to be of similar quality for the few common events, with an average mislocation of about 20 km. The NORSAR reviewed bulletin is more complete at low magnitudes compared to pIDC, and there appears to be a potential for significant improvements in the PIDC processing of small seismic events in this region.

Section 6.2 is entitled "Continuous assessment of upper limit M_S ". It describes a new application of the continuous seismic threshold monitoring technique (TM) to long-period data, for the purpose of obtaining a continuous assessment of surface wave magnitude (M_S). We present initial results from investigating the relation between pIDC station magnitudes and STA based estimates calculated from bandpass filtered data, as well as a case study with monitoring of surface waves from a mining area on the Kola peninsula during and after a M_S 7.6 earthquake in Turkey.

An important result of this study is the demonstration of the significant benefits of using a shorter period band (8-12 seconds) instead of the traditional processing band (17-24 seconds) for processing surface waves at regional distances during an aftershock sequence. In future work, we will investigate further whether the use of this shorter period band could be applicable also during "normal" background noise conditions. In an operational setting, it is clearly an advantage to use a fixed frequency band for each station-site combination, but it requires a

careful assessment of the relations between surface wave magnitudes calculated in different frequency bands.

In this study, we have used the three IMS arrays ARCES, NOA and SPITS, and applied a site-specific technique to investigate the threshold trace during a large earthquake sequence. A natural follow-up of this work would be to include additional long-period and broadband IMS stations for the same time interval, in order to assess the improvements in monitoring capability when using a network with better azimuthal coverage.

As in the short period case, there is a tradeoff between optimizing the TM process for site-specific studies and developing a more general TM application for global surface wave monitoring. Among the main issues is the sharpness of the beam lobe, which depends upon the filter setting, the STA time windows and the tolerance for travel-time deviations. Another issue is the need for regional corrections, which may be greater than in the short-period case. For example, the significant difference between oceanic, continental and combined oceanic-continental paths are important for surface wave propagation, but have little or no counterpart in analyzing short-period P and S waves.

Section 6.3 describes results from tuning of the Threshold Monitoring processing parameters for IMS stations BRAR and NVAR. In general, the processing parameters for all stations in the IMS Threshold Monitoring System processing must be tuned for reliable estimation of the detection capability. The IMS array stations BRAR and NVAR, discussed in this contribution, have recently been incorporated into the pIDC processing, and therefore need such tuning.

The tuning study requires events with good SNR's, preferably occurring at a range of distances from the stations. This was done by searching the pIDC data base for good SNR events at various distances, and then requesting and receiving the data intervals using the AutoDRM. Between 40 and 50 events were used for each of the stations BRAR and NVAR, with epicentral distances ranging from less than 5 degrees (local events) to more than 140 degrees (core phases).

The general procedure in the tuning study has been in accordance with the Threshold Monitoring Operations Manual, and has included studies of short-term-averages (STAs) in various frequency bands, SNR as a function of frequency and epicentral distance, effects of beamsteering losses, and evaluation of the number of beams required for a given "worst-case" missteering loss. The results of this study have been communicated to the pIDC and the IDC for operational implementation.

Section 6.4 is entitled "The MASI-99 Field Experiment". This paper describes an experimental regional seismic network of 13 three-component seismometer systems deployed in Finnmark, northern Norway during May-September 1999. The experiment was a joint undertaking between NORSAR and the University of Potsdam, Germany. Its purpose was to study neotectonic fault movements, microseisms, and travel times/attenuation of seismic phases from earthquakes and mining explosions in northern Fennoscandia and adjacent areas. Examples of seismic recordings by the network are presented. The high sampling rate (125 samples per second) in combination with the "broadband" characteristics of the seismometers (eigenperiod of 5 seconds), enables studying a range of seismic phases and signal frequencies, from P and S waves above 50 Hz to regional surface waves of periods around 10 seconds. All the data have been stored continuously on CDs, and will be made available as a data base for future scientific investigations.

Section 6.5 describes recent developments in connection with the seismic station in Amderma, Russia. Initially, Amderma operated as a standard Russian analog recording station. In 1993, KRSC installed a microarray (with digital recording) at the site. The hardware comprised short-period S-500 vertical and horizontal seismometers, Nanometric 18 bit digitizer and a Norac array controller. From August 1998, the microarray has been replaced by a broadband 3-component seismometer system of the type RefTek DAS 72A.

Data is sampled at 100 Hz and registered on a local disk system. Continuous data are transferred to an Exabyte cassette recorder and shipped by mail to Apatity. Typically, these data are available within 1-2 months of the date of recording. Software to connect the Amderma station to Apatity by Inmarsat services was developed by KRSC in 1998/99. The software allows for the retrieval of a) waveform segments for specified time intervals, b) detection lists, c) compressed STA trace of filtered vertical channel data (filter band 4-12 Hz) and d) state-of health indicators. The link can furthermore be used to remotely controlling the station parameters, and restarting the system in case of occasional failure. Examples of waveform segments from the broad-band Amderma station are given, including data for the earthquake in the Kola Peninsula on 17 August 1999 and selected teleseismic P-wave recordings.

Section 6.6 describes our analysis of data from the Eurobridge experiment, which comprised a 1130 km seismic refraction profile crossing the Baltic Shield in the northwest and the Ukrainian Shield in the southeast. There were three series of shots, one in 1995 and two in 1996. Observations of these explosions at the Fennoscandian arrays (ARCES, FINES, Hagfors, and NORES) provide an opportunity to check the accuracy of the travel-time tables in use at NORSAR for Fennoscandia. At the same time, these refraction shots provide a useful extension to the pIDC ground-truth database.

P-phases from most of the Eurobridge shots were observed at the FINES, HAGFORS and NORES arrays, and even at the more distant ARCES array as many as 12 out of the 29 events were seen. We have compared the event locations provided by the GBF method to the ground-truth locations of the Eurobridge shots. In order to take advantage of recent developments in the GBF methodology, we reprocessed the days of the Eurobridge shots using the currently implemented GBF parameters. It turns out that all events located with two or more S-phases had automatic GBF location errors less than 27.1 km, which is an excellent result taking into account the low magnitudes (all events below magnitude 2.5) and the large distances involved.

For each array, seismic sections were plotted with a reduction velocity of 8 km/s (13.9 s/deg), and compared with the predicted arrivals using the travel-time curves of the Fennoscandian model. We observe significant differences between the model predictions and the P-onsets, and it is our plan to investigate these in more detail. A striking feature is the difference between the Hagfors and NORES sections, which appear to be associated with a timing problem at the Hagfors array. This and other features of the seismic sections will be further investigated.

Frode Ringdal

Beginning 1 January 1999, the responsibility for funding the operational activities of the seis-
mic field systems and the Norwegian National Data Center (NDC) has been taken over by the
Norwegian Government, with the understanding that the funding of IMS-related activities will
gradually be arranged through the CTBTO/PTS.

Table of Contents

1   Summary

This Semiannual Technical Summary describes the operation, maintenance and research activities at the Norwegian Seismic Array (NOA), the Norwegian Regional Seismic Array (NORES), the Arctic Regional Seismic Array (ARCES) and the Spitsbergen Regional Array for the period 1 April - 30 September 1999. Statistics are also presented for additional seismic stations, which through cooperative agreements with institutions in the host countries provide continuous data to the NORSAR Data Processing Center (NPDC). These stations comprise the Finnish Regional Seismic Array (FINES), the German Regional Seismic Array (GERES), the Hagfors array in Sweden and the regional seismic array in Apatity, Russia.

Beginning 1 January 1999, the responsibility for funding the operational activities of the seismic field systems and the Norwegian National Data Center (NDC) has been taken over by the Norwegian Government, with the understanding that the funding of IMS-related activities will gradually be arranged through the CTBTO/PTS. Research activities described in this report, as well as transmission of selected data to the United States NDC, are continuing to be funded by the United States Department of Defense.

The NOA Detection Processing system has been operated throughout the period with an average uptime of 99.93%. A total of 2244 seismic events have been reported in the NOA monthly seismic bulletin for April through September 1999. The performance of the continuous alarm system and the data transfer to AFTAC has been satisfactory. Processing of requests for full NOA and regional array data on magnetic tapes has progressed according to established schedules.

This Semiannual Report also presents statistics from operation of the Regional Monitoring System (RMS). The RMS has been operated in a limited capacity, with continuous automatic detection and location and with analyst review of selected events of interest for GSETT-3. Data sources for the RMS have comprised all the regional arrays processed at NORSAR. The Generalized Beamforming (GBF) program continues to be used as a pre-processor to RMS.

On-line detection processing and data recording at the NORSAR Data Processing Center (NDPC) of NORES, ARCES, FINES and GERES data have been conducted throughout the period. Data from two small-aperture arrays at sites in Spitsbergen and Apatity, Kola Peninsula, as well as the Hagfors array in Sweden, have also been recorded and processed. Processing statistics for the arrays as well as results of the RMS analysis for the reporting period are given.

The operation of the regional arrays has proceeded normally in the period. Maintenance activities in the period comprise preventive/corrective maintenance in connection with all of the NOA subarrays. The ARCES array has been completely refurbished, under a contract with the CTBTO/PTS. Other activities have involved repair of defective electronic equipment, cable splicing and work in connection with the small-aperture array in Spitsbergen. Work is also progressing in making the modifications required for formal station certification of the NOA array.

A summary of the activities related to the GSETT-3 experiment and experience gained at the Norwegian NDC during the reporting period is provided in Section 4. Norway has been contributing primary station data from three arrays: ARCES, NORES and NOA and one auxiliary array (Spitsbergen). Norway's NDC is also acting as a regional data center, forwarding data to the IDC from GSETT-3 primary and auxiliary stations in several countries. The work at the Norwegian NDC has continued to focus on operational aspects, like stable forwarding of data using the Alpha protocol, proper handling of outgoing and incoming messages, improvement to routines

for dealing with failure of critical components, as well as implementation of other measures to ensure maximum reliability and robustness in providing data to the IDC. The NDC will continue the efforts towards improvements and hardening of all critical data acquisition and data forwarding hardware and software components, so as to meet future requirements related to operation of IMS stations to the maximum extent possible.

The PrepCom has tasked its Working Group B with overseeing, coordinating and evaluating the GSETT-3 experiment until the end of 1999. The PrepCom has also encouraged states that operate IMS-designated stations to continue to do so on a voluntary basis and in the framework of the GSETT-experiment until such time that the stations have been certified for formal inclusion in IMS. In line with this, we envisage continuing the provision of data from Norwegian IMS-designated stations without interruption to the PIDC, and later on, following certification, to the IDC in Vienna, via the new global communications infrastructure.

Summaries of six scientific and technical contributions are presented in Chapter 6 of this report.

Section 6.1 is entitled "Earthquake location accuracies in Norway based on a comparison between local and regional networks". Detailed studies of the low to intermediate seismicity in two coastal regions of Norway have been used in a comparison between earthquake locations from local high-precision networks on the one side and locations using a sparse regional array network on the other side. To this end, a reference set of 32 low-magnitude earthquakes have been located using two local temporary networks in northern and western Norway, with estimated epicenter accuracies better than 5 and 10 km, respectively.

Comparisons are made between the local network solutions and the NORSAR Generalized Beamforming (GBF) system, which provides automatic phase association and location estimates using the Fennoscandian regional array network. The median automatic GBF location error is of the order of 20-30 km when four or more arrays detect the event, increasing to about 80-100 km when only two arrays are available, and the automatic GBF bulletin is essentially complete down to magnitude M_L=2.0. Most of the mislocation vectors of the NORSAR GBF solutions are oriented perpendicular to the Norwegian coast, and with a tendency to pull the location in a southeasternly direction. The GBF performance is clearly better, both in terms of accuracy and completeness, than the performance of the automatic bulletin of the Prototype International Data Center (pIDC) which uses data from essentially the same network.

The analyst reviewed NORSAR and pIDC bulletins show, not unexpectedly, an improvement in location accuracy compared to the automatic solutions and appear to be of similar quality for the few common events, with an average mislocation of about 20 km. The NORSAR reviewed bulletin is more complete at low magnitudes compared to pIDC, and there appears to be a potential for significant improvements in the PIDC processing of small seismic events in this region.

Section 6.2 is entitled "Continuous assessment of upper limit M_S ". It describes a new application of the continuous seismic threshold monitoring technique (TM) to long-period data, for the purpose of obtaining a continuous assessment of surface wave magnitude (M_S). We present initial results from investigating the relation between pIDC station magnitudes and STA based estimates calculated from bandpass filtered data, as well as a case study with monitoring of surface waves from a mining area on the Kola peninsula during and after a M_S 7.6 earthquake in Turkey.

An important result of this study is the demonstration of the significant benefits of using a shorter period band (8-12 seconds) instead of the traditional processing band (17-24 seconds) for processing surface waves at regional distances during an aftershock sequence. In future work, we will

investigate further whether the use of this shorter period band could be applicable also during "normal" background noise conditions. In an operational setting, it is clearly an advantage to use a fixed frequency band for each station-site combination, but it requires a careful assessment of the relations between surface wave magnitudes calculated in different frequency bands.

In this study, we have used the three IMS arrays ARCES, NOA and SPITS, and applied a site-specific technique to investigate the threshold trace during a large earthquake sequence. A natural follow-up of this work would be to include additional long-period and broadband IMS stations for the same time interval, in order to assess the improvements in monitoring capability when using a network with better azimuthal coverage.

As in the short period case, there is a tradeoff between optimizing the TM process for site-specific studies and developing a more general TM application for global surface wave monitoring. Among the main issues is the sharpness of the beam lobe, which depends upon the filter setting, the STA time windows and the tolerance for travel-time deviations. Another issue is the need for regional corrections, which may be greater than in the short-period case. For example, the significant difference between oceanic, continental and combined oceanic-continental paths are important for surface wave propagation, but have little or no counterpart in analyzing short-period P and S waves.

Section 6.3 describes results from tuning of the Threshold Monitoring processing parameters for IMS stations BRAR and NVAR. In general, the processing parameters for all stations in the IMS Threshold Monitoring System processing must be tuned for reliable estimation of the detection capability. The IMS array stations BRAR and NVAR, discussed in this contribution, have recently been incorporated into the pIDC processing, and therefore need such tuning.

The tuning study requires events with good SNR's, preferably occurring at a range of distances from the stations. This was done by searching the pIDC data base for good SNR events at various distances, and then requesting and receiving the data intervals using the AutoDRM. Between 40 and 50 events were used for each of the stations BRAR and NVAR, with epicentral distances ranging from less than 5 degrees (local events) to more than 140 degrees (core phases).

The general procedure in the tuning study has been in accordance with the Threshold Monitoring Operations Manual, and has included studies of short-term-averages (STAs) in various frequency bands, SNR as a function of frequency and epicentral distance, effects of beamsteering losses, and evaluation of the number of beams required for a given "worst-case" missteering loss. The results of this study have been communicated to the pIDC and the IDC for operational implementation.

Section 6.4 is entitled "The MASI-99 Field Experiment". This paper describes an experimental regional seismic network of 13 three-component seismometer systems deployed in Finnmark, northern Norway during May-September 1999. The experiment was a joint undertaking between NORSAR and the University of Potsdam, Germany. Its purpose was to study neotectonic fault movements, microseisms, and travel times/attenuation of seismic phases from earthquakes and mining explosions in northern Fennoscandia and adjacent areas. Examples of seismic recordings by the network are presented. The high sampling rate (125 samples per second) in combination with the "broadband" characteristics of the seismometers (eigenperiod of 5 seconds), enables studying a range of seismic phases and signal frequencies, from P and S waves above 50 Hz to regional surface waves of periods around 10 seconds. All the data have been stored continuously on CDs, and will be made available as a data base for future scientific investigations.

Section 6.5 describes recent developments in connection with the seismic station in Amderma, Russia. Initially, Amderma operated as a standard Russian analog recording station. In 1993, KRSC installed a microarray (with digital recording) at the site. The hardware comprised short-period S-500 vertical and horizontal seismometers, Nanometric 18 bit digitizer and a Norac array controller. From August 1998, the microarray has been replaced by a broadband 3-component seismometer system of the type RefTek DAS 72A.

Data is sampled at 100 Hz and registered on a local disk system. Continuous data are trans-ferred to an Exabyte cassette recorder and shipped by mail to Apatity. Typically, these data are available within 1-2 months of the date of recording. Software to connect the Amderma station to Apatity by Inmarsat services was developed by KRSC in 1998/99. The software allows for the retrieval of a) waveform segments for specified time intervals, b) detection lists, c) compressed STA trace of filtered vertical channel data (filter band 4-12 Hz) and d) state-of health indicators. The link can furthermore be used to remotely controlling the station parameters, and restarting the system in case of occasional failure. Examples of waveform segments from the broad-band Amderma station are given, including data for the earthquake in the Kola Peninsula on 17 August 1999 and selected teleseismic P-wave recordings.

Section 6.6 describes our analysis of data from the Eurobridge experiment, which comprised a 1130 km seismic refraction profile crossing the Baltic Shield in the northwest and the Ukrainian Shield in the southeast. There were three series of shots, one in 1995 and two in 1996. Observations of these explosions at the Fennoscandian arrays (ARCES, FINES, Hagfors, and NORES) provide an opportunity to check the accuracy of the travel-time tables in use at NORSAR for Fennoscandia. At the same time, these refraction shots provide a useful extension to the pIDC ground-truth database.

P-phases from most of the Eurobridge shots were observed at the FINES, HAGFORS and NORES arrays, and even at the more distant ARCES array as many as 12 out of the 29 events were seen. We have compared the event locations provided by the GBF method to the ground-truth locations of the Eurobridge shots. In order to take advantage of recent developments in the GBF methodology, we reprocessed the days of the Eurobridge shots using the currently implemented GBF parameters. It turns out that all events located with two or more S-phases had automatic GBF location errors less than 27.1 km, which is an excellent result taking into account the low magnitudes (all events below magnitude 2.5) and the large distances involved.

For each array, seismic sections were plotted with a reduction velocity of 8 km/s (13.9 s/deg), and compared with the predicted arrivals using the travel-time curves of the Fennoscandian model. We observe significant differences between the model predictions and the P-onsets, and it is our plan to investigate these in more detail. A striking feature is the difference between the Hagfors and NORES sections, which appear to be associated with a timing problem at the Hagfors array. This and other features of the seismic sections will be further investigated.

Frode Ringdal

2   Operation of International Monitoring System (IMS) Stations in Norway

2.1   PS27 — Primary Seismic Station NOA

The average recording time was 99.93% as compared to 99.92% for the previous reporting period.

Table 2.1.1 lists the reasons for and times of the main outages in the reporting period.

Date	Time	Cause
20 Aug	0658 - 0945	Hardware failure at NDPC

Table 2.1.1. *The major downtimes in the period 1 April - 30 September 1999.*

Monthly uptimes for the NORSAR on-line data recording task, taking into account all factors (field installations, transmissions line, data center operation) affecting this task were as follows:

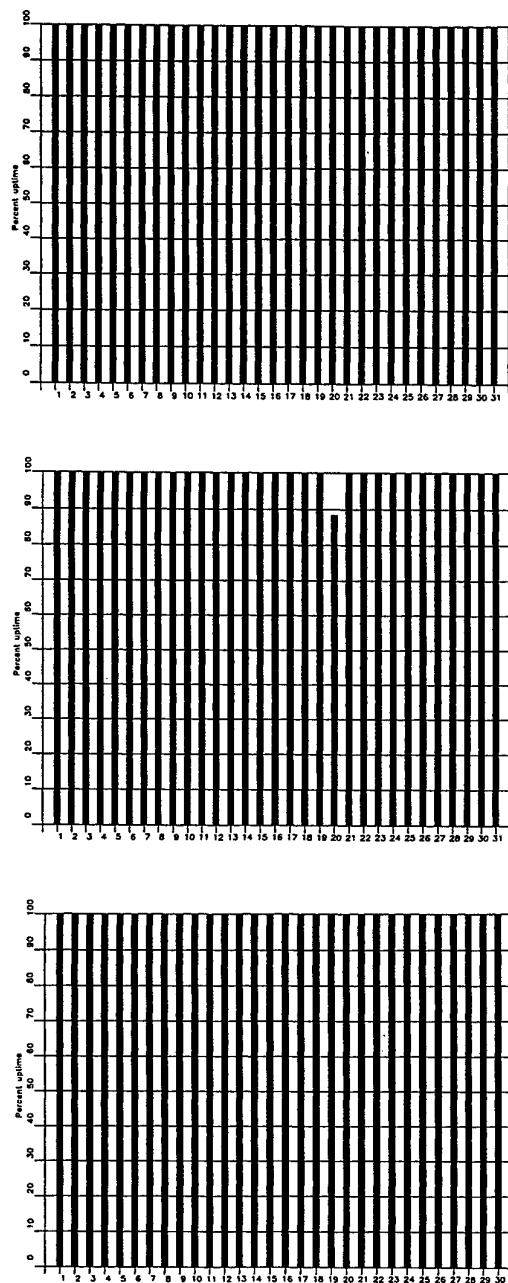| April	:	100.00%
May	:	99.98%
June	:	100.00%
July	:	100.00%
August	:	99.62%
September	:	100.00%

J. Torstveit

Fig. 2.1.1. *The figure shows the uptime for the data recording task, or equivalently, the availability of NOA data in our tape archive, on a day-by-day basis, for the reporting period. (Page 1 of 2, Apr-Jun 1999).*
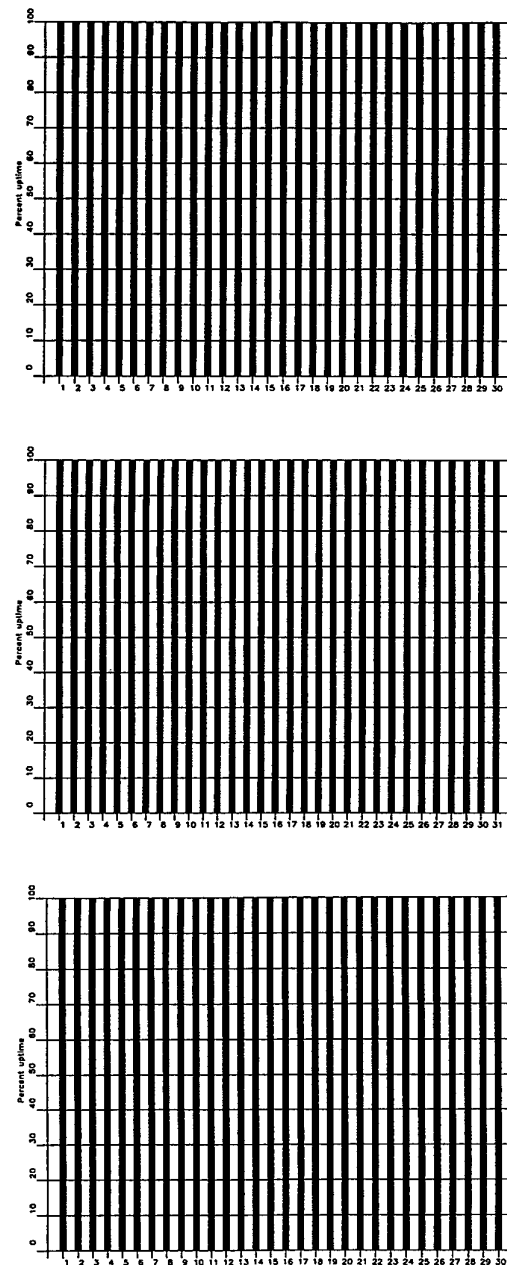
Fig. 2.1.1. *(cont.) (Page 2 of 2, Jul-Sep 1999).*

NOA Event Detection Operation

In Table 2.1.2 some monthly statistics of the Detection and Event Processor operation are given. The table lists the total number of detections (DPX) triggered by the on-line detector, the total number of detections processed by the automatic event processor (EPX) and the total number of events accepted after analyst review (teleseismic phases, core phases and total).

	Total DPX	Total EPX	Accepted Events		Sum	Daily
			P-phases	Core Phases		
Apr	6922	756	262	56	318	10.6
May	5324	798	289	72	361	11.6
Jun	4322	594	246	44	290	9.7
Jul	5426	648	267	62	329	10.6
Aug	8753	990	421	78	499	16.1
Sep	8047	881	400	47	447	14.9
	38794	4667	1885	359	2244	12.25

Table 2.1.2. *Detection and Event Processor statistics, 1 April - 30 September 1999.*

NOA detections

The number of detections (phases) reported by the NORSAR detector during day 091, 1999, through day 273 , 1999, was 38,794, giving an average of 212 detections per processed day (183 days processed).

B. Paulsen

U. Baadshaug

2.2   PS28 — Primary Seismic Station ARCES

The average recording time was 94.84% as compared to 99.72% for the previous period.

Table 2.2.1 lists the reasons for and times of the main outages in the reporting period.

Date	Time			Cause
18 Apr	0152	-	0744	Corrupted data
25 May	1416	-	1717	Installation of UPS
12 Jun	0634	-	0655	Maintenance NDPC
01 Sep	0604	-		Field upgrading
20 Sep		-	1700	

Table 2.2.1. *The main interruptions in recording of ARCES data at NDPC 1 April - 30 September 1999.*

Monthly uptimes for the ARCESS on-line data recording task, taking into account all factors (field installations, transmission lines, data center operation) affecting this task were as follows:

April	:	99.35%
May	:	99.59%
June	:	99.57%
July	:	99.99%
August	:	99.99%
September	:	35.15%

J. Torstveit
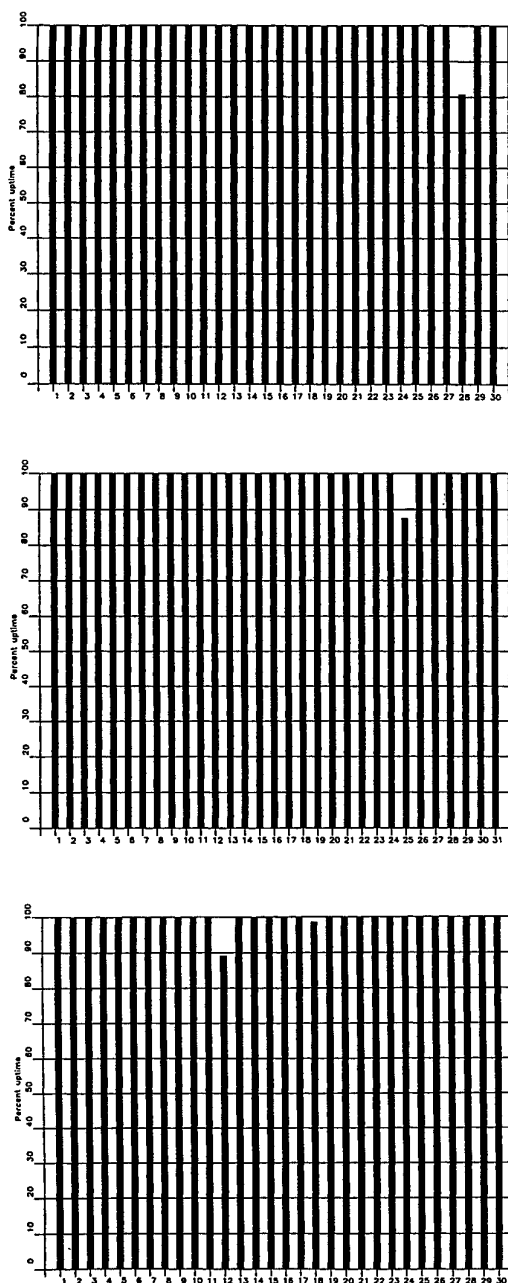
Fig. 2.2.1. *The figure shows the uptime for the data recording task, or equivalently, the availability of ARCES data in our tape archive, on a day-by-day basis, for the reporting period. (Page 1 of 2, Apr-Jun 1999)*
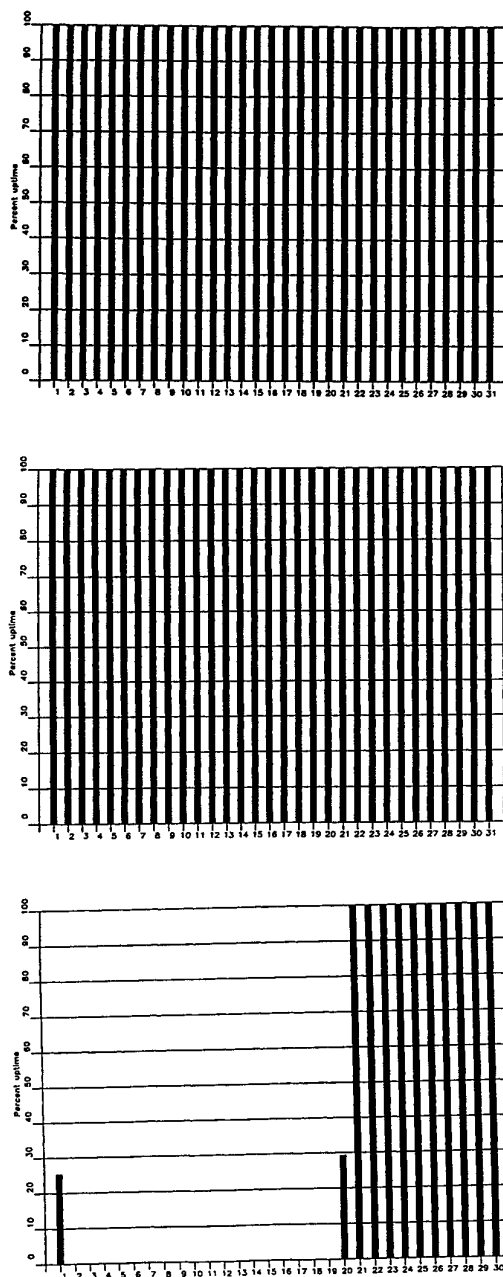
Fig. 2.2.1 *(cont.) (Page 2 of 2, Jul-Sep 1999).*

Event Detection Operation

ARCES detections

The number of detections (phases) reported during day 091, 1999, through day 273, 1999, was 101,261, giving an average of 614 detections per processed day (165 days processed).

Events automatically located by ARCES

During days 091, 1999, through 273, 1999, 5626 local and regional events were located by ARCES, based on automatic association of P- and S-type arrivals. This gives an average of 34.1 events per processed day (165 days processed). 57% of these events are within 300 km, and 85% of these events are within 1000 km.

U. Baadshaug

2.3   AS72 — Auxiliary Seismic Station Spitsbergen

The average recording time was 98.62% as compared to 97.53% for the previous reporting period.

Table 2.3.1 lists the reasons for and time periods of the main downtimes in the reporting period.

Date	Time			Cause
19 Apr	0012	-	0026	Transmission failure
25 May	1316	-	1717	Transmission failure
15 Jun	2003	-	2020	Transmission failure
17 Jun	0705	-	0720	Transmission failure
24 Jun	2008	-	2044	Transmission failure
24 Jun	2206	-	2258	Transmission failure
25 Jun	0652	-	0709	Transmission failure
25 Jun	0729	-	0800	Transmission failure
27 Jun	1723	-	1750	Transmission failure
27 Jun	1808	-	1838	Transmission failure
27 Jun	1854	-	1909	Transmission failure
31 Jul	0049	-	1031	Hardware failure NDPC
29 Aug	0124	-		Disk failure NDPC
30 Aug		-	0557	
31 Aug	0845	-	0939	Transmission failure
02 Sep	1016	-	1032	Transmission failure
06 Sep	1338	-	1353	Transmission failure
06 Sep	1426	-	1437	Transmission failure
11 Sep	2201	-	2221	Transmission failure
12 Sep	0010	-	0025	Transmission failure
13 Sep	0315	-	0343	Transmission failure
13 Sep	0805	-	0855	Transmission failure
14 Sep	1645	-	1719	Transmission failure

Table 2.3.1. *The main interruptions in recording of Spitsbergen data at NDPC, 1 April - 30 September 1999.*

Monthly uptimes for the Spitsbergen on-line data recording task, taking into account all factors (field installations, transmissions line, data center operation) affecting this task were as follows:

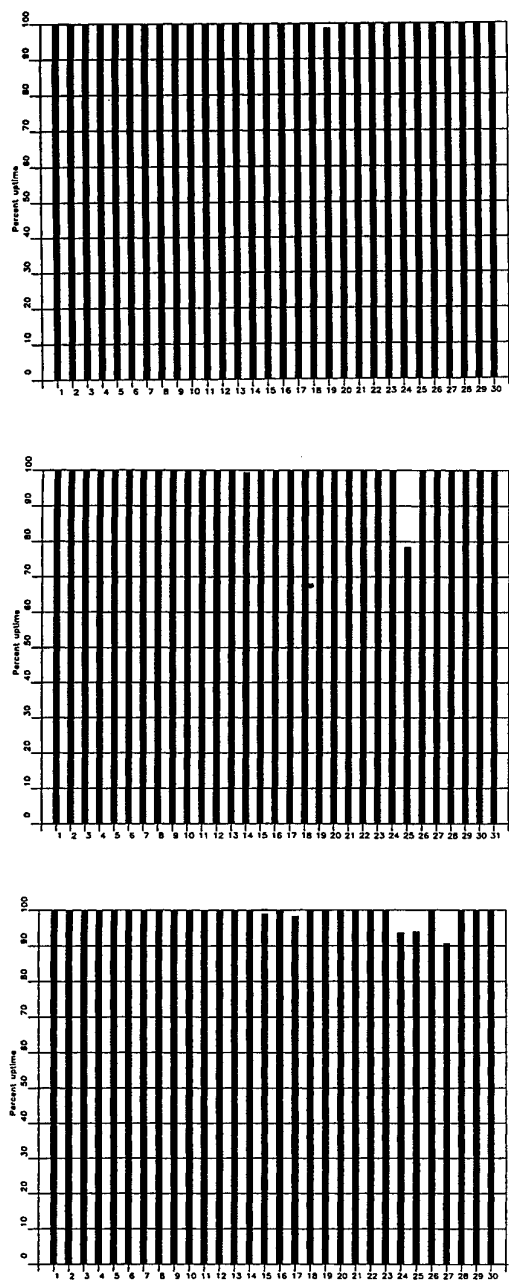|		
April	:	99.95%
May	:	99.27%
June	:	99.17%
July	:	98.69%
August	:	95.37%
September	:	99.25%

J. Torstveit

Fig. 2.3.1. *The figure shows the uptime for the data recording task, or equivalently, the availability of Spitsbergen data in our tape archive, on a day-by-day basis, for the reporting period. (Page 1 of 2, Apr-Jun 1999).*
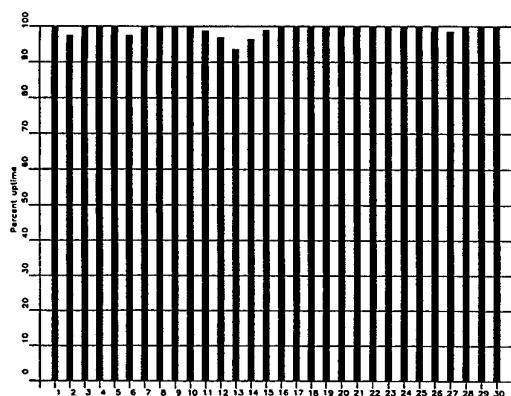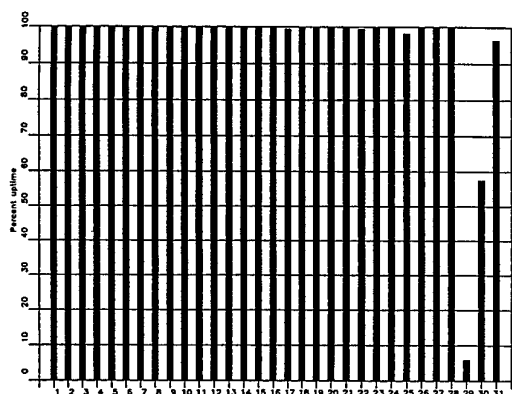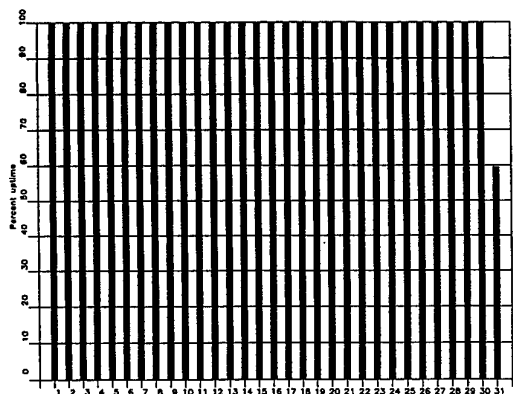
Fig. 2.3.1 *(cont.) (Page 2 of 2, Jul-Sep 1999).*

Event Detection Operation

Spitsbergen array detections

The number of detections (phases) reported from day 091, 1999, through day 273, 1999, was 317,967, giving an average of 1738 detections per processed day (183 days processed).

Events automatically located by the Spitsbergen array

During days 091, 1999, through 273, 1999, 28,522 local and regional events were located by the Spitsbergen array, based on automatic association of P- and S-type arrivals. This gives an average of 155.9 events per processed day (183 days processed). 63% of these events are within 300 km, and 85% of these events are within 1000 km.

U. Baadshaug

2.4   AS73 — Auxiliary Seismic Station Jan Mayen

The IMS auxiliary seismic network will include a three-component station at the Norwegian island of Jan Mayen. The station location given in the protocol to the Comprehensive Nuclear Test-Ban Treaty is 70.9°N, 8.7°W.

The University of Bergen has operated a seismic station at this location since 1970. An investment in the new station at Jan Mayen will be made in due course and in accordance with Prep-Com budget decisions. In the meanwhile, NORSAR will, in cooperation with the University of Bergen, look into technical possibilities of transmitting data from the existing station at Jan Mayen to the NDC at Kjeller. Such data may also be forwarded to the IDC in Vienna.

S. Mykkeltveit

2.5   IS37 — Infrasound Station at Karasjok

The IMS infrasound network will include a station at Karasjok in northern Norway. The coordinates given for this station are 69.5°N, 25.5°E. These coordinates coincide with those of the primary seismic station PS28.

A site survey for this station was carried out during June/July 1998 as a cooperative effort between the Provisional Technical Secretariat of the CTBTO and NORSAR. Analysis of the data collected at several potential locations for this station in and around Karasjok will soon be completed. The results of this analysis will lead to a decision on the exact location of the infrasound station. We expect that the new station will be installed some time during the summer or fall of year 2000.

S. Mykkeltveit

2.6   RN49 — Radionuclide Station on Spitsbergen

The IMS radionuclide network will include a station at Longyearbyen on the island of Spitsbergen, at location 78.2°N, 16.4°E. These coordinates coincide with those of the auxiliary seismic station AS72. According to PrepCom decision, this station will also be among those IMS radionuclide stations that will have a capability of monitoring for the presence of relevant noble gases upon entry into force of the CTBT.

A site survey for this station was carried out in August of 1999 by NORSAR, in cooperation with the Norwegian Radiation Protection Authority. The site survey report to the PTS contains a recommendation to establish this station at Platåberget, some 20 km away from the Treaty location. The station will be established in the year 2000 or later, depending on future PrepCom decisions.

S. Mykkeltveit

3 Operation of Regional Seismic Arrays

3.1 NORES

Average recording time was 99.77 as compared to 99.33 for the previous period.

Table 3.1.1 lists the reasons for and times of the main outages in the reporting period.

Date	Time			Cause
21 May	0955	-	1129	Data line failure
25 May	1416	-	1717	Installation of UPS
18 Jun	0635	-	0808	Maintenance NDPC
13 Aug	1052	-	1130	Maintenance NDPC
16 Aug	1136	-	1341	Maintenance NDPC
23 Sep	0913	-	0941	Disk failure

Table 3.1.1. *The main interruptions in recording of NORES data at the NDC 1 April - 30 September 1999.*

Monthly uptimes for the NORES on-line data recording task, taking into account all factors (field installations, transmissions line, data center operation) affecting this task were as follows

April	:	99.99%
May	:	99.36%
June	:	99.77%
July	:	99.99%
August	:	99.57%
September	:	99.92%

J. Torstveit
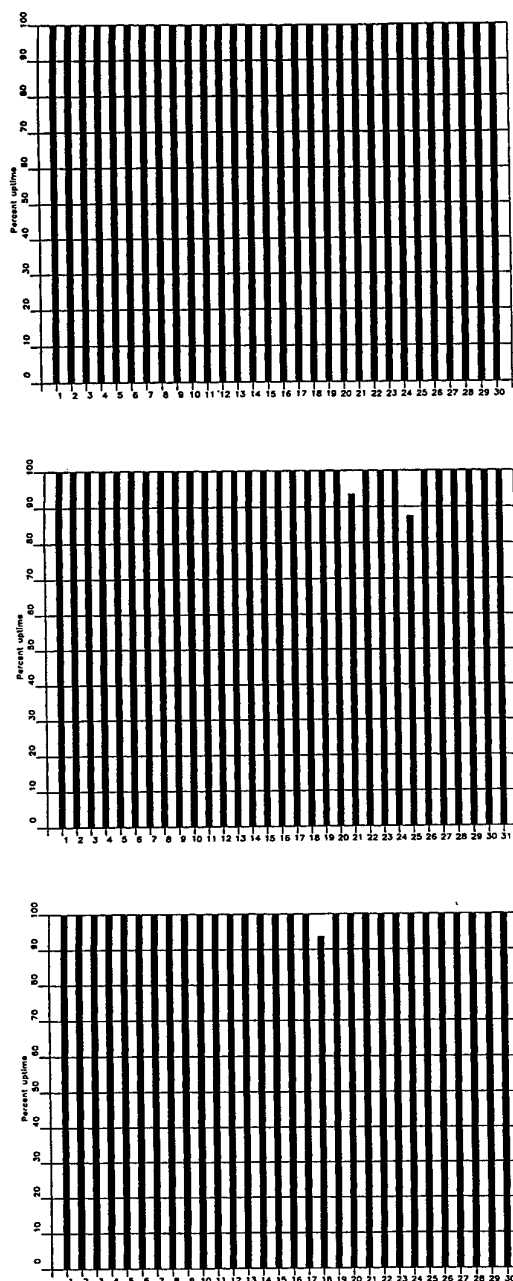
Fig. 3.1.1. *The figure shows the uptime for the data recording task, or equivalently, the availability of NORES data in our tape archive, on a day-by-day basis, for the reporting period (Page 1 of 2, Apr-Jun 1999).*

Fig. 3.1.1 *(cont.) (Page 2 of 2, Jul-Sep1999).*

NORES Event Detection Operation

NORES detections

The number of detections (phases) reported from day 091, 1999, through day 273, 1999, was 72,401, giving an average of 396 detections per processed day (183 days processed).

Events automatically located by NORES

During days 091, 1999, through 273, 1999, 2009 local and regional events were located by NORES, based on automatic association of P- and S-type arrivals. This gives an average of 11.0 events per processed day (183 days processed). 56% of these events are within 300 km, and 84% of these events are within 1000 km.

U. Baadshaug

3.2   Hagfors (IMS Station AS101)

The average recording time was 99.99% in the reporting period.

Table 3.2.1 lists the reasons for and times of the main outages in the reporting period.

Date	Time	Cause
11 Jun	0624 - 0636	Transmission line failure

Table 3.2.1. *The main interruptions in Hagfors recordings at the NDC, 1 April - 30 September 1999.*

Monthly uptimes for the Hagfors on-line data recording task, taking into account all factors (field installations, transmissions line, data center operation) affecting this task were as follows:

|		
April	:	100.00%
May	:	100.00%
June	:	99.98%
July	:	100.00%
August	:	100.00%
September	:	100.00%

J. Torstveit
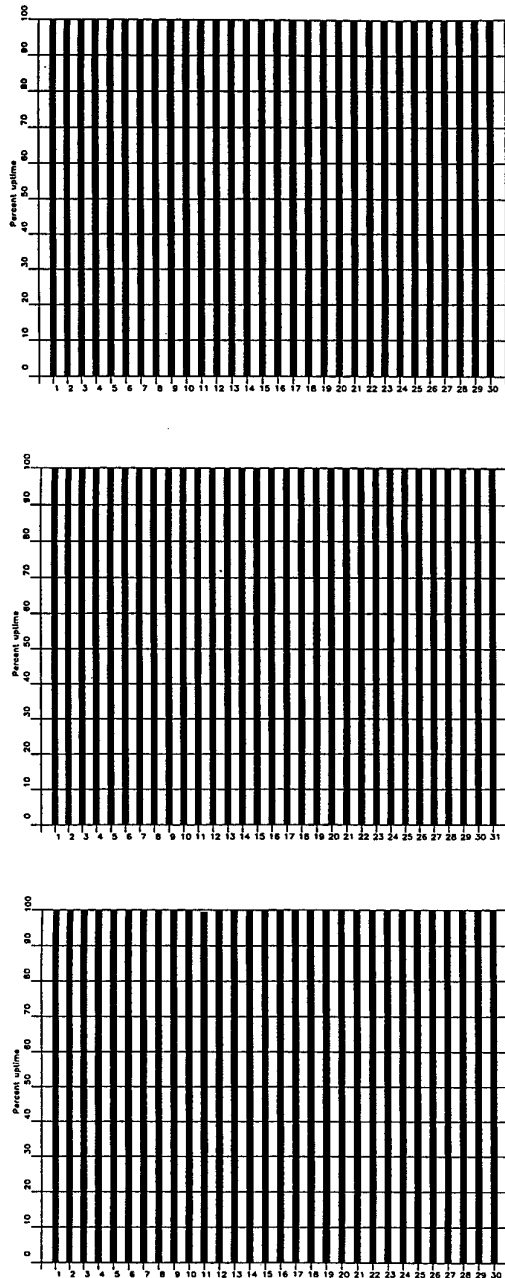
Fig. 3.2.1. *The figure shows the uptime for the data recording task, or equivalently, the availability of Hagfors data in our tape archive, on a day-by-day basis, for the reporting period (Page 1 of 2, Apr-Jun 1999).*
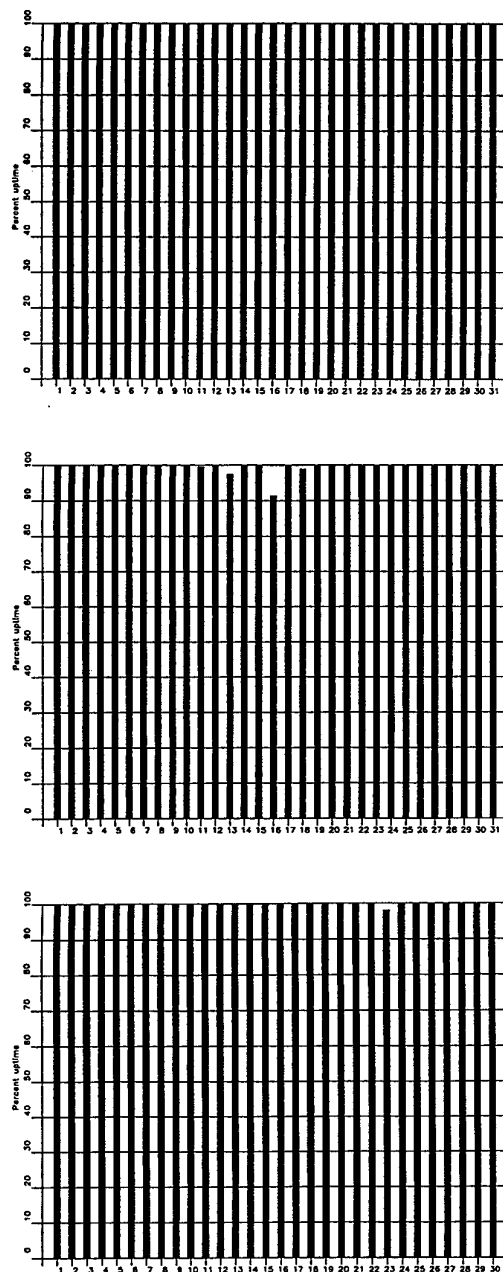
Fig. 3.2.1 *(cont.) (Page 2 of 2, Jul-Sep 1999).*

Hagfors Event Detection Operation

Hagfors array detections

The number of detections (phases) reported from day 091, 1999, through day 273, 1999, was 62,508, giving an average of 342 detections per processed day (183 days processed).

Events automatically located by the Hagfors array

During days 091, 1999, through 273, 1999, 2091 local and regional events were located by the Hagfors array, based on automatic association of P- and S-type arrivals. This gives an average of 11.4 events per processed day (183 days processed). 61% of these events are within 300 km, and 85% of these events are within 1000 km

U. Baadshaug

3.3   FINES

The average recording time was 73.78% as compared to 99.68% for the previous reporting period.

Table 3.3.1 lists the reasons for and times of the main outages during the reporting period..

Date	Time			Cause
08 Apr	0509	-	0643	SIM reset in Helsinki
30 May	1207	-	1220	Problems in Helsinki
07 Jun	0458	-		Transmission line failure
09 Jun		-	0714	
09 Jun	0807	-	0903	Transmission line failure
15 Jun	1329	-	1702	Power drop in array
26 Jun	2122	-		Power drop in array
28 Jun		-	1300	
30 Jun	0807	-		Upgrading AIMs
13 Aug		-	1102	
23 Aug	2303	-		Problems in Helsinki
24 Aug		-	0440	
19 Sep	2356	-		Problems in Helsinki
20 Sep		-	0549	

Table 3.3.1. *The main interruptions in FINES recordings at the NDC, 1 April - 30 September 1999.*

Monthly uptimes for the FINES on-line data recording task, taking into account all factors (field installations, transmissions line, data center operation) affecting this task were as follows:

|		
April	:	99.78%
May	:	99.97%
June	:	84.69%
July	:	0
August	:	59.05%
September	:	99.18%

J. Torstveit
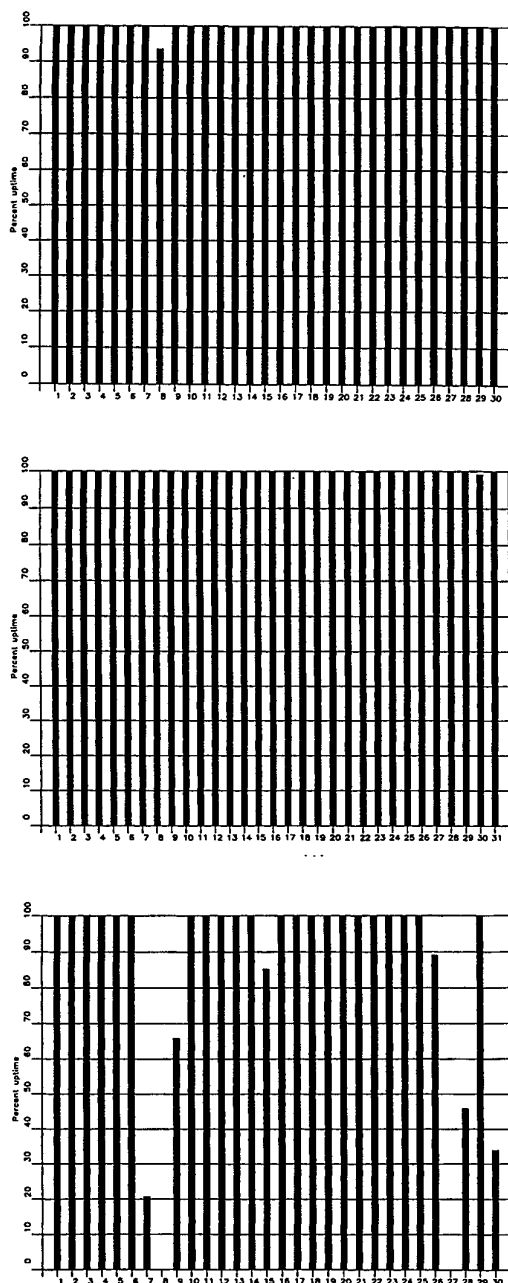
Fig. 3.3.1. *The figure shows the uptime for the data recording task, or equivalently, the availability of FINES data in our tape archive, on a day-by-day basis, for the reporting period (Page 1 of 2, Apr-Jun 1999).*
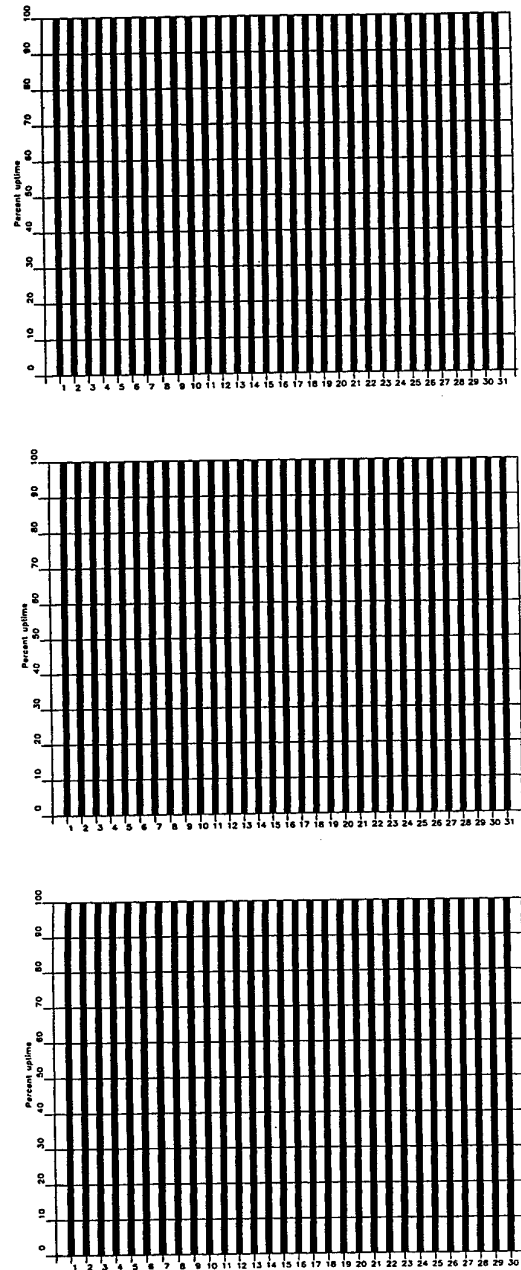
Fig. 3.3.1 *(cont.) (Page 2 of 2, Jul-Sep 1999)*

FINES Event Detection Operation

FINES detections

The number of detections (phases) reported during day 091, 1999, through day 273, 1999, was 30,842, giving an average of 241 detections per processed day (128 days processed).

Events automatically located by FINES

During days 091, 1999, through 273, 1999, 2322 local and regional events were located by FINESS, based on automatic association of P- and S-type arrivals. This gives an average of 16.8 events per processed day (138 days processed). 79% of these events are within 300 km, and 90% of these events are within 1000 km.

U. Baadshaug

3.4   Apatity

The average recording time was 99.01% in the reporting period compared to 98.98% during the previous period.

Table 3.4.1 lists the reasons for and times of the main outages during the reporting period.

Date	Time			Cause
18 Apr	0000	-	0009	Timing problems
23 May	0000	-	0006	Timing problems
24 May	0000	-	0005	Timing problems
14 Jun	0000	-	0008	Timing problems
05 Jul	0605	-	1258	Problems in Apatity
17 Jul	0031	-		Problems in Apatity
18 Jul		-	0514	
22 Jul	0045	-	0412	Problems in Apatity
23 Jul	1223	-	1245	Problems in Apatity
23 Jul	1355	-	1417	Problems in Apatity
22 Aug	0000	-	0021	Timing problems
21 Sep	1125	-	1442	Problems in Apatity

Table 3.4.1. *The main interruptions in Apatity recordings at the NDC, 1 April -*
30 September 1999.

Monthly uptimes for the Apatity on-line data recording task, taking into account all factors (field installations, transmissions line, data center operation) affecting this task were as follows:

|		
April	:	99.96%
May	:	99.97%
June	:	99.98%
July	:	94.68%
August	:	99.95%
September	:	99.54%

J. Torstveit

Fig. 3.4.1. *The figure shows the uptime for the data recording task, or equivalently, the availability of Apatity data in our tape archive, on a day-by-day basis, for the reporting period (Page 1 of 2, Apr-Jun 1999).*
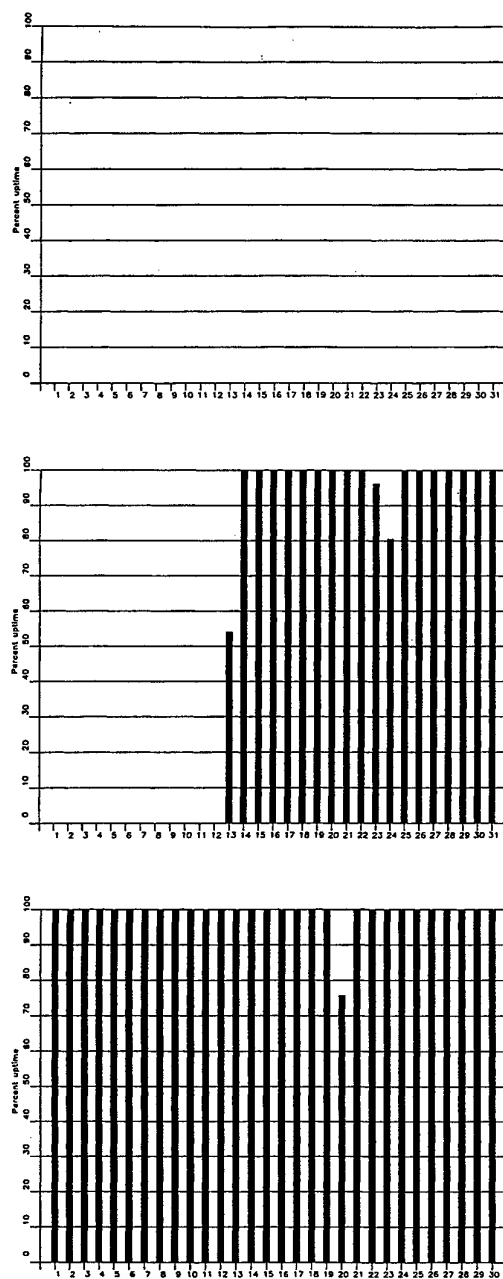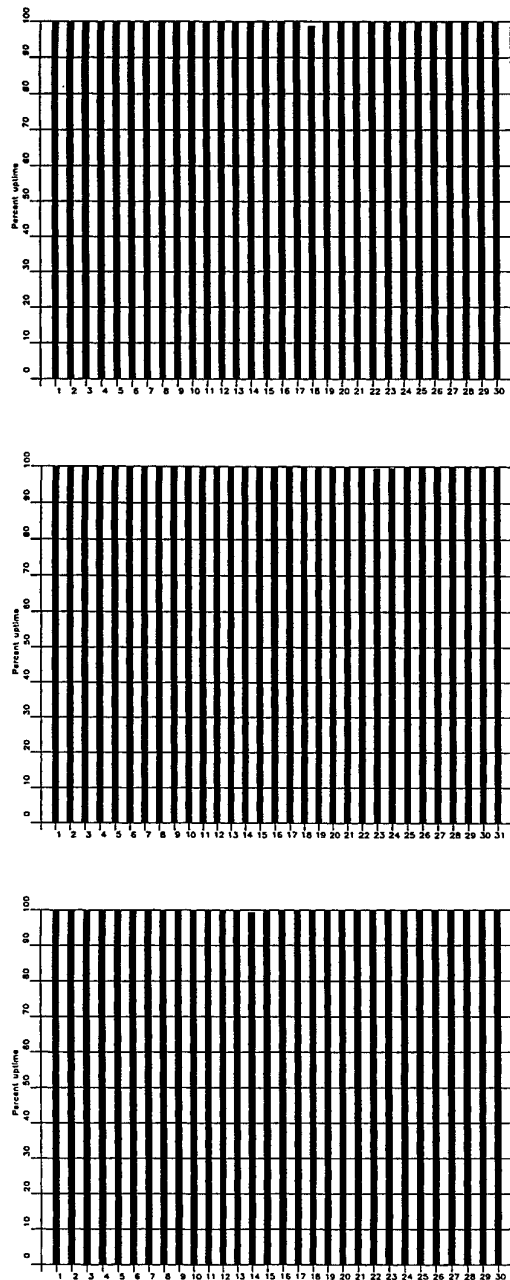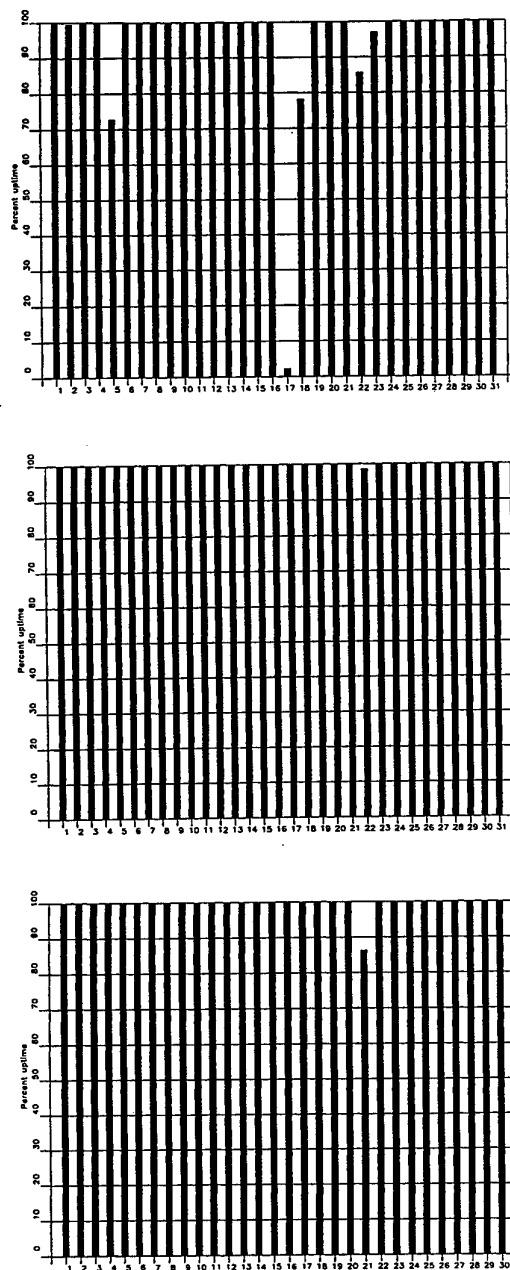
Fig. 3.4.1 *(cont.) (Page 2 of 2, Jul-Sep 1999)*

Apatity Event Detection Operation

Apatity array detections

The number of detections (phases) reported from day 091, 1999, through day 273, 1999, was 194,486, giving an average of 1075 detections per processed day (181 days processed).

As described in earlier reports, the data from the Apatity array are transferred by one-way (simplex) radio links to Apatity city. The transmission suffers from radio disturbances that occasionally result in a large number of small data gaps and spikes in the data. In order for the communication protocol to correct such errors by requesting retransmission of data, a two-way radio link would be needed (duplex radio). However, it should be noted that noise from cultural activities and from the nearby lakes cause most of the unwanted detections. These unwanted detections are "filtered" in the signal processing, as they give seismic velocities that are outside accepted limits for regional and teleseismic phase velocities.

Events automatically located by the Apatity array

During days 091, 1999, through 273, 1999, 3031 local and regional events were located by the Apatity array, based on automatic association of P- and S-type arrivals. This gives an average of 17.2 events per processed day (176 days processed). 37% of these events are within 300 km, and 74% of these events are within 1000 km.

U. Baadshaug

3.5   GERES

GERES Event Detection Operation

GERESS detections

The number of detections (phases) reported from day 091, 1999, through day 273, 1999, was 91,773, giving an average of 504 detections per processed day (182 days processed).

Events automatically located by GERESS

During days 091, 1999, through 273, 1999, 5842 local and regional events were located by GERESS, based on automatic association of P- and S-type arrivals. This gives an average of 32.1 events per processed day (182 days processed). 59% of these events are within 300 km, and 82% of these events are within 1000 km.

U. Baadshaug

3.6   Regional Monitoring System Operation and Analysis

The Regional Monitoring System (RMS) was installed at NORSAR in December 1989 and was operated at NORSAR from 1 January 1990 for automatic processing of data from ARCESS and NORESS. A second version of RMS that accepts data from an arbitrary number of arrays and single 3-component stations was installed at NORSAR in October 1991, and regular operation of the system comprising analysis of data from the 4 arrays ARCESS, NORESS, FINESS and GERESS started on 15 October 1991. As opposed to the first version of RMS, the one in current operation also has the capability of locating events at teleseismic distance.

Data from the Apatity array were included on 14 December 1992, and from the Spitsbergen array on 12 January 1994. Detections from the Hagfors array were available to the analysts and could be added manually during analysis from 6 December 1994. After 2 February 1995, Hagfors detections were also used in the automatic phase association.

Since 24 April 1999, RMS has processed data from all the seven regional arrays ARCES, NORES, FINES, GERES, Apatity, Spitsbergen, and Hagfors. Starting 19 September 1999, waveforms and detections from the NORSAR array have also been available to the analyst.

Phase and event statistics

Table 3.6.1 gives a summary of phase detections and events declared by RMS. From top to bottom the table gives the total number of detections by the RMS, the number of detections that are associated with events automatically declared by the RMS, the number of detections that are not associated with any events, the number of events automatically declared by the RMS, the total number of events defined by the analyst, and finally the number of events accepted by the analyst without any changes (i.e., from the set of events automatically declared by the RMS).

Due to reductions in the FY94 funding for RMS activities (relative to previous years), new criteria for event analysis were introduced from 1 January 1994. Since that date, only regional events in areas of special interest (e.g, Spitsbergen, since it is necessary to acquire new knowledge in this region) or other significant events (e.g, felt earthquakes and large industrial explosions) were thoroughly analyzed. Teleseismic events were analyzed as before.

To further reduce the workload on the analysts and to focus on regional events in preparation for Gamma-data submission during GSETT-3, a new processing scheme was introduced on 2 February 1995. The GBF (Generalized Beamforming) program is used as a pre-processor to RMS, and only phases associated to selected events in northern Europe are considered in the automatic RMS phase association. All detections, however, are still available to the analysts and can be added manually during analysis.

	Apr 99	May 99	Jun 99	Jul 99	Aug 99	Sep 99	Total
Phase detections	78831	116967	163258	140943	147326	136403	783728
- Associated phases	3250	4556	5282	3054	5553	3683	25378
- Unassociated phases	75581	112411	157967	137889	141773	132720	758350
Events automatically declared by RMS	532	715	931	635	983	773	4569
No. of events defined by the analyst	114	91	114	58	84	84	545
No. of events accepted without modifications	0	0	1	0	0	0	1

Table 3.6.1. *RMS phase detections and event summary.*

U. Baadshaug
B. Paulsen

4   NDC and Field Activities

4.1   NDC Activitities

NORSAR will function as the Norwegian National Data Center (NDC) for treaty verification. Six monitoring stations, comprising altogether 119 field instruments, will be located on Norwegian territory as part of the future IMS as described elsewhere in this report. The four seismic IMS stations are all in operation today, with three of them contributing data to GSETT-3. The infrasound station in northern Norway and the radionuclide station at Spitsbergen will need to be established within the next few years. Data recorded by the Norwegian stations will be transmitted in real time to the Norwegian NDC, and provided to the IDC through the Global Communications Infrastructure (GCI). Norway is now connected to the GCI with a frame relay link to Vienna.

Operating the Norwegian IMS stations will require increased resources and additional personnel both at the NDC and in the field. It will require establishing new and strictly defined procedures as well as increased emphasis on regularity of data recording and timely data transmission to the IDC in Vienna. Anticipating these requirements, a new organizational unit has been established at NORSAR to form a core group for the future Norwegian NDC for treaty monitoring. The NDC will carry out all the technical tasks required in support of Norway's treaty obligations. NORSAR will also carry out assessments of events of special interest, and advise the Norwegian authorities in technical matters relating to treaty compliance.

Verification functions

After the CTBT enters into force, the IDC will provide data for a large number of events each day, but will not assess whether any of them are likely to be nuclear explosions. Such assessments will be the task of the States Parties, and it is important to develop the necessary national expertise in the participating countries.

Monitoring the Arctic region

Norway will have monitoring stations of key importance for covering the Arctic, including Novaya Zemlya, and Norwegian experts have a unique competence in assessing events in this region. On several occasions in the past, seismic events near Novaya Zemlya have caused political concern, and NORSAR specialists have contributed to clarifying these issues.

Information received from IDC

The IDC will provide regular bulletins of detected events as well as numerous other products, but will not assess the nature of each individual event. An important task for the Norwegian NDC will be to make independent assessments of events of particular interest to Norway, and to communicate the results of these analyses to the Norwegian Ministry of Foreign Affairs.

International cooperation

After entry into force of the treaty, a number of countries are expected to establish national expertise to contribute to the treaty verification on a global basis. Norwegian experts have been in contact with experts from several countries with the aim to establish bilateral or multilateral

cooperation in this field. One interesting possibility for the future is to establish NORSAR as a regional center for European cooperation in the CTBT verification activities.

NORSAR event processing

The automatic routine processing of NORSAR events as described in NORSAR Sci. Rep. No. 2-93/94, has been running satisfactorily. The analyst tools for reviewing and updating the solutions have been continuously modified to simplify operations and improve results. NORSAR is currently applying teleseismic detection and event processing using the large-aperture NORSAR array as well as regional monitoring using the network of small-aperture arrays in Fennoscandia and adjacent areas.

Y2K related problems

NORSAR is currently finalizing its efforts in ensuring that all systems at the NDC and in the field are Y2K compliant. The GPS week-rollover problem was addressed, and all systems passed the roll-over without problems.

Technical Training Program

The Norwegian NDC organized the second international training program for seismic station operators at NORSAR in the fall of 1999, with participation from 13 countries in all areas of the world. The course contents included functions at the NDC as well as field maintenance procedures, with emphasis on hands-on demonstrations. The program was carried out very successfully, and will probably be followed by additional such training courses in the future.

Certification of PS27

IMS station PS27-NOA is currently being considered by the PTS for formal certification. PTS personnel visited the station in June 1998, and carried out a detailed technical evaluation. As a result of this inspection and subsequent discussions between NORSAR and the PTS, and following further discussions of the certification requirements during Working Group B meetings, it is now concluded that PS27 needs the following enhancements:

- A tamper detector to be emplaced at every seismometer and at the subarray central vaults
- A centralized authentication process in each subarray as well as at the central array recording facility
- Establishment of a GCI connection at the central array facility
- Addition of a 3-component seismometer in order to satisfy the technical requirements for short-period 3-component recording.

These enhancements are now being implemented.

Establishing an independent subnetwork

Norway has elected to use the option for an independent subnetwork, which will connect with all the IMS stations operated by NORSAR with an interface to the GCI. A contract has been concluded and VSAT antennas have been installed at each station in the network.

Currently, the Norwegian NDC cooperates with several institutions in other countries for transmission of IMS data to the Prototype IDC during GSETT-3, using a variety of data communi-

cations solutions in combination with a high speed link between the Norwegian NDC and the Prototype IDC, and a frame relay link to the IDC in Vienna:

- Data from IMS station PS17 — FINES array — is buffered in Helsinki and thereafter forwarded to the Norwegian NDC, where data is also buffered. From the Norwegian NDC, the data is reformatted and transmitted to the PIDC and the IDC.

- Data from IMS station PS19 — GERES array — is transmitted via simplex satellite from the array to the Norwegian NDC, where it is buffered, reformatted and transmitted to the PIDC.

- Data from IMS station PS40 — Sonseca array — is transmitted from Madrid to the PIDC, using a satellite connection between the Norwegian NDC and Spain NDC. At the Norwegian NDC, the data is routed through to the PIDC.

- Continuous data from IMS station AS101 — Hagfors array — is transmitted by VSAT from Hagfors to the Norwegian NDC, where the data is buffered for data requests from PIDC.

- Data from the station Nilore in Pakistan can be requested by the PIDC, using a VSAT connection between Pakistan and the Norwegian NDC.

It is anticipated that after these stations have been connected to the GCI, these communication links will be discontinued.

Upgrade of PS28

IMS station PS28-ARCES was selected by the PrepCom for hardware upgrade in 1999, and this effort has been concluded. All the digitizers and data acquisition equipment have been replaced. Data from the upgraded array are now being transmitted from the NDC to PIDC, IDC and US_NDC.

Jan Fyen

4.2   Status Report: Norway's Participation in GSETT-3

Introduction

This contribution is a report for the period April - September 1999 on activities associated with Norway's participation in the GSETT-3 experiment, which is now being coordinated by PrepCom's Working Group B. This report represents an update of contributions that can be found in the previous five editions of NORSAR's Semiannual Technical Summary.

Norwegian GSETT-3 stations and communications arrangements

During the reporting interval 1 April - 30 September 1999, Norway has provided data to the GSETT-3 experiment from the three seismic stations shown in Fig. 4.2.1. The NORSAR array (station code NOA) is a 60 km aperture teleseismic array, comprised of 7 subarrays, each containing six vertical short period sensors and a three-component broadband instrument. ARCES is a 25-element regional array with an aperture of 3 km, whereas the Spitsbergen array (station code SPITS) has 9 elements within a 1-km aperture. ARCES and SPITS both have a broadband three-component seismometer at the array center.

Data from these three stations are transmitted continuously and in real time to NOR_NDC. The NOA data are transmitted using dedicated land lines, whereas data from the other two arrays are transmitted via VSAT satellite links of capacity 64 Kbits/s and 19.2 Kbits/s for the ARCES and SPITS arrays, respectively. From the NOR_NDC, relevant data (see below) are forwarded to the prototype IDC (PIDC) in Arlington, Virginia, USA, via a dedicated fiber optical 256 Kbits/s link between the two centers.

The NOA and ARCES arrays are primary stations in the GSETT-3 network, which implies that data from these stations are transmitted continuously to the PIDC with a delay not exceeding 5 minutes. The SPITS array is an auxiliary station in GSETT-3, and the SPITS data are available to the PIDC on a request basis via use of the AutoDRM protocol (Kradolfer, 1993; Kradolfer, 1996). The Norwegian stations are thus participating in GSETT-3 with the same status (primary/auxiliary seismic stations) they have in the International Monitoring System (IMS) defined in the protocol to the Comprehensive Nuclear Test-Ban Treaty.

Uptimes and data availability

Figs. 4.2.2 - 4.2.3 show the monthly uptimes for the Norwegian GSETT-3 primary stations ARCES and NOA, respectively, for the period 1 April - 30 September 1999, given as the hatched (taller) bars in these figures. These barplots reflect the percentage of the waveform data that are available in the NOR_NDC tape archives for these two arrays. The downtimes inferred from these figures thus represent the cumulative effect of field equipment outages, station site to NOR_NDC communication outage, and NOR_NDC data acquisition outages. The low uptime value for ARCES for September (Fig. 4.2.2) is due to the fact that the array operation was halted during the period 1 - 20 September in connection with a complete refurbishment of the electronics of the array.

Figs. 4.2.2-4.2.3 also give the data availability for these two stations as reported by the PIDC in the PIDC Station Status reports. The main reason for the discrepancies between the NOR_NDC and PIDC data availabilities as observed from these figures is the difference in the ways the two data centers report data availability for arrays: Whereas NOR_NDC reports an array station to be up and available if at least one channel produces useful data, the PIDC uses weights where the reported availability (capability) is based on the number of actually operating channels.

Experience with the AutoDRM protocol

NOR_NDC's AutoDRM has been operational since November 1995 (Mykkeltveit & Baadshaug, 1996).

The PIDC started actively and routinely using NOR_NDC's AutoDRM service after SPITS changed its station status from primary to auxiliary on 1 October 1996. For the month of October 1996, the NOR_NDC AutoDRM responded to 12338 requests for SPITS waveforms from two different accounts at the PIDC: 9555 response messages were sent to the "pipeline" account and 2783 to "testbed". Following this initial burst of activity, the number of "pipeline" requests stabilized at a level between 5000 and 7000 per month. Requests from the "testbed" account show large variations. More recently, the number of requests has decreased further. "Pipeline" requests for the reporting period range between 700 and 1200 per month.

The monthly number of requests for SPITS data for the period April - September 1999 is shown in Fig. 4.2.4.

NDC automatic processing and data analysis

These tasks have proceeded in accordance with the descriptions given in Mykkeltveit and Baadshaug (1996). For the period April - September 1999, NOR_NDC derived information on 547 supplementary events in northern Europe and submitted this information to the Finnish NDC as the NOR_NDC contribution to the joint Nordic Supplementary (Gamma) Bulletin, which in turn is forwarded to the PIDC. These events are plotted in Fig. 4.2.5.

Data forwarding for GSETT-3 stations in other countries

NOR_NDC continues to forward data to the PIDC from GSETT-3 primary stations in several countries. These currently include FINESS (Finland), GERESS (Germany) and Sonseca (Spain). In addition, communications for the GSETT-3 auxiliary station at Nilore, Pakistan, are provided through a VSAT satellite link between NOR_NDC and Pakistan's NDC in Nilore. The PIDC obtains data from the Hagfors array (HFS) in Sweden through requests to the Auto-DRM server at NOR_NDC (in the same way requests for Spitsbergen array data are handled, see above). Fig. 4.2.6 shows the monthly number of requests for HFS data from the two PIDC accounts "pipeline" and "testbed".

Current developments and future plans

NOR_NDC is continuing the efforts towards improvements and hardening of all critical data acquisition and data forwarding hardware and software components, so as to meet future requirements related to operation of IMS stations to the maximum extent possible.

The PrepCom has tasked its Working Group B with overseeing, coordinating, and evaluating the GSETT-3 experiment. The PrepCom has also encouraged states that operate IMS-designated stations to continue to do so on a voluntary basis and in the framework of the GSETT-experiment until such time that the stations have been certified for formal inclusion in IMS. In line with this, and provided that adequate funding is obtained, we envisage continuing the provision of data from Norwegian IMS-designated stations without interruption to the PIDC, and to the IDC in Vienna.

Plans for a so-called Independent Subnetwork for transfer of data from IMS stations on Norwegian territory to the NOR_NDC have been finalized and a contract has been concluded with the carrier Telenor. As part of this contract, a new VSAT link was installed between ARCES and NOR_NDC in September, replacing the old NORSAT B link.

Data from Norwegian IMS stations will be sent to the IDC in Vienna via the Norwegian NDC at Kjeller. A new line from Kjeller to the IDC (a so-called frame relay link) was installed in September. The current connection to the PIDC will be terminated when reliable transport of all data from Norwegian IMS-designated stations to the IDC in Vienna has been verified.

The certification process for NOA was initiated by an overview station inspection visit by a PTS (Provisional Technical Secretariat of the PrepCom) team in mid-June 1998. The PTS has pointed out certain modifications that have to be made to the NOA installation to make it fully compatible with the IMS requirements. Implementation of these modifications are now under-way.

During September 1999, ARCES was upgraded with completely new electronics, under a contract with the Provisional Technical Secretariat. We have developed the necessary data conversion software to provide the ARCES data in a format compatible with that used by the IDC. Data from the refurbished ARCES array are as of 1 October 1999 being transmitted to the PIDC and the IDC.

U. Baadshaug
S. Mykkeltveit
J. Fyen

References

Kradolfer, U. (1993): Automating the exchange of earthquake information. *EOS, Trans., AGU*, 74, 442.

Kradolfer, U. (1996): AutoDRM — The first five years, *Seism. Res. Lett.*, 67, 4, 30-33.

Mykkeltveit, S. & U. Baadshaug (1996): Norway's NDC: Experience from the first eighteen months of the full-scale phase of GSETT-3. *Semiann. Tech. Summ., 1 October 1995 - 31 March 1996*, NORSAR Sci. Rep. No. 2-95/96, Kjeller, Norway.
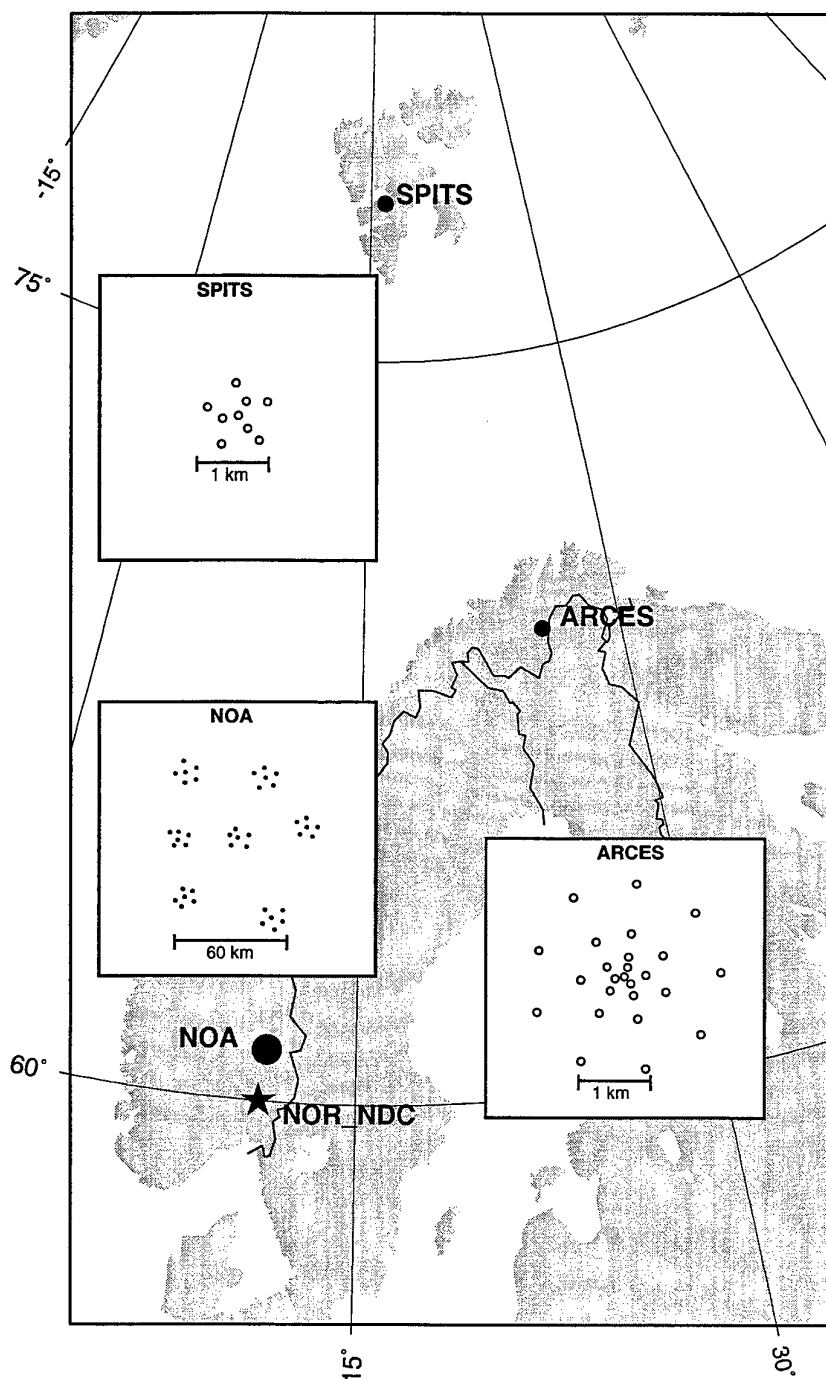
Fig. 4.2.1. *The figure shows the locations and configurations of the three Norwegian seismic array stations that have provided data to the GSETT-3 experiment during the period 1 April - 30 September 1999. The data from these stations are transmitted continuously and in real time to the Norwegian NDC (NOR_NDC). The stations NOA and ARCES have participated in GSETT-3 as primary stations, whereas SPITS has contributed as an auxiliary station.*

ARCES data availability at NDC and PIDC
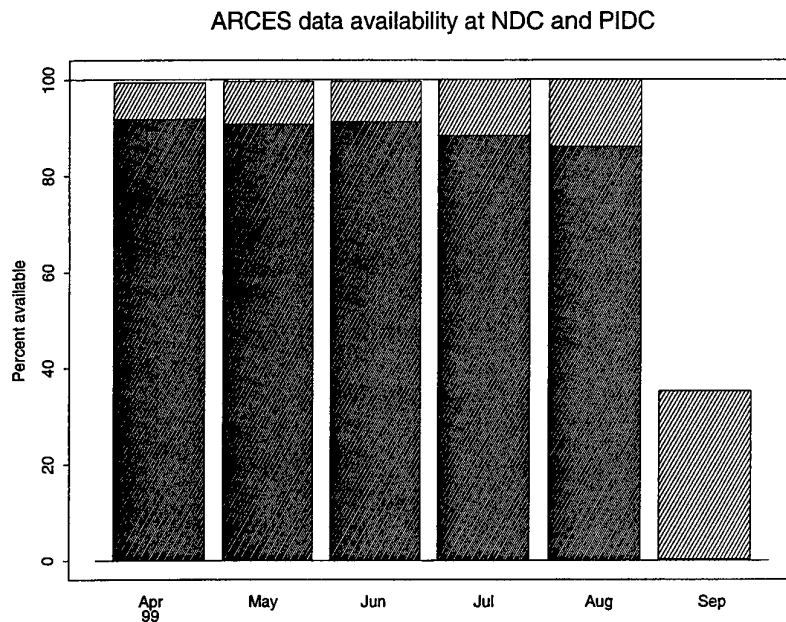
Fig. 4.2.2. The figure shows the monthly availability of ARCESS array data for the period April -
September 1999 at NOR_NDC and the PIDC. See the text for explanation of differences in
definition of the term "data availability" between the two centers. The higher values
(hatched bars) represent the NOR_NDC data availability.

NOA data availability at NDC and PIDC
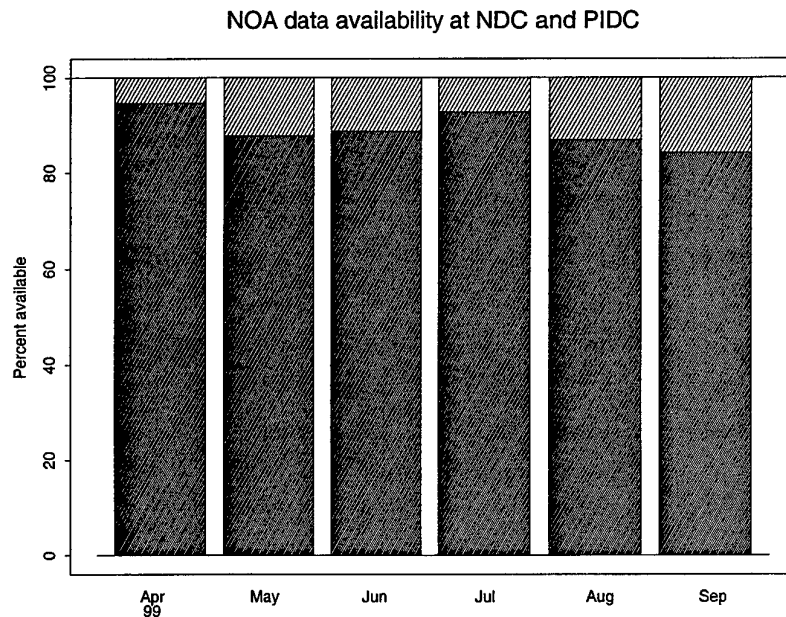
Fig. 4.2.3. The figure shows the monthly availability of NORSAR array data for the period April -
September 1999 at NOR_NDC and the PIDC. See the text for explanation of differences in
definition of the term "data availability" between the two centers. The higher values
(hatched bars) represent the NOR_NDC data availability.

AutoDRM SPITS requests received by NOR_NDC from pipeline and testbec
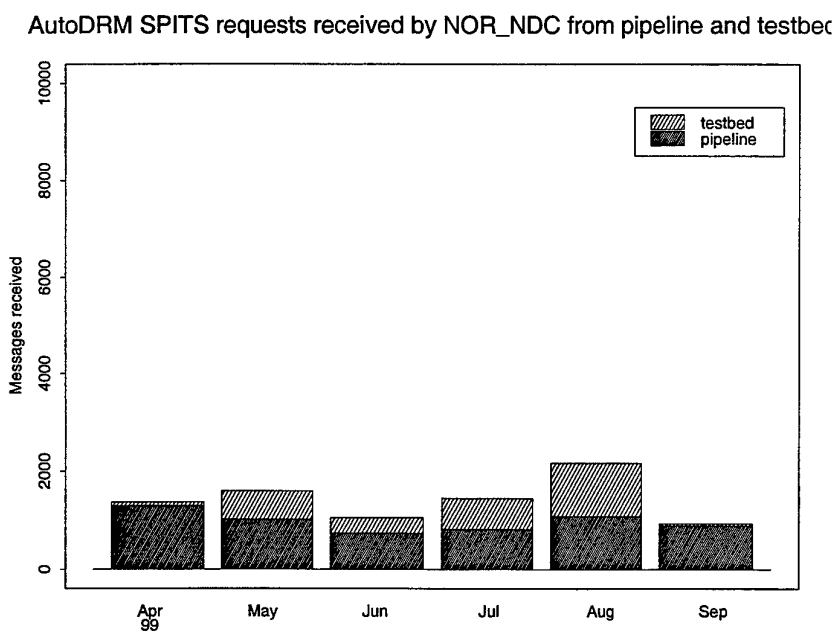
*Fig. 4.2.4. The figure shows the monthly number of requests received by NOR_NDC from the
PIDC for SPITS waveform segments during April - September 1999.*

Reviewed Supplementary events

Fig. 4.2.5. The map shows the 547 events in and around Norway contributed by NOR_NDC during April - September 1999 as Supplementary (Gamma) data to the PIDC, as part of the Nordic Supplementary data compiled by the Finnish NDC. The map also shows the seismic stations used in the data analysis to define these events.

AutoDRM HFS requests received by NOR_NDC from pipeline and testbed
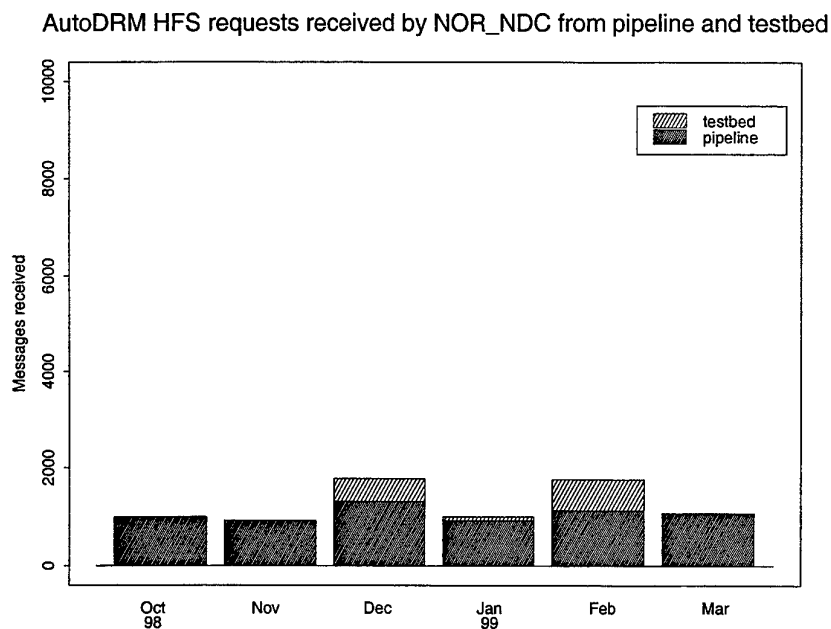
Fig. 4.2.6. The figure shows the monthly number of requests received by NOR_NDC from the
PIDC for HFS waveform segments during April - September 1999.

4.3   Field Activities
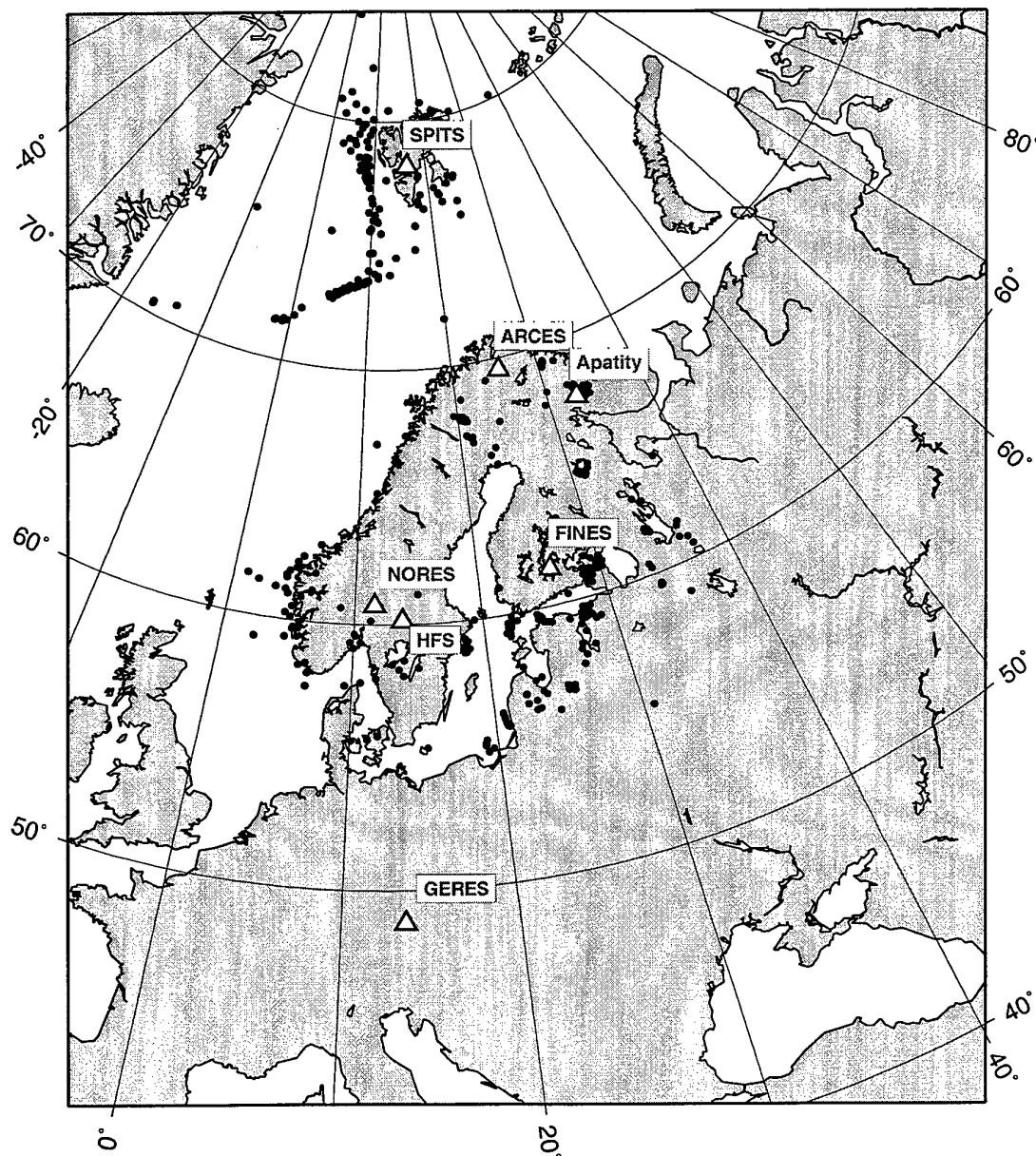
Activities in the field and at the Maintenance Center

This section summarizes the activities at the Maintenance Center (NMC) Hamar, and includes activities related to monitoring and control of the NORSAR teleseismic array, as well as the NORES, ARCES, FINES, GERES, Apatity, Spitsbergen, and Hagfors small-aperture arrays.

Activities also involve preventive and corrective maintenance, planning and activities related to the refurbishment of the NORSAR teleseismic array.

Details for the reporting period are provided in Table 4.3.1 below.

P.W. Larsen
K.A. Løken

Subarray/ area	Task	Date
April 1999		
NORSAR		April
02C-01-02	Preventive maintenance of vault	8-9/4
01B-05	Preventive maintenance of vault	15-16/4
SPITS	Replaced windmill, repaired defective cable going to B4, and installed new fuses for B2	26-29/4
NMC	Repair of defective electronic equipment	April
May 1999		
NORSAR		May
01A-02	Preventive maintenance of vault, including installation of new lid and pole for the GPS receiver	19/5
01A-02-00		20/5
01A-03-04		21/5
01A-04-05		25/5
01A-05-01		26/5
06C-00		27/5
04C-02		28/5
04C-00		31/5

Subarray/area	Task	Date
NMC	Repair of defective electronic equipment.	May
June 1999		
NORSAR		June
04C-04	Preventive maintenance of vault, including installation of new lid and pole for the GPS receiver	1/6
04C-03		2/6
03C-02		3/6
03C-01-05		7/6
02B-02		8/6
02B-03		11/6
02B-00		14/6
01B-00		15/6
01B-03		16/6
01B-01		17/6
02B-04		18/6
01B-02-04		21/6
01B-04-05		22/6
02B-01		23/6
06C-04		24/6
06C-03		25/6
03C-01		28/6
03C-00		29/6
04C-01		30/6
NMC	Repair of defective electronic equipment. Planning new equipment for ARCES	June

Subarray/ area	Task	Date
July 1999		
NORSAR		July
02C-03-00	Preventive maintenance of vault, including installation of new lid and pole for the GPS receiver	1/7
02C-05-00		2/7
03C-04		5/7
NMC	Planning, acquisition and system integration of equipment for ARCES	July
August 1999		
NORSAR		August
01A-00-02-03	Installation of new software for the AIM-24 digitizers and mounted new GPS receivers.	11/8
01B-01-02-03		11/8
01A-04-05-00		12/8
01B-04-05-00		13/8
06C-03-04-05-00		18/8
02B-02-03-04-00-01		18/8
03C-01-02-03-04-05-00		19/8
04C-02-04-05-00		19/8
02C-01-02-04-03-00		20/8
02B05		20/8
NMC	Planning, acquisition and system integration of equipment for the upgrade of ARCES	August

Subarray/ area	Task	Date
	September 1999	
ARCES	Splicing of fiber cables, installation of new digitizers, fiber multiplexers and new acquisition system	September

Table 4.3.1. *Activities in the field and the NORSAR Maintenance Center during 1April - 30 September 1999.*

5 Documentation Developed

Asming, V., I. Kuzmin & F. Ringdal (1999): Recent developments in connection with the seismic station in Amderma, Russia, **In:** *Semiannual Tech. Summ., 1 April - 30 September 1999*, NORSAR Sci. Rep. 1-1999/2000, Kjeller, Norway.

Hicks, E.C., H. Bungum & F. Ringdal (1999): Earthquake location accuracies in Norway based on a comparison between local and regional networks, **In:** *Semiannual Tech. Summ., 1 April - 30 September 1999*, NORSAR Sci. Rep. 1-1999/2000, Kjeller, Norway.

Kremenetskaya, E.O., V. Asming, A. Jevtjugina & F. Ringdal (1999): Study of regional surface waves and frequency-dependent M_s:m_b discrimination in the European Arctic, Spec. Issue *PAGEOPH*, submitted June 99.

Kværna, T. & L. Taylor (1999): Threshold Monitoring processing parameters for IMS stations BRAR and NVAR, **In:** *Semiannual Tech. Summ., 1 April - 30 September 1999*, NORSAR Sci. Rep. 1-1999/2000, Kjeller, Norway.

Kværna, T., F. Ringdal, J. Schweitzer & L. Taylor (1999a): Oprtimized seismic threshold monitoring. Part 1: Regional processing, Spec. Issue *PAGEOPH*, submitted June 99.

Kværna, T., F. Ringdal, J. Schweitzer & L. Taylor (1999b): Oprtimized seismic threshold monitoring. Part 2: Teleseismic processing, Spec. Issue *PAGEOPH*, submitted June 99.

Kværna, T., L. Taylor, J. Schweitzer & F. Ringdal (1999): Continuous assessment of upper limit M_s, **In:** *Semiannual Tech. Summ., 1 April - 30 September 1999*, NORSAR Sci. Rep. 1-1999/2000, Kjeller, Norway.

NORSAR (1999): *Semiannual Technical Summary, 1 October 1998 - 31 March 1999*, NORSAR Sci. Rep. 2-98/99, Kjeller, Norway.

Ringdal, F., E.O. Kremenetskaya & V. Asming (1999): Observed characteristics of regional seismic phases and implications for P/S discrimination in the European Arctic, Spec. Issue *PAGEOPH*, submitted June 99.

Schweitzer, J. (1999), The MASI-1999 field experiment, **In:** *Semiannual Tech. Summ., 1 April - 30 September 1999*, NORSAR Sci. Rep. 1-1999/2000, Kjeller, Norway.

Schweitzer, J. (1999): Slowness corrections — One way to improve IDC results, Spec. Issue *PAGEOPH*, submitted June 99.

Schweitzer, J. (1999): HYPOSAT — A new routine to locate seismic events, Spec. Issue *PAGEOPH*, submitted June 99.

Taylor, L., J. Schweitzer & T. Kværna (1999): Eurobridge — ground truth observations at the Fennoscandian arrays, **In:** *Semiannual Tech. Summ., 1 April - 30 September 1999*, NORSAR Sci. Rep. 1-1999/2000, Kjeller, Norway.

6.1 Earthquake location accuracies in Norway based on a comparison between local and regional networks

Abstract

Detailed studies of the low to intermediate seismicity in two coastal regions of Norway have been used in a comparison between earthquake locations from local high-precision networks on the one side and locations using a sparse regional array network on the other side. To this end, a reference set of 32 low-magnitude earthquakes have been located using two local temporary networks in northern and western Norway, with estimated epicenter accuracies better than 5 and 10 km, respectively. Comparisons are made between the local network solutions and the NORSAR Generalized Beamforming (GBF) system, which provides automatic phase association and location estimates using the Fennoscandian regional array network. The median automatic GBF location error is of the order of 20-30 km when four or more arrays detect the event, increasing to about 80-100 km when only two arrays are available, and the automatic GBF bulletin is essentially complete down to magnitude M_L=2.0. Most of the mislocation vectors of the NORSAR GBF solutions are oriented perpendicular to the Norwegian coast, and with a tendency to pull the location in a southeasternly direction. The GBF performance is clearly better, both in terms of accuracy and completeness, than the performance of the automatic bulletin of the Prototype International Data Center (PIDC) which uses data from essentially the same network. The analyst reviewed NORSAR and PIDC bulletins show, not unexpectedly, an improvement in location accuracy compared to the automatic solutions and appear to be of similar quality for the few common events, with an average mislocation of about 20 km. The NORSAR reviewed bulletin is more complete at low magnitudes compared to PIDC, and there appears to be a potential for significant improvements in the PIDC processing of small seismic events in this region.

Introduction

A considerable effort is currently taking place to develop and apply location calibration information for seismic events recorded by the International Monitoring System (IMS) for the Comprehensive Nuclear-Test-Ban Treaty (CTBT) (e.g., Bondar and North, 1999). One important source of such calibration information is sets of explosions or earthquakes with very accurate locations (so-called Ground Truth information). Earthquakes monitored by local microseismic networks with high location precision are in many cases appropriate as calibration events, and in this paper we present a number of earthquake hypocenters calculated from local networks in northern and western Norway (located within the two boxes in Fig. 1, where also the regional seismicity is shown). We use these results to evaluate the accuracy of automatic and interactive location estimates using a sparse regional array network, essentially comprising the IMS seismic stations in Fennoscandia. While most of our emphasis is on evaluating the NORSAR automatic processing system, we also compare the results with those of the automatic PIDC process, as well as with analyst reviewed results at NORSAR and the PIDC.

NORSAR and PIDC detection and location processing

The NORSAR automatic system makes use of the Generalized Beamforming (GBF) method, which was developed by Ringdal and Kværna (1989), and which has been applied routinely at

NORSAR since 1990. The GBF algorithm is based upon processing data from a sparse network of regional arrays, and associates detected phases by forming a regional grid system and "steering" the network towards each individual grid point. Each detected phase at one of the arrays is treated as a 0-1 valued function, where the value 1 is assigned if the detection corresponds in azimuth and slowness to the grid point. By simply adding these functions, suitably delayed in time, one obtains an efficient phase association of seismic events as well as a preliminary location. By using a denser grid ("beampacking") around this initial epicenter, the location estimates are subsequently refined.

The automatic association and event definition procedure at the PIDC makes use of the same basic principles as the NORSAR GBF, but introduces a set of weighting criteria (different from the 0/1 weightings used at NORSAR) in the beamforming procedure. A seismic event is defined when the weighted sum of detected phases exceeds a predefined threshold. The threshold setting represents a tradeoff between the desire for completeness (no missed events) and for avoiding spurious events (false associations). In contrast to the NORSAR GBF, the threshold at the PIDC is set to a relatively high value in order to minimize the number of spurious (false) events. On the other hand, this results in several real seismic events being missed by the PIDC automatic procedure, as will be further shown by examples in this paper.

The Local Networks and their Capabilities

The two local networks studied in this paper are located in the Ranafjord area (northern Norway) and the Bremanger area (western Norway). Fig. 1 shows the two study areas along with a seismicity map of Fennoscandia. The technical installations for both networks are similar, relying on radio links to transmit data to a central station, where the data are digitized, and a real-time STA/LTA analysis is performed by a local, PC-based acquisition system (Hicks et al., 1999a). Triggers are stored locally and downloaded to NORSAR on a daily basis. Sampling rates are 40 Hz for both networks. Whenever convenient, the readings from the two networks have been supplemented by readings from nearby permanent seismic stations part of the National Norwegian Seismic Network. However, these additional stations did not provide any significant improvement of the locations, but rather acted as confirmation.

The Ranafjord network (Fig. 2) comprised initially six seismic stations installed in June 1997 as part of a research project (NEONOR, Neotectonics in Norway), with the main purpose of monitoring possibly seismic activity along potentially active local faults (Hicks et al., 1999a). The network was reduced to four stations in September 1998, but without significant loss in location precision. The Bremanger network (Fig. 3) has been in operation since October 1998, but has not been operating continuously since it was installed, and less data are therefore available here than one otherwise should have expected in view of the proximity to seismically active areas of the North Sea (Bungum et al., 1991).

The location algorithms used for both networks is a version of the Hypocenter program (Lienert et al., 1986), which uses scaled, adaptively damped least squares to determine hypocenter location. Due to the close distances from hypocenter to station, (5-40 km for the Rana network) the phase arrivals for events of this magnitude can pe picked with a high accuracy. This is especially the case for the 'larger' events ($M_L > 1.5$) such as those used in this study. The short distances also mean that first arrivals are direct waves, so the only velocities used in the location are the upper 15 km of the crust. Consequently, RMS traveltime residuals are less than 0.1s for all earthquakes in the Rana network, and generally less than 0.5s for the earthquakes in West-

ern Norway, using arrival times from the local and permanent networks. The velocity models used are fairly accurate for the relatively consistent geophysical properties in the areas surrounding the networks.

Based on a detailed analysis of the location error ellipsoids, we estimate that the accuracy of the epicenter locations in Rana is better than 5 km, and most likely within 2-3 km for the events near the network. The events located in the Bremanger area are somewhat farther from the network itself, and of higher magnitude. In this case there is, however, a more significant contribution from the permanent network, which is better in western than in northern Norway. A conservative estimate of the location accuracy near Bremanger would be between 5 and 10 km. This means that the local earthquakes from Rana and Bremanger will qualify as GT5 and GT10 events (GT = Ground Truth), i.e., with location accuracies better than 5 and 10 km, respectively.

Seismicity in and around the Local Networks

The offshore and onshore parts of Northern Norway have long been considered an area of elevated seismic activity with regard to the rest of the Baltic shield and margin areas, albeit not particularly high as compared to some other passive (rifted) continental margins globally (Bungum et al., 1991; Byrkjeland et al., in press). The largest known onshore earthquake in Fennoscandia in historical times occurred in the Ranafjord area, where the Rana network is located, on August 31, 1819, and with an estimated magnitude of M_S 5.8-6.2 (Muir Wood, 1989). This earthquake was felt over most of Fennoscandia, as far away as Stockholm and Oslo.

The northern parts of the North Sea, adjacent to the Bremanger network, are among the most seismically active areas in northern Europe, in a structurally very complex region. The largest recent earthquakes in this area occurred on August 8, 1988, and on January 23, 1989, with respective magnitudes of M_L 5.1 and 4.9 (Hansen et al., 1989). The 1988 earthquake occurred around 200 km northwest of the current network, while the 1989 earthquake was around 50 km due west of the current network.

Of the 420 events located by the Rana network, 340 are located in the immediate vicinity of the network, and 40 of these are confirmed explosions or probable explosions, leaving around 300 as probable earthquakes. Magnitudes range from M_L 0.1 to 2.8, with most events in the M_L 1.0 to 1.5 range. The hypocenter depths are shallow, mainly from 4 to 12 km, thereby indicating that this is essentially a swarm activity of the type seen also elsewhere in this region (Bungum et al., 1979; Atakan et al., 1994).

Fig. 2 shows the 1997-1999 micro-seismic activity in the Rana region plotted according to magnitude (explosions removed). Five main groups of events are visible in the western part of the network. These groups occur as swarms, having well defined activity periods and hypocenter depths. The largest events within the network occurred within the two westernmost groups, which are also located in the vicinity of many of the reported phenomena concerning the 1819 earthquake. The easternmost group has hypocenter depths predominantly around 4-6 km, while the other three mainland groups mainly have depths in the 10-12 km range. The depth estimate for the large westernmost group is slightly more uncertain since these events lie further outside the network, but since several of the earthquakes were noticed as loud bangs/cracking noises the depths are most likely less than five km for this group also.

Focal mechanism solutions determined using data from the Rana network show an σ_{Hmax} orientation parallel to the coast, which is a 90° rotation with respect to the regional, ridge push dominated, stress field (Hicks et al., 1999b). This implicates a strong local stress influence on the seismic activity in the area. The northern North Sea is a geologically very complex area, with an intricate system of rifted basins and highs. However, focal mechanisms in this area do largely comply with the expected direction of the ridge push force, although some mechanisms southwest of the network (Lindholm et al.; in press) do have a similar inversion of the σ_{Hmax} direction as seen in the Rana area.

The Bremanger area has of yet not shown any clear patterns of seismicity, the activity appears to be fairly well distributed, as shown in Fig. 3. The largest earthquake (M_L 3.9) located occurred in an area were there has been no earlier known activity. The other two earthquakes with magnitudes larger than 2.0 occured within the areas known to have the highest seismic activity from earlier instrumental data.

Location Results using the Regional Array Network

A total of 32 of the local earthquakes detected by the local networks were also detected and located by NORSARs automatic GBF system. Of these, 21 were reviewed by the NORSAR analysts. Eight events were detected by the PIDC automatic bulletin, six of which were reviewed. All of these events are listed in Table 1, together with locations and location differences. For the Rana region the details of the magnitude information are given in Fig. 4, where it is seen that the PIDC system has a detection threshold near M_L 2.5 (but with two missing M_L 2.7 events), while the GBF system seems to have a detection threshold of about M_L 2.0 (but with one missing M_L 2.1 event).

The location differences are plotted vs. number of stations used in the solution in Fig. 5, with a second order regression line for the GBF solutions, and the median location differences are also shown in the same figure. It can be inferred from these results that both the GBF and PIDC location accuracies are quite sensitive to number of stations used (and thereby event magnitude). In contrast, the NORSAR analyst reviewed solutions retain good accuracy (median error about 20 km) even for the smaller events, although events detected on only 1 or 2 stations are usually not reviewed. It is, however, because of the large scatter, difficult to use Fig. 5 in comparing the performance of the two systems in more detail, except that the analyst review causes a clear improvement in the location accuracies for both systems. Table 2 shows average location 'errors' for the five events for which all four types of solutions are available (all from Rana, see Table 1), and it is appears that the GBF has better automatic solutions than the PIDC (32 versus 60 km) while the reviewed solutions are quite similar (22 versus 20 km). However, the low number of events in the PIDC bulletins combined with the large scatter makes it difficult to conclude very clearly here.

It can be seen from Table 1 (see also Fig. 5) that the automatic GBF system provides epicenters with median location error about 20-30 km for events that are detectable on four or more stations. For the smaller events, detectable at only 1 or 2 stations, the GBF location accuracy deteriorates, with a median error of about 80-100 km and with a large scatter. The azimuthal distribution of the location differences for the GBF solutions are shown in Fig. 6. The mislocation vectors are generally oriented NW-SE (perpendicular to the coast), and it is also apparent that the GBF system tends to bias the solutions towards the southeast, in particular for events with the largest uncertainties (fewer detecting stations).

Concluding Remarks

The following main conclusions can be drawn from this study of detection and location of small events in northern and western Norway:

- Using essentially the same network of seismic stations (arrays), the automatic NORSAR GBF is significantly better than the automatic PIDC system both in terms of location accuracy (~30 and ~60 km for common events) and detectability (M_L 2.0 and 2.5).
- The quality of the automatic GBF locations deteriorates quite rapidly when fewer stations are used in the solution, whereas the accuracy of the NORSAR analyst reviewed solutions remains high.
- The analyst reviewed NORSAR and PIDC bulletins have similar location accuracies (~20 km) for the few common events, but the NORSAR bulletin is more complete at low magnitudes.

In this paper we have sometimes used the term 'location error' or 'location accuracy' when comparing results from the local and regional networks. We note that the local network solutions, which have been used as reference, may themselves be mislocated by up to 5 or 10 km. The real performance of the regional network locations should therefore be slightly better than evaluated here. We should also note that the grid spacing for the GBF system is 33.3 km (0.3°), so the solutions within 20 km are therefore in general located to the closest grid point. Potentials for further improvements here are apparent. With respect to the PIDC solutions we finally note that, for the region considered in this paper, the only significant difference between the arrays and stations used by the two systems is that the PIDC system uses the large-aperture NOA array instead of the regional small-aperture NORES array. While this could explain some of the difference between the two systems, it seems that there should still be potentials for the PIDC to detect events at a lower magnitude level than what is done today, and possibly also with better precisions in its automatic solutions which are quite important in an operational situation within a CTBT context.

In closing we note that events located by local networks as analyzed here provide an interesting potential for extending the data base of Ground Truth events.

Acknowledgments

E.C. Hicks, NORSAR & Dept. for Geology, Univ. of Oslo
H. Bungum, NORSAR & Dept. for Geology, Univ. of Oslo
F. Ringdal

References

Atakan, K., C.D. Lindholm, and J. Havskov (1994): *Earthquake swarm in Steigen, Northern Norway: an unusual example of intraplate seismicity*, Terra Nova, 6, 180-194.

Blystad, P., H. Brekke, R.B. Færseth, B.T. Larsen, J. Skogseid, and B. Tørudbakken (1995): *Structural elements of the Norwegian continental shelf, Part II: The Norwegian Sea region*, NPD Bulletin, 8.

Bondar, I. and R.G. North (1999): *Development of calibration techniques for the Comprehensive Nuclear-Test-Ban Treaty (CTBT) international monitoring system*. Phys. Earth. Plan. Int., 113, 11-24.

Bungum, H., A. Alsaker, L.B. Kvamme, and R.A. Hansen (1991): *Seismicity and seismotectonics of Norway and surrounding continental shelf areas*, J. Geophys. Res., 96, 2249-2265.

Bungum, H., B.K. Hokland, E.S. Husebye, and F. Ringdal (1979): *An exceptional intraplate earthquake sequence in Meløy, Northern Norway*, Nature, 280, 32-35.

Byrkjeland, U., H. Bungum, and O. Eldholm (in press): *Seismotectonics of the Norwegian margin*, J. Geophys. Res.

Hansen, R.A., H. Bungum, and A. Alsaker (1989): *Three recent larger earthquakes offshore Norway*, Terra Nova, 1, 284-295.

Hicks, E., H. Bungum, and C.D. Lindholm (1999a): *Seismic activity, inferred from crustal stresses and seismotectonics in the Rana region, Northern Norway*, Quaternary Sci. Rev., in press.

Hicks, E., H. Bungum, and C.D. Lindholm (1999b): *Crustal stresses in Norway and surrounding areas as derived from earthquake focal mechanism solutions and in-situ stress measurements*, Nor. Geol. Tidsskr., submitted.

Lienert, B.R.E., E. Berg, and L.N. Frazer (1986): *Hypocentre: An earthquake location method using centerd, scaled and adaptively damped leas squares*, Bull. Seis. Soc. Am., 76, 771-783.

Lindholm, C.D., H. Bungum, E. Hicks, and M. Villagran (in press): *Crustal stress and tectonics in Norwegian regions determined from earthquake focal mechanisms*, Geol. Soc. Lond., Spec. Publ.

Muir Wood, R. (1989): *The Scandinavian Earthquakes of 22 December 1759 and 31 August 1819*, Disasters, 12, 223-236.

Ringdal, F. and T. Kværna (1989), *A multichannel processing approach to real time network detection, phase association and threshold monitoring*, Bull. Seism. Soc. Am., 79, 1927-1940.

Vaage, S. (1980): *Seismic evidence of complex tectonics in the Meløy earthquake area*, Nor. Geol. Tidsskr., 60, 213-217.

Table 1

Date & time	Mag	Local solutions			NORSAR GBF			NORSAR reviewed			PIDC automatic (SEL1)			PIDC reviewed (REB)		
		Depth	Lat.	Lon.	Δ (km)	azi	nsta	Δ (km)	azi	nsta	Δ (km)	azi	nsta	Δ (km)	azi	nsta
99.05.29 - 00:31:44	3.9	8.7	62.189	4.741	22.6	234.2	7	20.5	65.2	8	52.3	355.8	3	24.5	210.0	8
98.06.18 - 22:54:00	2.7	11.4	66.376	13.111	22.1	97.3	5				39.3	111.3	1	59.0	78.5	3
98.12.16 - 20:57:46	2.7	8.7	66.270	12.983	36.8	131.6	5	30.5	102.4	5						
98.10.26 - 13:17:22	2.5	4.0	66.227	13.050	31.4	128.7	5	28.5	116.5	5	98.8	170.9	2	9.2	28.1	4
99.02.25 - 14:11:43	2.3	4.9	66.295	13.247	17.0	68.7	5	39.9	112.1	5	31.4	74.9	2			
98.02.09 - 12:59:05	2.8	10.7	66.385	13.088	56.6	93.4	4	22.3	114.7	6	55.5	94.4	2	24.6	100.2	4
98.03.09 - 14:19:57	2.8	6.6	65.854	13.529	37.1	107.8	4	5.6	93.4	6	54.7	68.3	3	2.1	190.5	4
97.11.25 - 22:24:17	2.7	11.0	66.500	12.403	88.5	100.0	4	15.4	118.4	5						
97.11.21 - 18:00:09	2.3	6.3	66.413	13.222	31.2	328.1	4	2.7	163.5	5						
98.10.13 - 22:21:59	2.3	3.0	66.241	13.015	14.2	328.7	4	34.7	101.3	4	36.8	98.6	2	38.2	112.0	4
99.01.07 - 14:04:13	2.3	0.0	66.856	13.894	21.4	60.5	4	45.5	108.0	4	11.9	83.4	2			
99.04.13 - 21:31:40	2.3	0.1	66.368	13.218	35.5	332.7	4	9.4	72.6	4						
98.10.29 - 21:07:29	2.3	3.0	66.222	13.045	21.1	204.8	4	36.2	102.6	4						
98.01.08 - 08:04:46	2.2	12.8	66.368	13.134	33.9	338.2	4	11.7	105.9	4						
98.01.11 - 20:01:18	2.2	12.3	66.373	13.110	33.0	339.6	4	16.0	105.6	4						
98.08.11 - 18:52:27	2.1	12.3	66.360	13.144	13.7	265.5	4									
98.12.24 - 07:50:10	2.1	16.6	66.395	13.288	14.8	109.6	4	18.6	79.1	4						
98.10.26 - 22:56:19	2.0	3.0	66.224	13.041	44.5	288.8	4	28.7	115.5	5						
99.06.26 - 21:30:46	2.5	23.7	61.728	4.274	23.4	47.2	3	10.2	167.3	2						
98.02.04 - 14:31:40	2.3	10.6	66.382	13.091	56.5	93.0	3	18.3	128.4	3						
98.12.04 - 12:39:29	2.3	22.2	66.163	12.275	103.0	115.6	3									
98.10.29 - 05:59:53	2.0	3.0	66.228	13.048	16.3	326.9	3	36.2	103.7	4						
98.12.05 - 22:14:53	1.9	13.0	66.751	13.812	26.3	115.1	3	23.4	102.2	4						
99.06.15 - 01:12:57	2.4	13.7	61.947	4.621	24.7	249.9	2	7.3	236.5	2						
98.02.28 - 16:53:26	2.0	11.6	66.701	13.316	179.3	90.0	2									
98.12.16 - 19:57:46	2.0	0.0	66.272	12.924	67.7	110.8	2									
99.04.09 - 08:04:28	2.0	8.0	66.389	13.351	159.0	115.2	2									
98.10.09 - 05:30:14	1.8	3.0	66.249	12.981	45.5	118.8	2									
98.12.17 - 18:33:24	1.8	0.0	66.262	13.000	181.7	118.3	2									
98.10.23 - 02:50:21	1.8	3.0	66.259	13.000	64.0	110.8	2									
98.12.21 - 17:09:47	1.6	33.0	66.488	14.259	161.3	119.3	2									
99.05.15 - 05:50:29	1.3	8.2	61.523	4.844	31.5	102.6	1									

Table 6.1.1. *Locations and location differences for the 32 events in this study. The reference locations are from the solutions determined by the local networks, where solutions north of 65°N are from Rana (six stations, four since September, 1998), the remaining from Bremanger (also six stations). Solutions using a sparse regional network (NORSAR, automatic (GBF) and reviewed; PIDC, automatic and reviewed) are given by location difference (Δ) in km, and azimuth, both compared to the local solution. The number of stations used in each case is also included. The events are sorted by number of stations in the GBF solution.*

Regional network loca-tion	Average location difference (km)
NORSAR GBF automatic	32 ± 16
PIDC automatic	60 ± 23
NORSAR reviewed	22 ± 11
PIDC reviewed (REB)	20 ± 14

Table 6.1.2. *Average location difference, with standard deviations, for five events from the Rana region covered by all solutions (see Table 6.1.1), between the local network solutions (location error less than 5 km) and the four regional network solutions, NORSAR and PIDC, automatic and reviewed.*
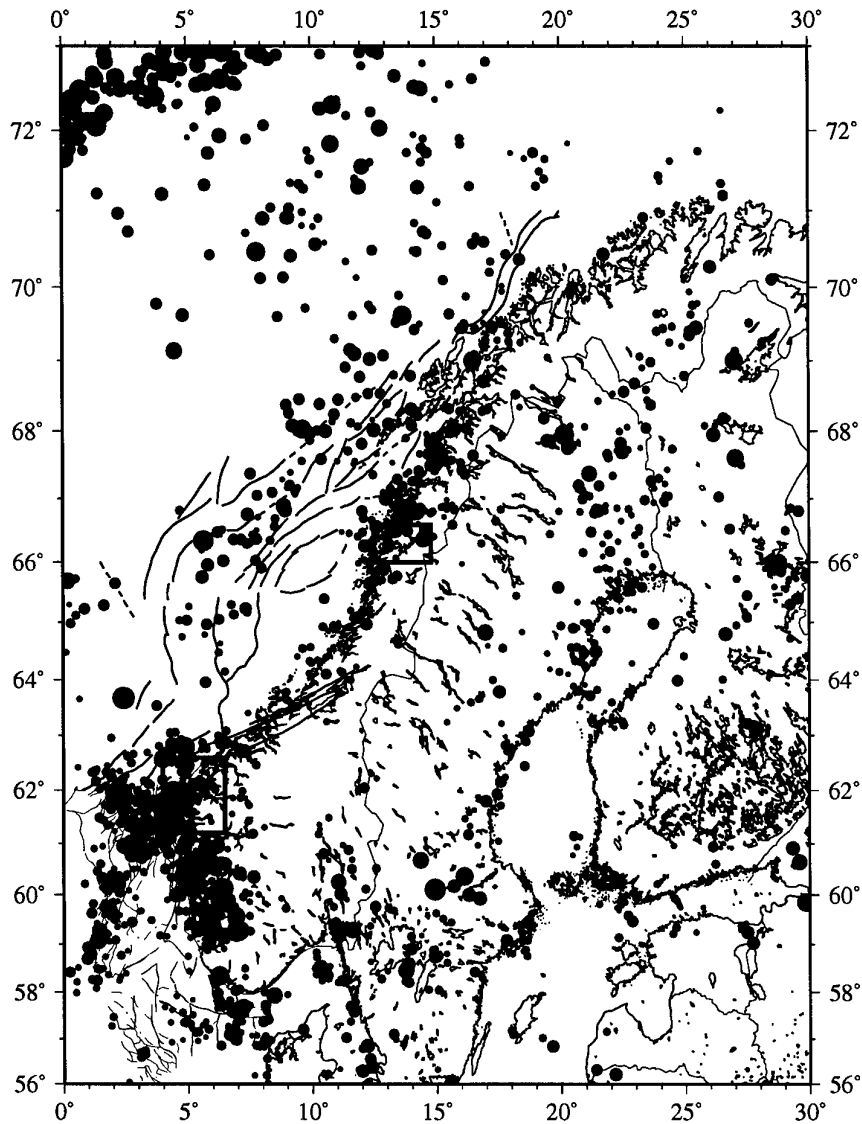
Fig. 6.1.1. *Seismic activity in Norway 1980-1999, M_ω > 2.0. The locations of the two study areas in this paper, Rana and Bremanger, are shown by the two rectangles in northern and western Norway, respectively. Structural information is from Blystad et al. (1995).*
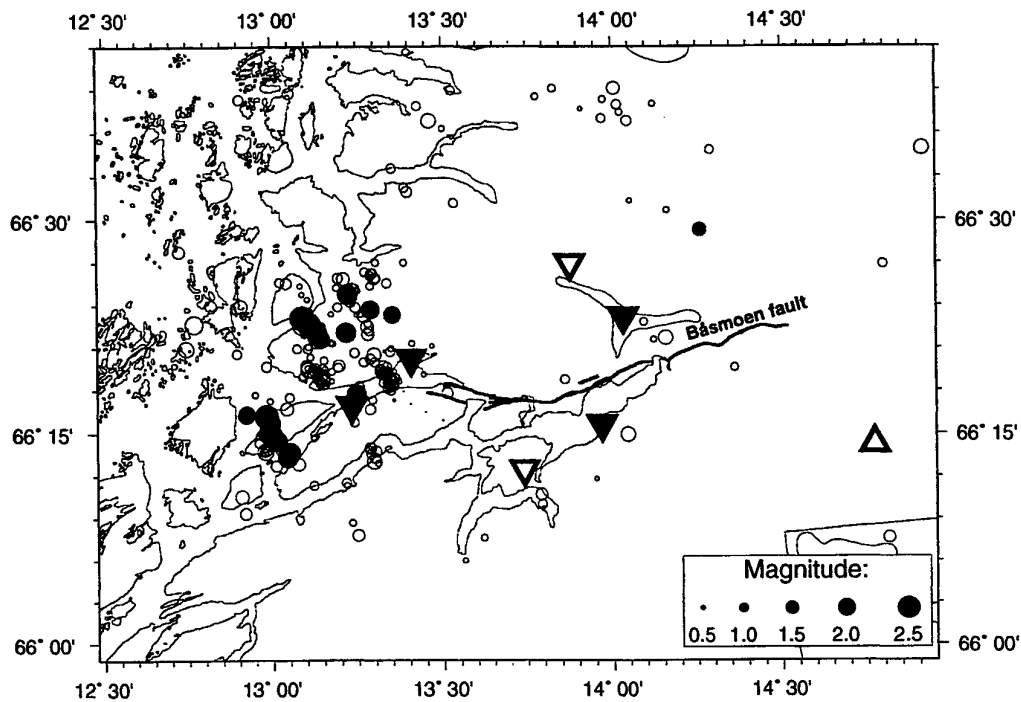
Fig. 6.1.2. *Local seismic activity located by the Rana network 1997-1999. The filled circles represent the events also located by the NORSAR GBF system. The stations are indicated by inverted triangles, the four stations remaining after September 1998 are filled. The three-component MOR8 station that is part of the national Norwegian seismic network, operated by the University of Bergen, is shown by a triangle to the east in the figure. The solid black line is the postglacial Båsmoen fault, considered to be potentially seismically active.*
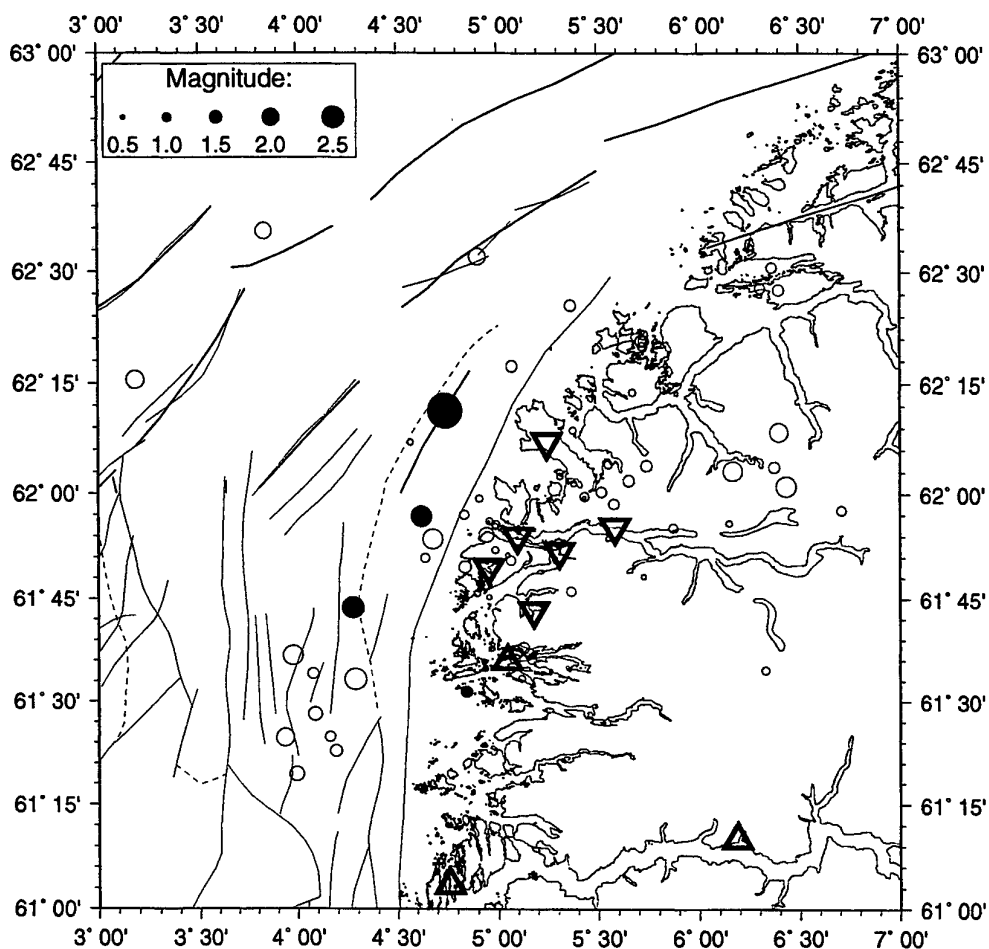
Fig. 6.1.3. *Local seismic activity located by the Bremanger network, 1998-1999. The filled circles represent the earthquakes also located by the NORSAR GBF system. The stations in the local network are indicated by inverted triangles. The NNSN stations in the area are shown as triangles.*
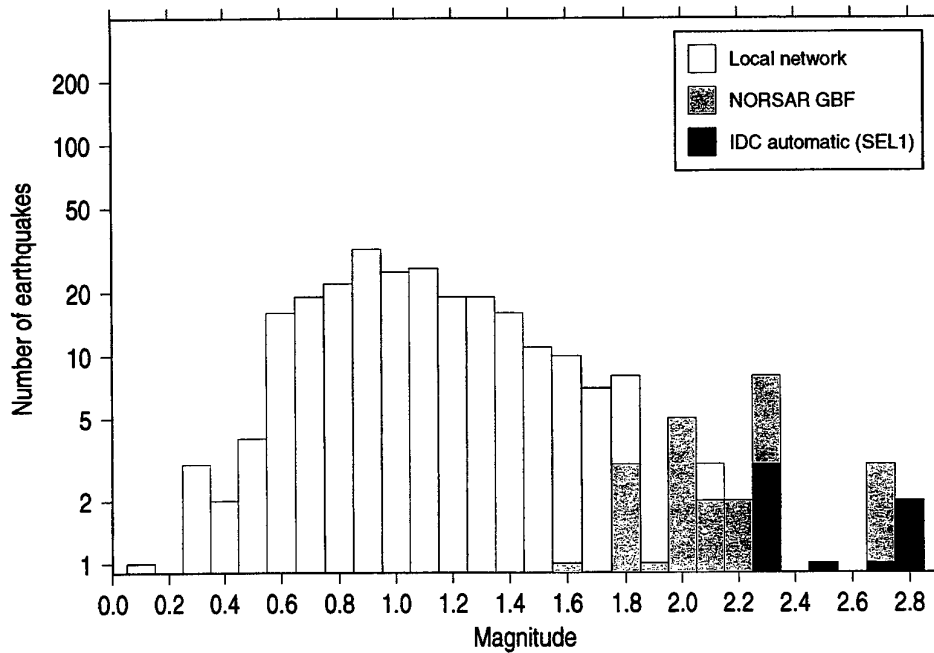
Fig. 6.1.4. *Histogram of frequency-magnitude distribution for the Rana local seismic network (based on about two years of operation) together with events reported by the automatic NORSAR GBF (Generalized Beamforming) system (shaded) and the automatic PIDC (Prototype International Data Center) system (black).*
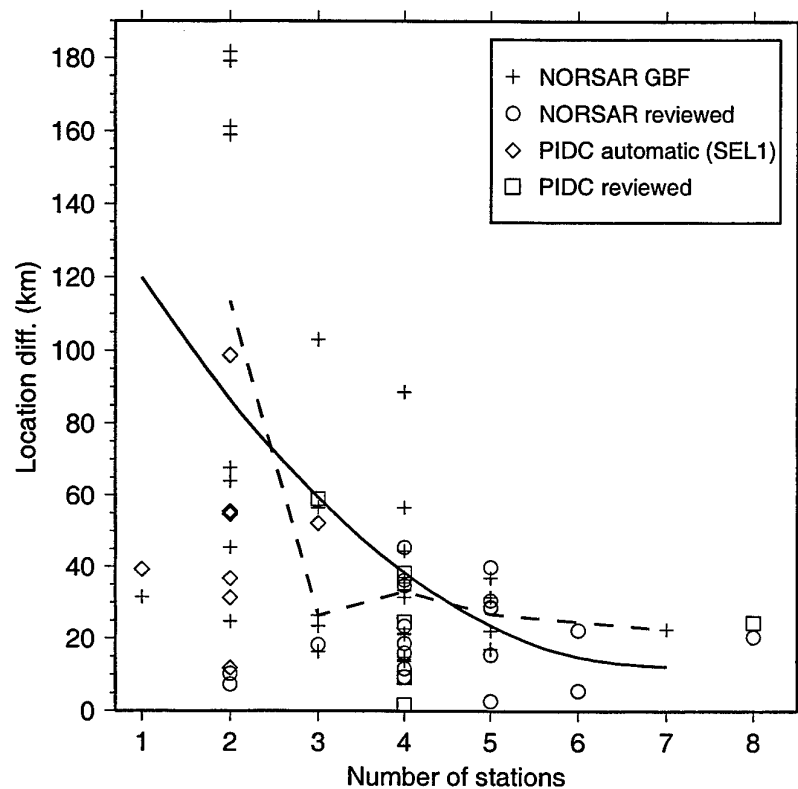
Fig. 6.1.5. *Scatter plot of the location differences between the local network locations and the NOR-SAR GBF (automatic) solutions (circles), the PIDC automatic (diamonds) and the PIDC reviewed (squares) solutions, respectively, plotted vs. number of stations used in the solution. A second order regression analysis for the GBF solutions is shown by the solid line, while the dashed line represents the median differences for the GBF solutions.*
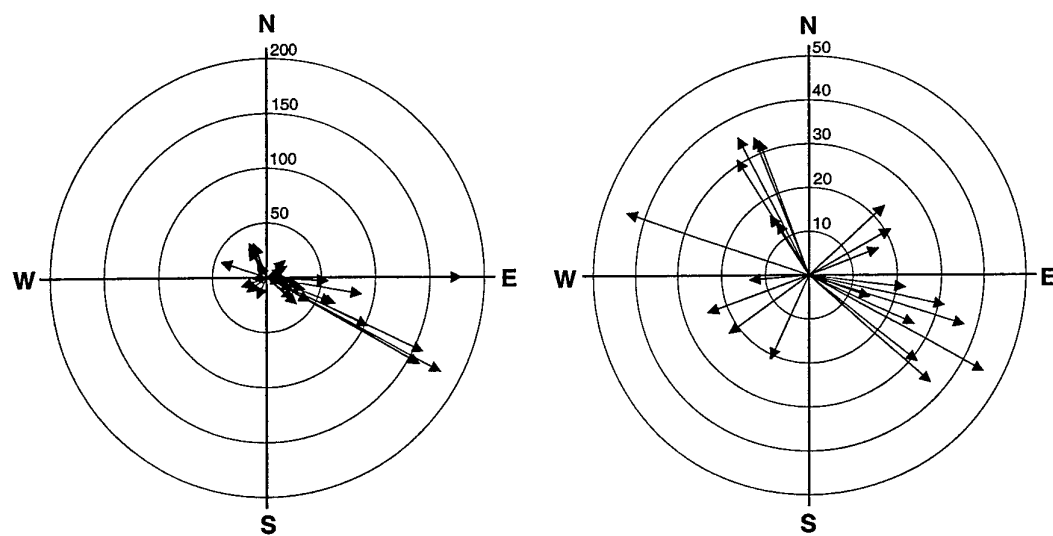
Fig. 6.1.6. *Location differences (in km) and azimuthal directions of the NORSAR GBF solutions with regard to the local solutions. The plot to the left contains all solutions, extending up to 200 km, while the plot to the right contains only events with location differences less than 50 km.*

6.2   Continuous assessment of upper limit M_S

Introduction

The continuous seismic threshold monitoring technique (TM) is used to provide a continuous assessment of the size of events that may have occurred in a given geographical area. The main application of this technique has until now been restricted to short-period seismic data, both at regional and teleseismic distances.

We have recently initiated an effort to apply the continuous TM technique to long-period data, for the purpose of obtaining a continuous assessment of surface wave magnitude (M_S). In principle, this application is straightforward, but in practice one has to take into account many factors, not all of which apply to the short-period case, such as surface wave dispersion, oceanic versus continental propagation paths, the difficulties in calculating surface wave magnitudes at regional distances, regional calibration formulas for *log(A/T)* vs. *log(STA)* and so on.

Nevertheless, the TM application promises to significantly improve monitoring of surface waves. One of the main considerations of TM is that it provides a realistic estimate of network detection thresholds during "unusual" noise conditions, such as in the coda of a large earthquake or during a large aftershock sequence. In the short-period case, we have demonstrated that the global detection capability can deteriorate significantly for many tens of minutes following a large earthquake. In the long-period case, this situation could be expected to be far worse, since surface waves from a large earthquake can last for many hours.

We present initial results from investigating the relation between PIDC station magnitudes and STA based estimates calculated from bandpass filtered data, as well as a case study with monitoring of surface waves from a mining area on the Kola peninsula during and after a M_S 7.6 earthquake.

TM measurements of M_S

When developing a strategy for threshold monitoring of surface waves, we have used the automatic surface wave measurements at the PIDC as the basis. Their procedure consists of the following steps:

- Shape Rayleigh wave observations to a common response type (KS36000)

- Search window for Rayleigh waves derived from regionalized group velocity windows

- Measure largest *A/T* with periods between 18 and 22 seconds

- Calculate station magnitudes using relation of Rezapour and Pearce (1998)

$$M_S = \log(A/T) + \frac{1}{3}\log(\Delta) + \frac{1}{2}\log(\sin(\Delta)) + 0.0046\Delta + 2.730$$

Our experience with threshold monitoring of body waves has shown that short-term averages (*STAs*) can efficiently be used to represent the traditional *A/T* measurements used for magnitude estimation. We will therefore attempt to adopt a similar procedure for surface waves. Concerning the search window for Rayleigh waves, the PIDC calculate these from a regionalized group velocity model. Currently we do not have this utility at hand and we have therefore chosen to analyze surface wave travel-time observations available in the PIDC database to derive

the STA search windows. For threshold monitoring of surface waves we have established the following procedure:

- Bandpass filter data between 17 and 24 seconds, zero phase Butterworth of 2nd order
- Generate short-term averages (*STAs*) with a window length of 30 seconds
- Measure largest *STA* within a search window derived from empirical PIDC data
- Derive *A/T* equivalent from the *STA* observation using station dependent empirical relations between $log(A/T)_{KS36000}$ and $log(STA)$
- Calculate station magnitudes using relation of Rezapour and Pearce (1998)

In Fig. 6.2.1 we show the travel-times and group velocities of PIDC M_S measurements at ARCES for continental propagations paths. Notice that a search window spanning the 2.5-3.3 km/s group velocity window covers all observations at ARCES.
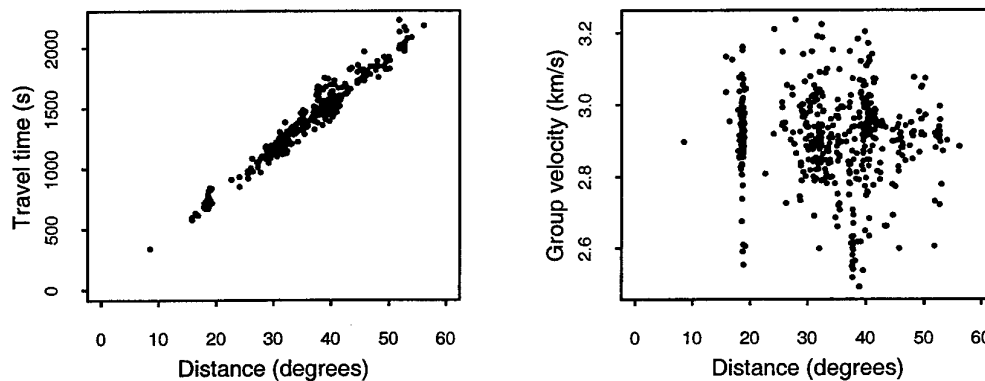

Fig. 6.2.1. *Travel-times and group velocities of PIDC M_S measurements at ARCES for continental propagations paths.*

Fig. 6.2.2 shows the relation between a small set of manual *log(A/T)* measurements made on the ARCES KS-36000 instrument, and *log(STA)* made on the same data filtered between 17 and 24 seconds. The difference between *log(A/T)* and *log(STA)* has a scatter with a standard deviation of 0.11 for this small data set, which is satisfactory in view of the scatter inherent in the magnitude-distance relation for surface waves (Rezapour and Pearce, 1998).
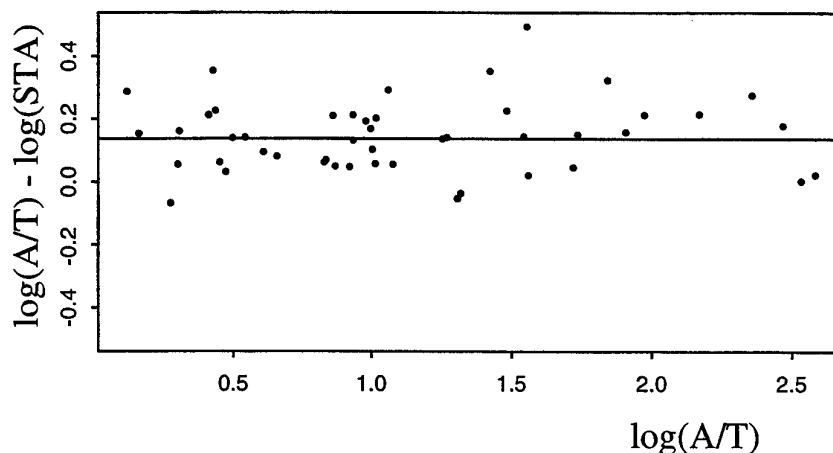
Fig. 6.2.2. *Difference between manual log(A/T) measurements made on the ARCES KS-36000 instrument, and log(STA) made on the same data filtered between 17 and 24 seconds.*
X-axis: log (A/T). Y-axis: $log(A/T)_{KS36000} - log(\frac{\pi}{2} \cdot STA \cdot \frac{cal_{20}}{20})$, where cal_{20} is the-sensitivity in nm at 20 seconds.

A first surface wave threshold monitoring experiment

As an example of TM processing of surface wave data, we have selected 17 August 1999, which was the day of the large Turkey earthquake ($M_S=7.6$). This earthquake was followed by numerous aftershocks, and therefore presents a good opportunity to assess the effects of such a situation on the surface wave detection capability. We focus our investigation on surface waves observed at the three Norwegian IMS stations NOA, ARCES and SPITS, as well as a TM trace based upon joint processing of the data from these three stations.

We have chosen to show a site-specific approach, with a TM beam focused towards the Lovoz-ero Massif, Kola Peninsula. Our reason for selecting this target area is that on the same day, about 4 hours and 40 minutes after the Turkey earthquake, a moderate earthquake ($m_b=4.2$) occurred in this place. We will in the following show a number of figures illustrating the sur-face wave observations and the results from surface wave threshold monitoring using two dif-ferent frequency bands.

Fig. 6.2.3 shows the locations of the station network, and the locations of the Turkey and Lovozero events.

The seismograms of the Turkey event as recorded at NOA, ARCES and SPITS are shown in Fig. 6.2.4. Different types of seismometers are used at these three stations; NOA - KS54000, ARCES - KS36000, SPITS - CMG-3T, and the epicentral distance to the three stations are 23.4, 28.9, and 37.9 degrees, respectively. Notice that the surface wave obser-vations at ARCES are clipped.
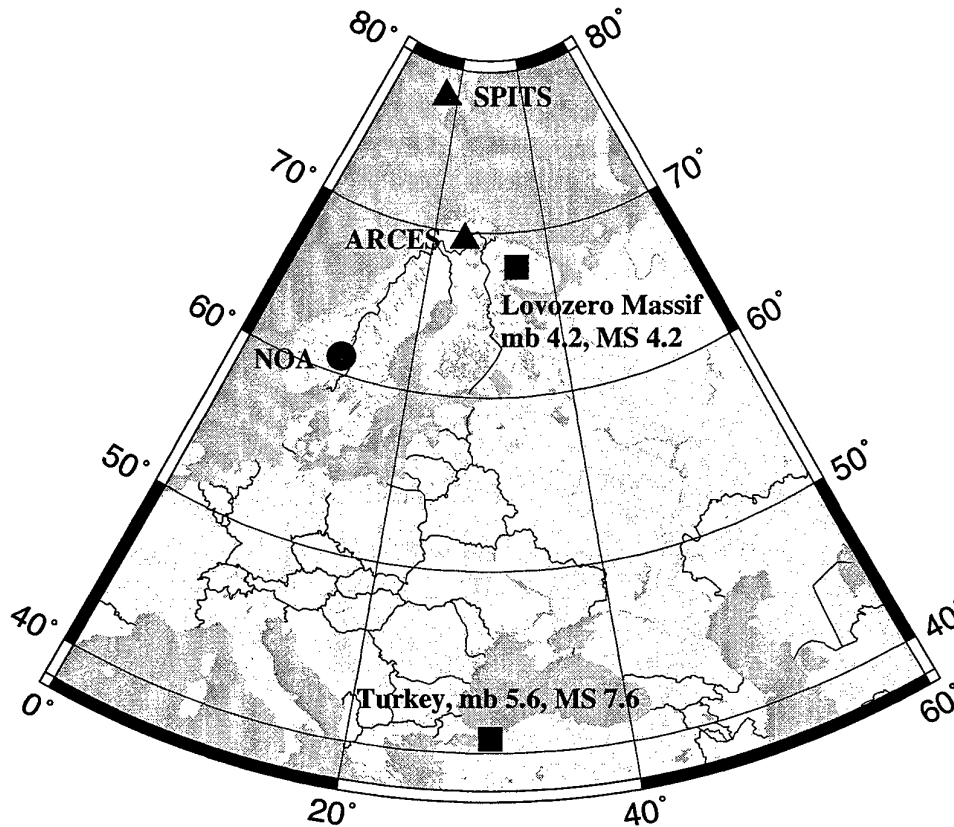
Fig. 6.2.3. *Map showing the locations of the station network, and the Turkey and Lovozero events.*

Fig. 6.2.5 shows the same time interval as in Fig. 6.2.4, but now with simulated KS36000 traces at NOA and SPITS. These are the data used for magnitude estimation at the PIDC. Band-pass filtered recordings of the Lovozero event are shown in Figs. 6.2.6 and 6.27. In the 17 - 24 s band (Fig. 6.2.6), the Rayleigh waves have a low SNR and is only visible at ARCES and NOA. In contrast, clear Rayleigh waves are seen at all stations in the 8 - 12 s period band (Fig. 6.2.7). The epicentral distance to ARCES, SPITS and NOA are 3.7, 11.5 and 12.1 degrees, respectively. Due to differences in the crustal and upper mantle structures, surface waves arrive later at SPITS than at NOA.

The NOA array consists of seven broad-band sensors deployed over an aperture of approximately 60 km. The surface waves from the Lovozero event arrive at NOA with an estimated back-azimuth of 42.4 degrees and an apparent velocity of 3.2 km/s. For the threshold monitoring experiment we beamform the NOA data using the estimated back-azimuth and slowness, resulting in improved SNR in both frequency bands. Based on 20 s Rayleigh wave observations at NOA and the ESDC array in Spain, we estimate a surface wave magnitude of 4.2 of the Lovozero event, using the relation of Rezapour and Pearce (1998).
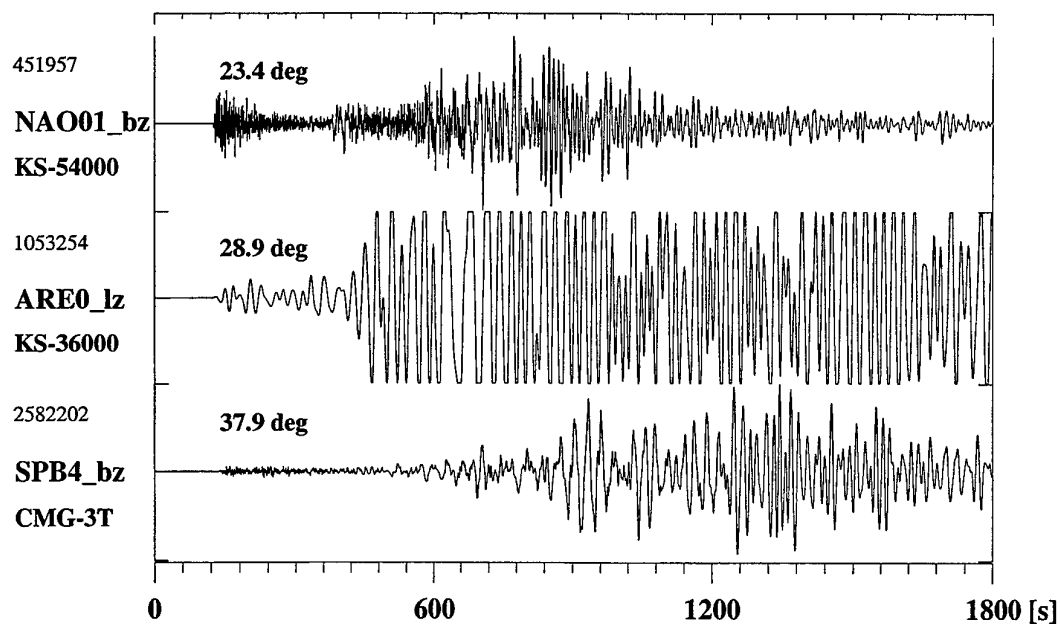
Fig. 6.2.4. *NOA, ARCES and SPITS recordings of the Turkey event. Different types of seismometers are used; NOA - KS54000, ARCES - KS36000, SPITS - CMG-3T. The epicentral distances are given above each trace.*
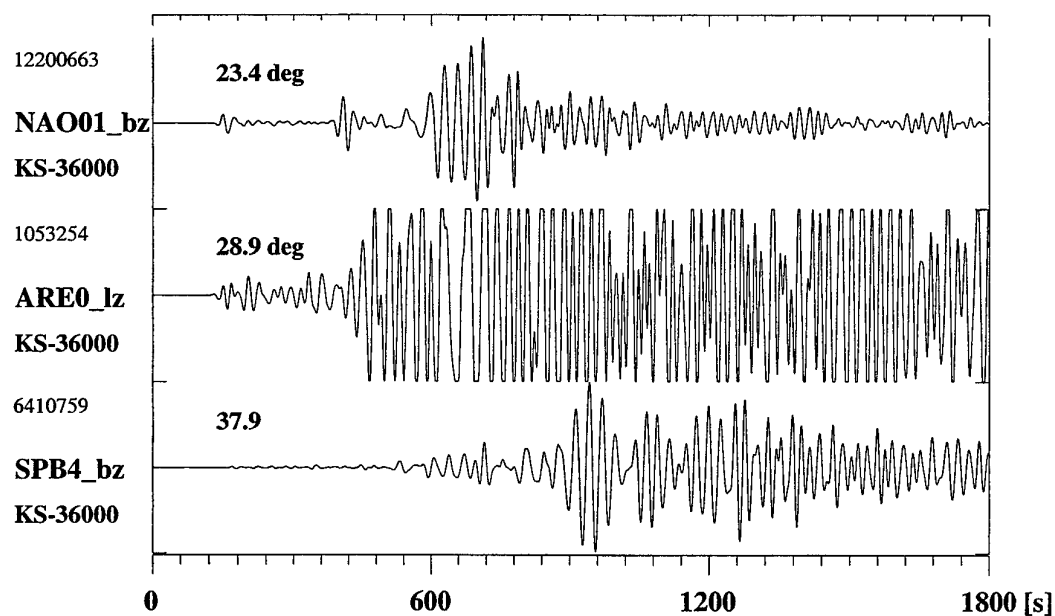
Fig. 6.2.5. *Simulated KS36000 traces at NOA and SPITS for the Turkey event. The ARCES recording is shown in its original form (KS36000).*

Zero phase Butterworth 17 - 24 s, 2. order
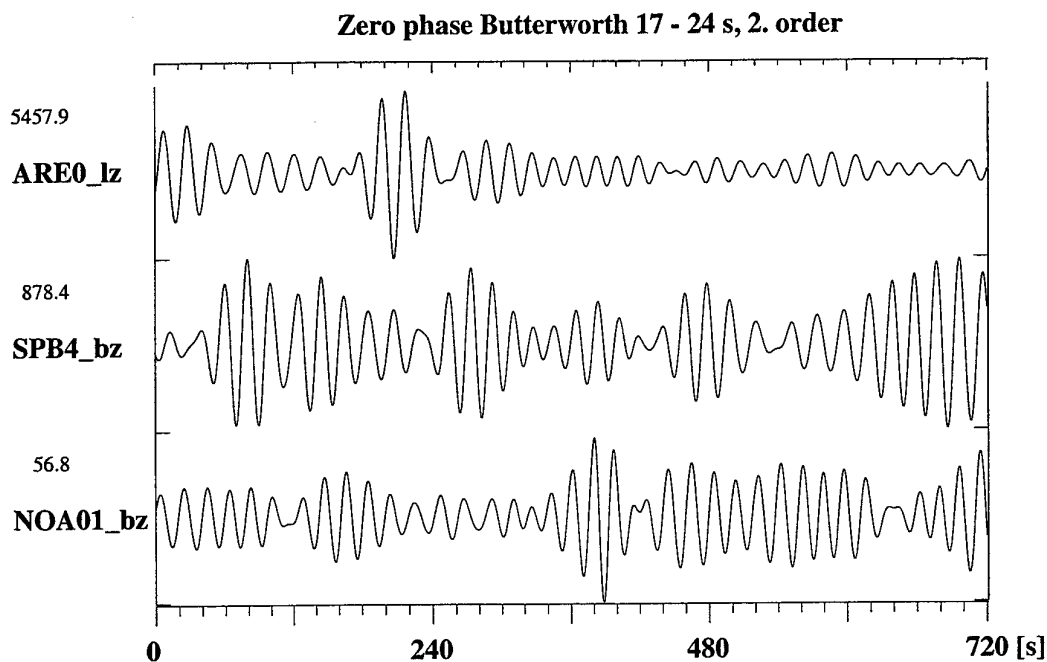
Fig. 6.2.6. *Bandpass filtered (17 - 24 s) recordings of the Lovozero event.*

Zero phase Butterworth 8 - 12 s, 2. order

Fig. 6.2.7. *Bandpass filtered (8 - 12 s) recordings of the Lovozero event. The epicentral distances are given above each trace.*

Using the site-specific threshold monitoring approach for the location of the Lovozero event, we have derived processing parameters such as travel-times, STA lengths, and amplitude-magnitude relations from the actual ARCES, SPITS and NOA observations. The threshold processing results in the "standard" PIDC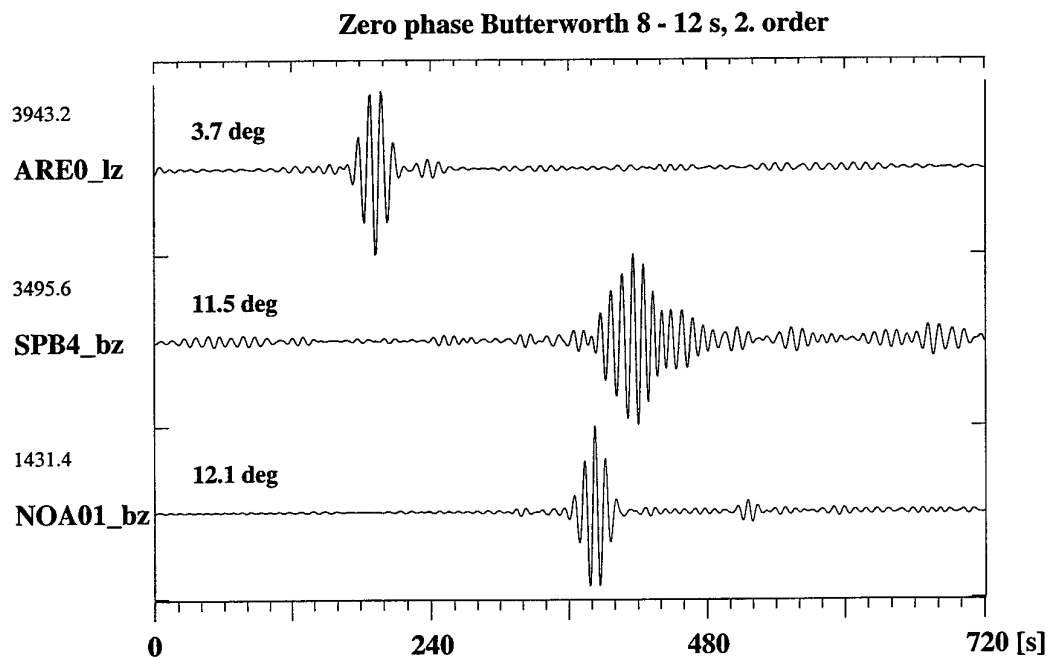 frequency band (17-24 s) are shown in Fig. 6.2.8. We see that the surface waves from the Lovozero event are effectively masked by the coda/aftershocks of the Turkey earthquake

However, in a more "high frequency" filter band (8-12 s) the surface waves from the Lovozero event stand out very clearly, see Fig. 6.2.9. This shows that "high frequency" processing of surface waves at regional distances can significantly improve detectability by suppressing the longer period energy from interfering distant earthquakes. Fig. 6.2.10 compares the threshold monitoring results for both frequency bands (17-24 and 8-12 s) for a 10 hour time period. This clearly illustrates that the amplitudes of surface wave coda of the Turkey event decay much more rapidly at higher frequencies.

Discussion

The continuous assessment of upper limits on surface wave magnitudes as described in this paper is an entirely new application of the Threshold Monitoring technique. Our results so far must be considered only as a preliminary indication of the potential of the method when applied to long-period seismic recordings, but it is already clear that there are significant possibilities for developing the TM process into a useful monitoring tool for surface waves.

In this study, we have used the three IMS arrays ARCES, NOA and SPITS, and applied a site-specific technique to investigate the threshold trace during a large earthquake sequence. A natural follow-up of this work would be to include additional long-period and broadband IMS stations for the same time interval, in order to assess the improvements in monitoring capability when using a network with better azimuthal coverage. It would also be interesting to steer the threshold beam to other sites, including the site of the earthquake sequence (Turkey), in order to assess the possibility for obtaining magnitude estimates (or upper limits) for individual aftershocks in the sequence.

An important result of this initial study is the demonstration of the significant benefits of using a shorter period band (8-12 seconds) instead of the traditional processing band (17-24 seconds) for processing surface waves at regional distances during an aftershock sequence. In future work, we will investigate further whether the use of this shorter period band could be applicable also during "normal" background noise conditions. In an operational setting, it is clearly an advantage to use a fixed frequency band for each station-site combination, but it requires a careful assessment of the relations between surface wave magnitudes calculated in different frequency bands.

As in the short period case, there is a tradeoff between optimizing the TM process for site-specific studies and developing a more general TM application for global surface wave monitoring. Among the main issues is the sharpness of the beam lobe, which depends upon the filter setting, the STA time windows and the tolerance for travel-time deviations. Another issue is the need for regional corrections, which may be greater than in the short-period case. For example, the significant difference between oceanic, continental and combined oceanic-continental paths are important for surface wave propagation, but have little or no counterpart in analyzing short-period P and S waves.

Since a main purpose of the MS measurements is to provide a basis for MS:mb screening (and discrimination), it is important to assess the effects of using shorter period surface waves on the MS:mb discrimination potential. Recent studies in the European Arctic (Krementetskaya et. al., 1998) have demonstrated some promising results using regional LP data from the Apatity long-period station for historic earthquakes and explosions in this region, including past nuclear explosions at Novaya Zemlya. This type of studies should be continued, using available regional recordings for earthquakes and underground nuclear explosions in various regions of the Earth.

T. Kværna
L. Taylor
J. Schweitzer
F. Ringdal

This work is conducted under contract DSWA01-97-C-0128

References

E.Kremenetskaya, V.Asming, Z. Jevtjugina and F. Ringdal (1998). Study of surface waves and Ms:mb using Apatity LP recordings. *Semiannual Technical Summary 1 April - 30 September 1998,* NORSAR Sci. Rep. 1-98/99, Kjeller, Norway.

Rezapour, M. and R.G. Pearce (1998): Bias in Surface-Wave Magnitude M_s due to Inadequate Distance Corrections. *Bull. Seism. Soc. Am.,* **88**, 43-61.
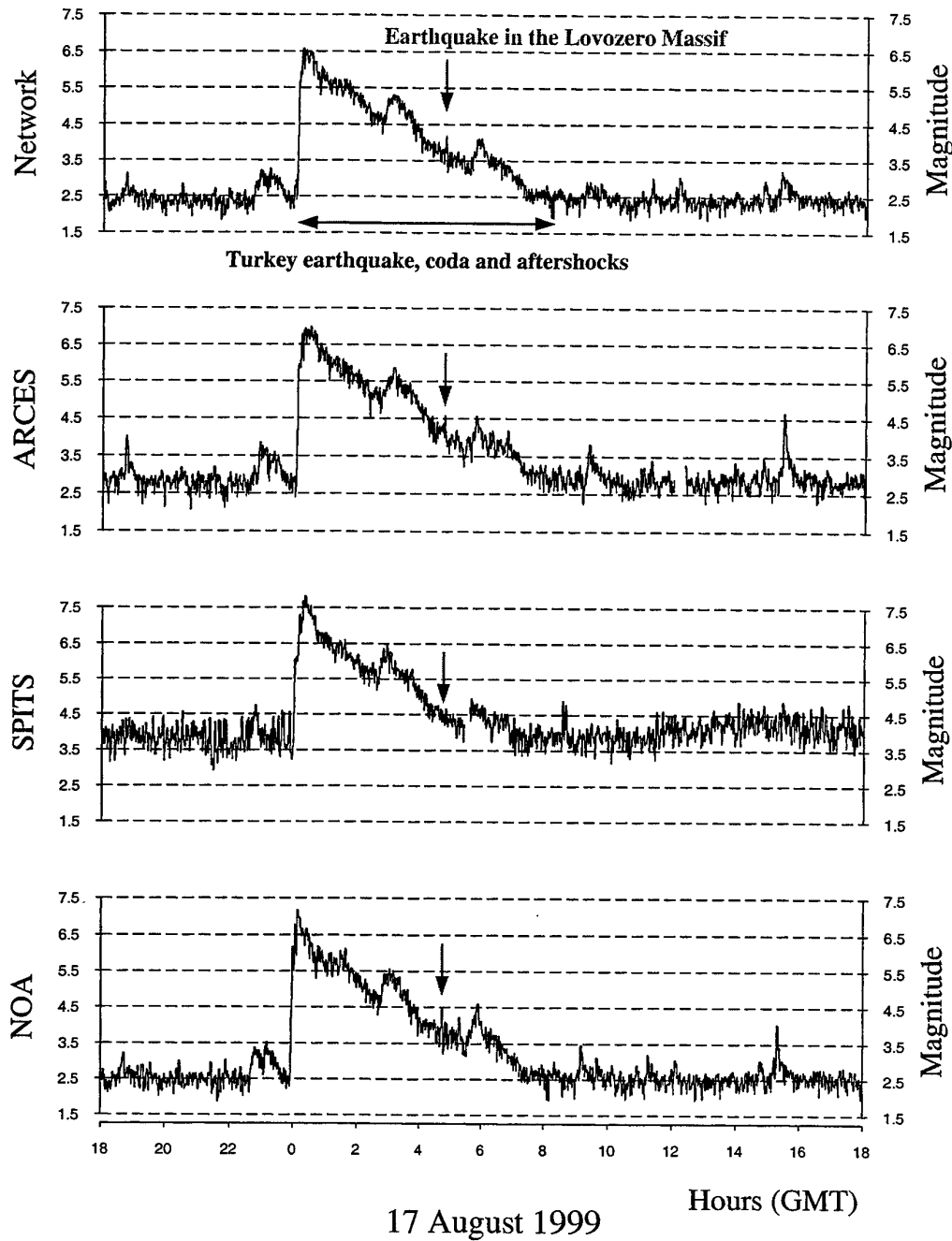
Fig. 6.2.8. Surface threshold monitoring for the location of the Lovozero event for 17 August 1999, using data filtered between 17 and 24 s. The lower three traces represent thresholds (upper 90% magnitude limits) obtained for each of the three stations, whereas the top trace shows the combined network thresholds. The peaks corresponding to the Lovozero event are indicated on each trace.
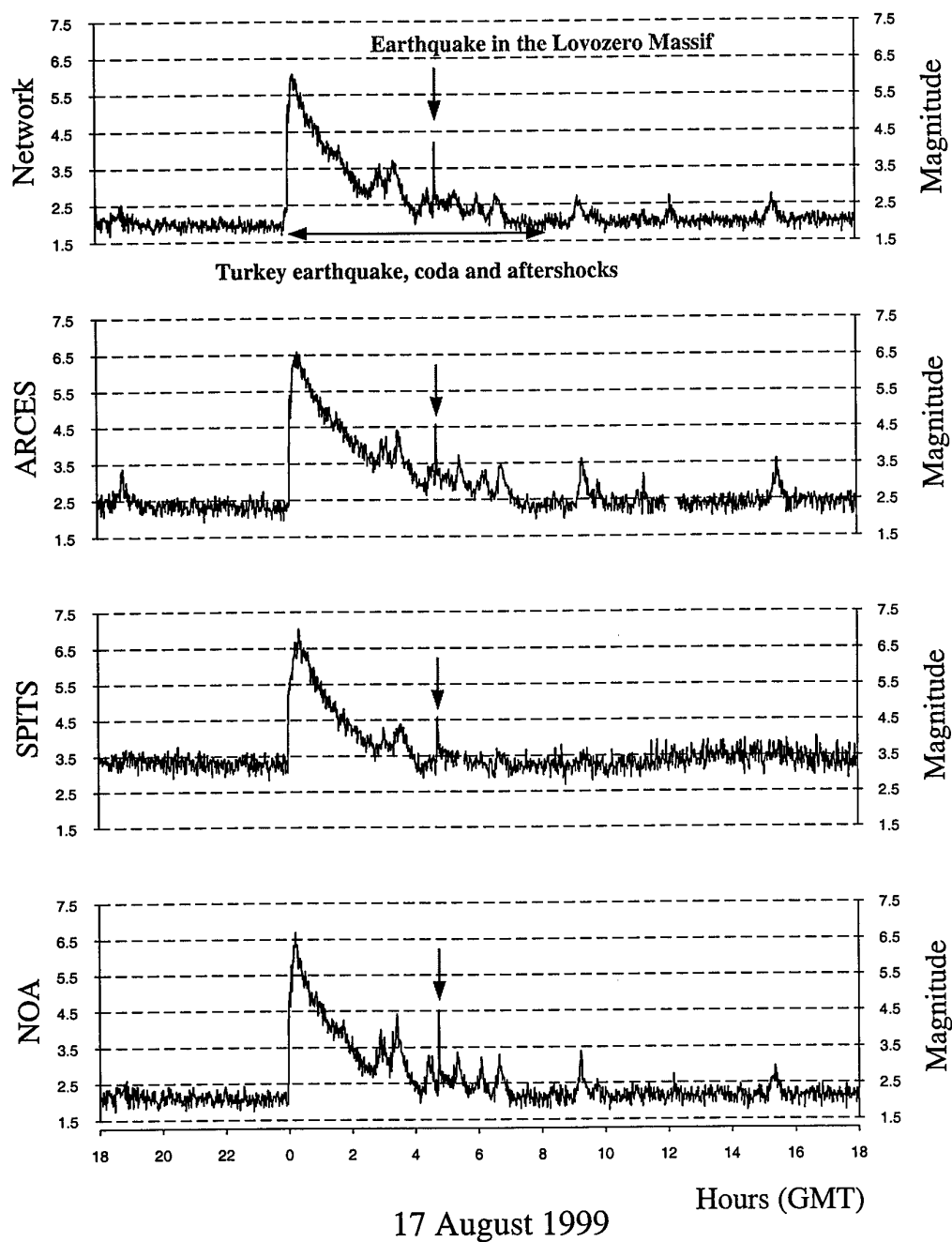
Fig. 6.2.9. Surface threshold monitoring for the location of the Lovozero event for 17 August 1999, using data filtered between 8 and 12 s. The lower three traces represent thresholds (upper 90% magnitude limits) obtained for each of the three stations, whereas the top trace shows the combined network thresholds. The peaks corresponding to the Lovozero event are indicated on each trace.
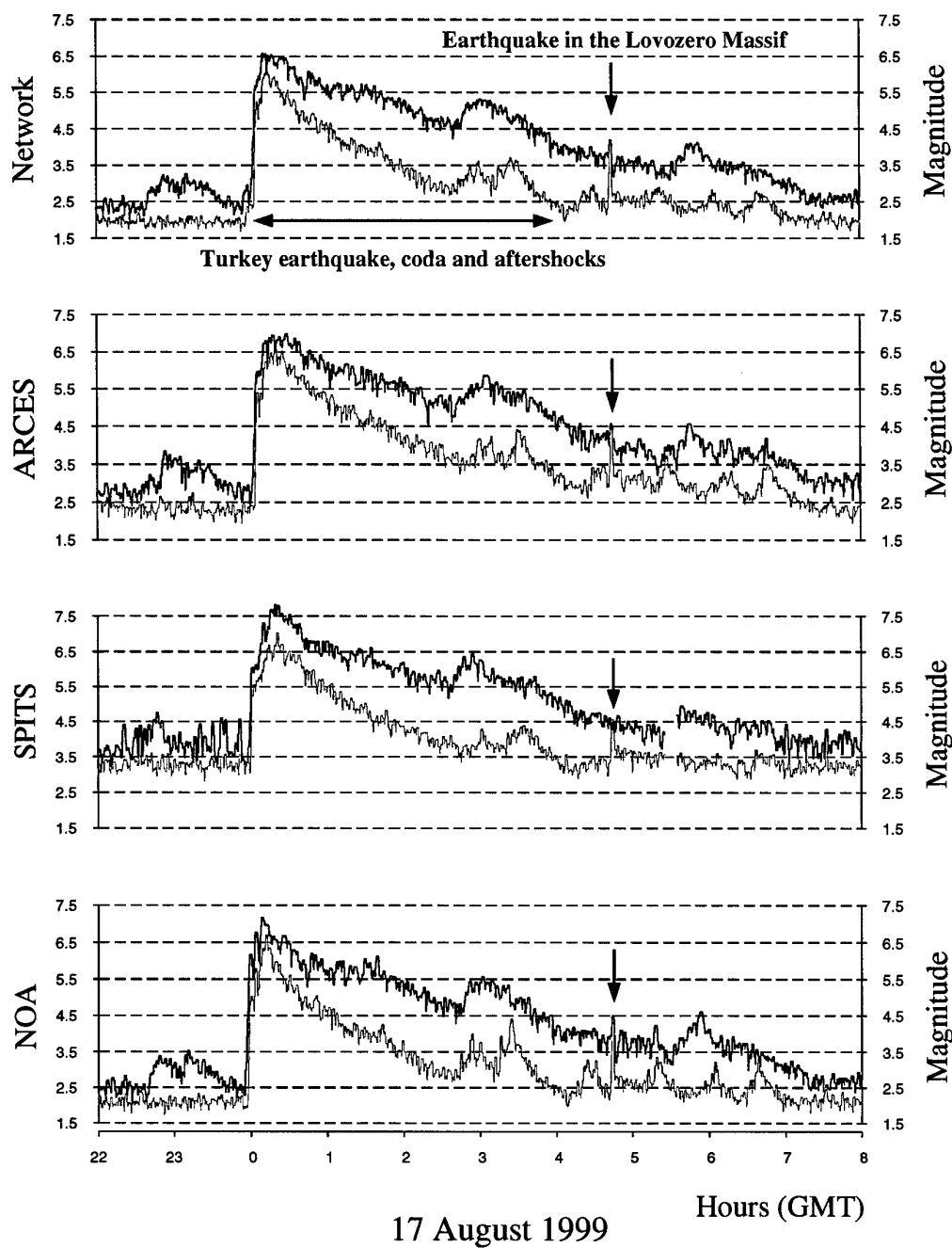
Fig. 6.2.10. Comparison between surface wave threshold monitoring using two different filter bands; red: 17 -24 s, green: 8-12 s. See captions of Figs. 6.2.8 and 9 for details.

6.3   Threshold Monitoring processing parameters for IMS stations BRAR and NVAR

Introduction

The processing parameters for all stations to be included in the IMS Threshold Monitoring System processing need to be tuned for reliable estimation of the detection capability. We will now report on the tuning of the IMS array stations BRAR and NVAR, and we follow the procedures described in the Threshold Monitoring Operations Manual (Taylor et. al., 1998).

Event Data Bases

For the tuning study we needed to find events with good SNR's, preferably occurring at various distances from the stations. This was done by searching the PIDC data base for good SNR events at various distances, and then requesting and receiving the data intervals using the Auto-DRM. In order to obtain information on the background noise field, the event data segments start one minute ahead of the P arrival, with a total length of two minutes. The lists of events for BRAR and NVAR are given in Table 6.3.1 and Table 6.3.2.

Table 6.3.1.   BRAR events used for TM tuning

STA	ORID	LAT	LON	DEPTH	UTM	MB	DELTA	PHASE	SNR	AZIMUTH	VEL
BRAR	20150736	40.8764	32.7625	0.0	1998-309:13.46.47.0	3.9	1.022	Pg	62.15	344.02	4.493
BRAR	20324105	38.4696	30.7440	22.5	1999-036:14.01.53.6	3.4	2.090	Pn	38.39	254.61	6.370
BRAR	20115701	39.9046	29.3379	0.0	1998-276:22.51.48.3	3.5	2.634	Pn	19.81	272.40	8.285
BRAR	19985229	36.5639	34.4738	0.0	1998-178:20.50.19.4	4.1	3.551	Pg	77.23	145.66	8.490
BRAR	20442069	36.3859	28.9362	50.2	1999-106:13.52.47.9	3.8	4.591	P	46.78	254.31	7.210
BRAR	20361880	37.2925	27.0861	0.0	1999-062:04.28.52.0	4.1	5.129	Pn	79.71	248.44	6.037
BRAR	20383875	37.3358	25.7638	0.0	1999-077:23.24.41.0	3.5	6.029	Pn	20.99	248.02	7.130
BRAR	20029578	35.1378	25.8938	55.6	1998-206:07.00.21.9	4.0	7.206	P	33.68	257.05	6.951
BRAR	20024862	34.5114	24.6733	0.0	1998-202:15.19.30.5	4.8	8.369	Pn	52.00	256.09	7.555
BRAR	20294097	41.1047	44.0036	0.0	1999-014:22.45.15.0	4.4	8.660	Pn	24.21	70.15	7.099
BRAR	20444408	36.1483	21.7937	21.3	1999-108:05.54.58.6	4.4	9.412	Pn	44.39	252.26	6.861
BRAR	20464018	44.2509	20.2049	0.0	1999-120:03.30.38.1	4.9	10.318	Pn	37.67	300.04	9.635
BRAR	20347857	43.2158	46.8683	65.8	1999-052:18.14.39.8	4.6	11.095	P	48.91	64.88	7.503
BRAR	20086480	39.9632	15.8369	0.0	1998-252:11.27.59.2	5.3	12.999	Pn	39.32	282.18	7.459
BRAR	19939287	31.6774	50.7966	0.0	1998-166:01.14.32.9	4.7	16.738	Pn	41.06	101.47	15.315
BRAR	20099400	31.0895	51.2981	0.0	1998-264:21.35.24.2	5.0	17.425	P	36.01	105.17	11.086
BRAR	20497730	29.5261	51.9812	37.0	1999-150:00.15.40.7	4.2	18.830	P	47.91	175.68	13.544
BRAR	20041925	37.3021	57.3062	0.0	1998-216:11.41.55.5	4.9	19.345	P	65.93	75.56	9.664
BRAR	20273106	27.8310	53.5947	0.0	1998-361:04.10.37.6	4.7	20.997	P	39.35	101.80	17.463
BRAR	20294086	28.9605	56.4352	27.6	1999-014:22.12.49.8	4.7	22.287	P	41.89	112.59	18.632
BRAR	20037412	27.7382	56.5350	11.6	1998-213:23.38.30.8	4.7	23.083	P	32.19	109.11	17.797
BRAR	19932006	28.1418	58.4602	92.0	1998-161:08.30.15.7	4.7	24.211	P	22.19	118.86	33.828
BRAR	1442288	26.4803	62.1511	44.5	1998-148:20.32.48.3	4.2	27.843	P	32.08	120.54	24.258
BRAR	1449288	37.1570	70.0682	0.0	1998-150:06.22.25.7	5.5	29.184	P	43.23	80.17	17.209
BRAR	20475724	13.1123	51.0996	20.4	1999-131:17.46.19.9	4.3	31.154	P	28.83	174.45	27.664
BRAR	20071443	39.7115	77.2874	0.0	1998-239:09.03.34.0	5.2	33.949	P	59.54	60.32	21.559

Table 6.3.1.   BRAR events used for TM tuning

STA	ORID	LAT	LON	DEPTH	UTM	MB	DELTA	PHASE	SNR	AZIMUTH	VEL
BRAR	20009735	47.6112	82.8839	0.0	1998-193:07.16.13.0	4.7	36.492	P	41.90	60.40	14.401
BRAR	20317144	41.6679	88.5307	24.2	1999-030:03.51.07.4	5.3	41.653	P	78.90	53.04	16.105
BRAR	20023426	30.0922	88.1782	15.5	1998-201:01.05.57.8	5.2	45.805	P	59.00	84.47	24.980
BRAR	20106764	27.6699	92.8437	18.5	1998-269:18.27.05.1	5.2	50.553	P	74.83	102.32	29.400
BRAR	20380814	.2875	-15.9980	0.0	1999-075:14.42.57.6	4.6	59.293	P	26.64	253.64	8.570
BRAR	20045432	7.3823	94.2112	23.7	1998-222:09.52.15.3	5.0	63.489	P	32.00	163.07	68.393
BRAR	20450290	-27.9021	26.6636	0.0	1999-112:22.19.38.1	5.3	67.646	P	97.50	217.30	19.799
BRAR	20020736	23.3870	120.7023	0.0	1998-198:04.51.14.0	5.2	73.899	P	88.56	63.37	33.831
BRAR	20260473	31.3683	131.3748	10.7	1998-350:00.18.42.2	5.0	76.585	P	55.90	53.43	29.598
BRAR	20127734	39.9974	143.3506	0.0	1998-286:20.41.10.1	4.7	78.423	P	57.47	24.94	29.781
BRAR	20392812	33.2443	141.4208	41.2	1999-082:04.23.36.5	4.5	81.844	P	30.92	58.95	25.541
BRAR	20072966	-.0124	125.1436	28.2	1998-240:12.40.55.9	6.0	91.842	P	64.63	74.66	35.691
BRAR	20075387	17.1042	148.1133	58.0	1998-242:01.48.13.2	5.7	97.391	P	44.57	48.70	30.704
BRAR	20289367	-5.3842	151.6759	24.9	1999-012:08.49.20.4	5.0	115.473	PKP	25.00	322.08	55.075
BRAR	20094396	-5.4521	151.6698	12.0	1998-258:08.35.44.0	5.2	115.513	PKP	21.31	37.89	45.611
BRAR	20082094	-29.4519	-71.5874	40.2	1998-246:17.38.01.9	5.8	118.596	PKP	56.62	267.35	20.377
BRAR	20232267	-7.8946	158.7221	41.2	1998-329:18.05.26.6	5.5	122.339	PKP	19.58	9.32	58.934
BRAR	20099497	-13.6857	166.6767	30.3	1998-264:12.09.41.4	5.8	131.992	PKP	35.47	42.53	34.298
BRAR	20029484	-13.7545	166.8566	43.2	1998-206:02.39.25.8	5.5	132.168	PKP	59.25	346.24	70.076
BRAR	20298247	-14.9618	-173.5653	0.0	1999-020:06.02.18.2	4.5	146.163	PKPbc	36.68	332.71	48.155
BRAR	20058843	-34.8503	-108.7204	0.0	1998-230:23.07.22.2	4.8	149.142	PKPbc	64.01	276.80	18.011
BRAR	20307295	-20.9029	-174.4590	0.0	1999-026:07.04.18.3	4.9	150.048	PKPbc	75.01	333.56	71.908

Table 6.3.2.   NVAR events used for TM tuning

STA	ORID	LAT	LON	DEPTH	UTM	MB	DELTA	PHASE	SNR	AZIMUTH	VEL
NVAR	20437988	36.6291	-120.7043	0.0	1999-105:03.20.34.0	3.5	2.621	Pn	16.37	105.22	4.627
NVAR	20413291	32.7819	-116.3265	0.0	1999-097:06.26.40.6	3.5	5.861	Pg	29.72	158.25	4.871
NVAR	20359687	40.8626	-126.0324	0.0	1999-059:15.33.36.9	3.8	6.440	Pn	26.11	280.87	5.836
NVAR	20499341	41.9474	-127.0332	19.3	1999-152:08.28.05.2	4.1	7.549	Pn	31.79	281.87	6.131
NVAR	20492320	43.5800	-127.3808	0.0	1999-145:23.39.47.7	4.1	8.575	Pn	25.11	301.88	7.830
NVAR	20474682	49.5528	-125.6061	32.8	1999-128:14.25.37.8	3.4	12.292	Pn	19.42	340.80	7.705
NVAR	20378288	24.9277	-108.8827	0.0	1999-072:09.11.44.3	4.1	15.654	Pn	50.85	149.49	7.607
NVAR	20413249	24.1840	-108.4301	0.0	1999-097:05.04.02.8	3.6	16.501	Pn	21.99	323.63	4.372
NVAR	20380739	22.6290	-107.2947	54.8	1999-075:06.14.16.7	3.7	18.359	P	51.37	153.63	7.000
NVAR	20491505	19.9238	-109.2556	16.4	1999-142:02.39.27.9	3.9	20.040	P	19.14	155.98	7.398
NVAR	20407926	19.4646	-101.2925	214.5	1999-092:13.05.44.1	3.2	23.982	P	15.44	145.91	8.587
NVAR	20451887	17.3752	-100.3793	45.6	1999-115:03.08.57.8	3.7	26.191	P	43.33	145.93	8.860
NVAR	20380697	16.2277	-100.0657	0.0	1999-074:17.05.12.3	3.9	27.313	P	17.86	142.80	9.142
NVAR	20404485	15.8712	-97.2961	19.2	1999-091:23.25.17.8	4.2	29.093	P	24.01	143.20	8.376
NVAR	20466045	60.5282	-153.1291	248.5	1999-122:21.53.00.6	3.1	31.037	P	30.90	151.24	6.768
NVAR	20483555	64.6161	-157.7441	0.0	1999-137:17.32.14.1	4.2	34.917	P	31.72	330.10	12.358
NVAR	20441919	11.4904	-86.0022	0.0	1999-106:16.03.17.1	4.4	39.355	P	17.78	146.86	13.974
NVAR	20400385	51.7195	-177.3390	67.6	1999-087:22.23.41.6	4.1	42.607	P	16.11	280.82	8.594
NVAR	20500785	7.0284	-82.2529	0.0	1999-154:14.17.33.3	4.6	45.128	P	53.43	124.84	12.197
NVAR	20349721	53.7654	171.1972	24.3	1999-054:12.23.45.8	4.3	49.175	P	18.47	303.18	14.956
NVAR	20345538	14.9705	-60.5649	0.0	1999-050:11.57.47.9	4.2	55.662	P	29.66	105.72	15.260

Table 6.3.2.   NVAR events used for TM tuning

STA	ORID	LAT	LON	DEPTH	UTM	MB	DELTA	PHASE	SNR	AZIMUTH	VEL
NVAR	20412001	24.4444	-46.3154	0.0	1999-096:04.51.05.4	5.0	61.572	P	21.00	83.41	14.575
NVAR	20393571	45.4446	149.9837	0.0	1999-080:13.32.29.6	4.4	64.970	P	19.73	285.77	9.668
NVAR	20444407	39.9178	145.3659	32.1	1999-108:20.41.16.4	4.0	70.790	P	23.51	278.19	9.450
NVAR	20361224	35.6290	141.7378	0.0	1999-061:07.12.17.6	4.7	75.621	P	30.76	283.12	19.221
NVAR	20350071	-21.3870	-173.7238	0.0	1999-054:18.56.50.4	4.8	78.988	P	68.10	212.54	13.781
NVAR	20367904	-34.5330	-69.3680	0.0	1999-064:03.35.14.5	4.9	85.604	P	21.27	164.69	16.450
NVAR	20408199	-19.2563	166.7876	0.0	1999-092:19.56.18.7	4.8	90.558	P	29.29	239.53	27.041
NVAR	20450367	-6.1334	150.8353	0.0	1999-113:09.58.02.6	4.8	94.441	P	38.38	245.01	21.372
NVAR	20413385	-6.5398	147.1112	0.0	1999-096:08.22.11.1	5.6	97.609	P	18.68	246.87	22.783
NVAR	20492167	12.8058	124.8997	44.0	1999-145:03.38.58.6	4.9	102.067	P	16.07	283.10	24.352
NVAR	20380686	2.6283	125.8539	86.1	1999-075:03.32.14.8	5.2	108.289	PKKP	22.70	122.42	15.237
NVAR	20382093	.0094	124.3615	57.8	1999-077:01.58.59.8	5.2	111.134	PKiKP	20.98	239.12	26.467
NVAR	20349505	-9.0232	112.5775	0.0	1999-054:05.45.58.2	4.9	125.868	PKP	16.34	276.90	34.571
NVAR	20368010	-5.8123	107.5961	326.0	1999-066:01.32.28.8	4.5	127.306	PKP	24.25	238.12	115.169
NVAR	20401468	-4.0128	87.1478	0.0	1999-088:06.17.58.3	5.3	138.633	PKhKP	15.01	281.21	17.318
NVAR	20500792	-8.5092	38.8420	0.0	1999-154:11.09.42.0	4.1	143.791	PKP	19.43	82.00	23.156
NVAR	20483009	-52.1677	20.3014	0.0	1999-137:00.30.33.1	4.3	148.270	PKPbc	16.53	124.22	23.300
NVAR	20450290	-27.9021	26.6636	0.0	1999-112:22.19.38.1	5.3	149.017	PKP	92.39	129.16	23.825
NVAR	20468597	-11.2676	66.1475	0.0	1999-126:06.54.45.8	4.6	152.660	PKPbc	35.62	266.08	17.035
NVAR	20417069	-41.9041	84.3861	0.0	1999-099:08.16.34.6	5.1	162.324	PKP	17.10	216.06	39.009

Signal-to-noise ratio vs. distance

We would like the TM procedure for estimating the network detection capability to resemble the IDC procedure for estimating m_b. At the IDC, a third order Butterworth filter with a pass-band between 0.8 and 4.5 Hz is applied to the data prior to the estimation of signal amplitude and period. The same prefilter should ideally be applied prior to the generation of the STA envelopes, but we also have to take into consideration the frequency band where we expect the highest SNR.

In Figures 6.3.1 and 6.3.2 we have plotted the average log(STA) for all noise segments preceding the P-phases versus frequency to see if there are noise peaks that should be avoided. It is apparent that for both stations there are increased noise levels above 2.0 Hz. To find the frequency range in which we expect the highest SNR, we have plotted the SNR (STA/LTA) measured in narrow frequency bands vs. the distance to the events in Figures 6.3.3 and 6.3.4. For each event we have normalized the maximum SNR to 50 dB. For both BRAR and NVAR we find the maximum SNR below 3.0 Hz at all distances. For the close distance range, good SNR is found up to 5 Hz.
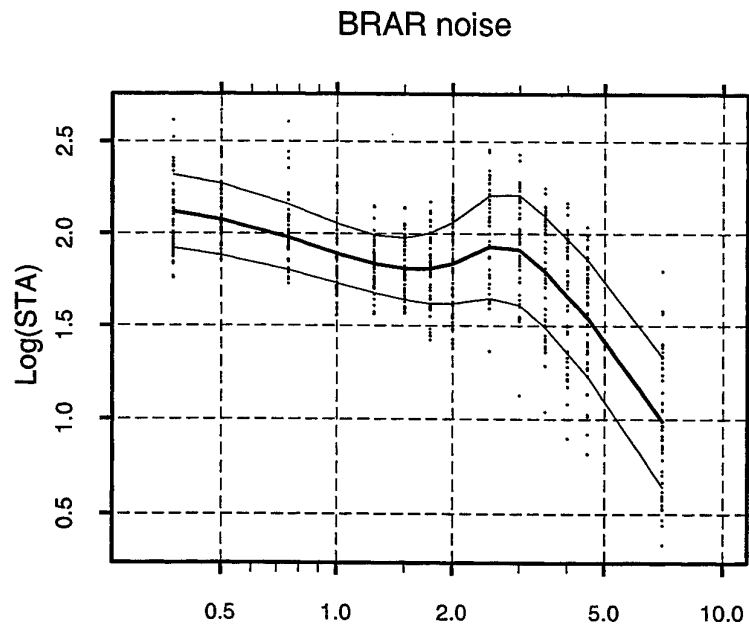
BRAR noise

Fig. 6.3.1. Average narrowband log(STA) of the BRAR noise segments plotted versus frequency. Lines ±1σ around the mean are also shown.

NVAR noise

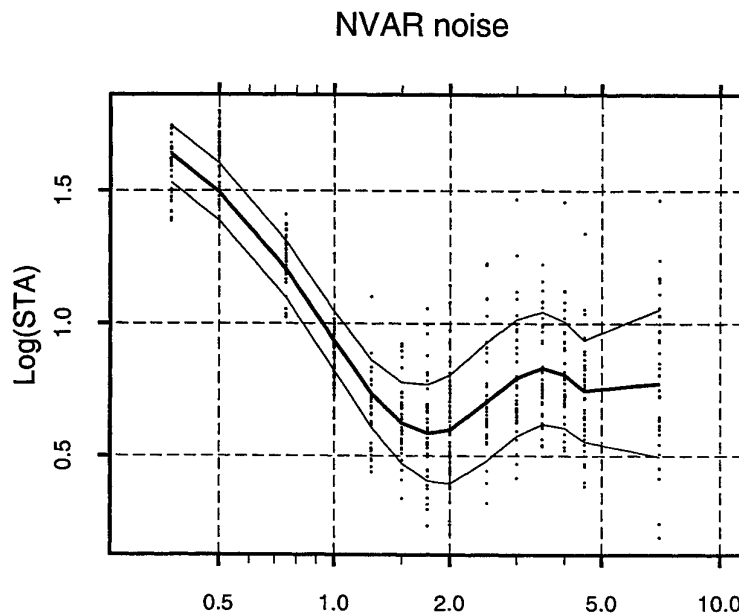*Fig. 6.3.2*. Average narrowband log(STA) of the NVAR noise segments plotted versus frequency. Lines ±1σ around the mean are also shown.
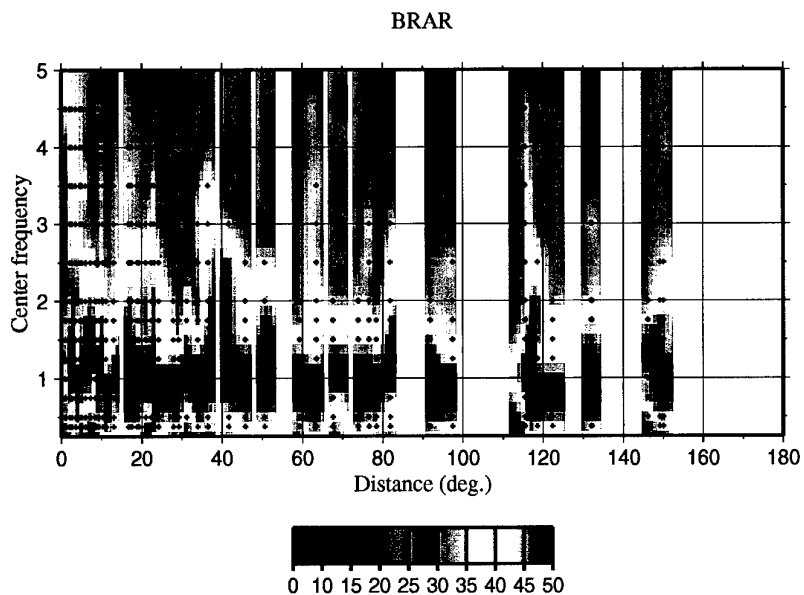
BRAR

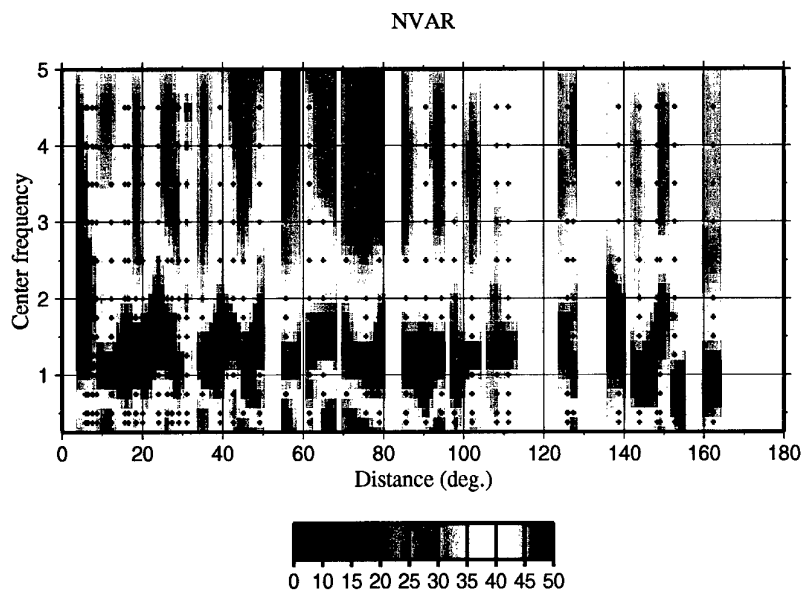*Fig. 6.3.3. SNR (STA/LTA) of BRAR events versus distance for events recorded at BRAR. The maximum SNR is normalized to 50 dB.*

NVAR

Fig. 6.3.4. SNR (STA/LTA) of NVR events versus distance for events recorded at NVAR. The maximum SNR is normalized to 50 dB.

Prefiltering

When choosing the prefilter cutoffs from the tuning events, we try to balance low amplitudes during noise conditions with a good recovery of the signal amplitudes. The frequencies may be different from those used for routine magnitude estimation.

To be able to relate the log(STA) estimates used by the TM system to the log(A/T) estimates used for magnitude estimation at the IDC, we manually measure log(A/T) of the tuning events. A/T is measured on beams steered with the azimuths and slownesses of the P-phases, and filtered between 0.8 and 4.5 Hz. The A/T measurements are made on the maximum amplitude occurring within 8 seconds of the first arrival.

Based on the average noise characteristics (see Figures 6.3.1 and 6.3.2) and the frequency range with the highest SNR (see Figures 6.3.3 and 6.3.4), we will test a series of filters for subsequent use in the TM system. For both BRAR and NVAR, the frequency ranges with maximum SNR show no significant distance dependent trend, and we therefore propose to use the same prefilter for all distances.

For BRAR and NVAR events we show in Figures 6.3.5 and 6.3.6 results from comparing the reference measurements in the 0.8-4.5 Hz filter band with the $\log((\pi/2) \cdot STA \cdot calib)$ measurements in three different filter bands (several other filters have also been tested). This average difference is later referred to as ATcomp. Mean (ATcomp) and Median give the average difference for the events. St.dev. gives the standard deviation of the differences and Noise gives the average STA level of the preceding noise.

For both stations we see that for STAs measured in the 0.8-4.5 Hz filter band (lower panel) there is, as expected, a very good correspondence with the reference A/T values. The mean difference for BRAR is only -0.01 m_b units with a standard deviation of 0.06 and an average noise value of -0.06 (m_b units). For NVAR the mean difference is -0.06 units with a standard deviation of 0.15 and an average noise value of -0.67 (m_b units).

When deciding which prefilter to use, we find that a 0.8-3.0 Hz filter band best combines low amplitudes during noise conditions with a good and stable recovery of the signal amplitudes for both stations. When processing BRAR and NVAR data in this frequency band we should subtract 0.01 m_b units for BRAR and 0.06 m_b units for NVAR (ATcomp) from the estimates to make them compatible with the magnitude estimation procedure at the IDC.
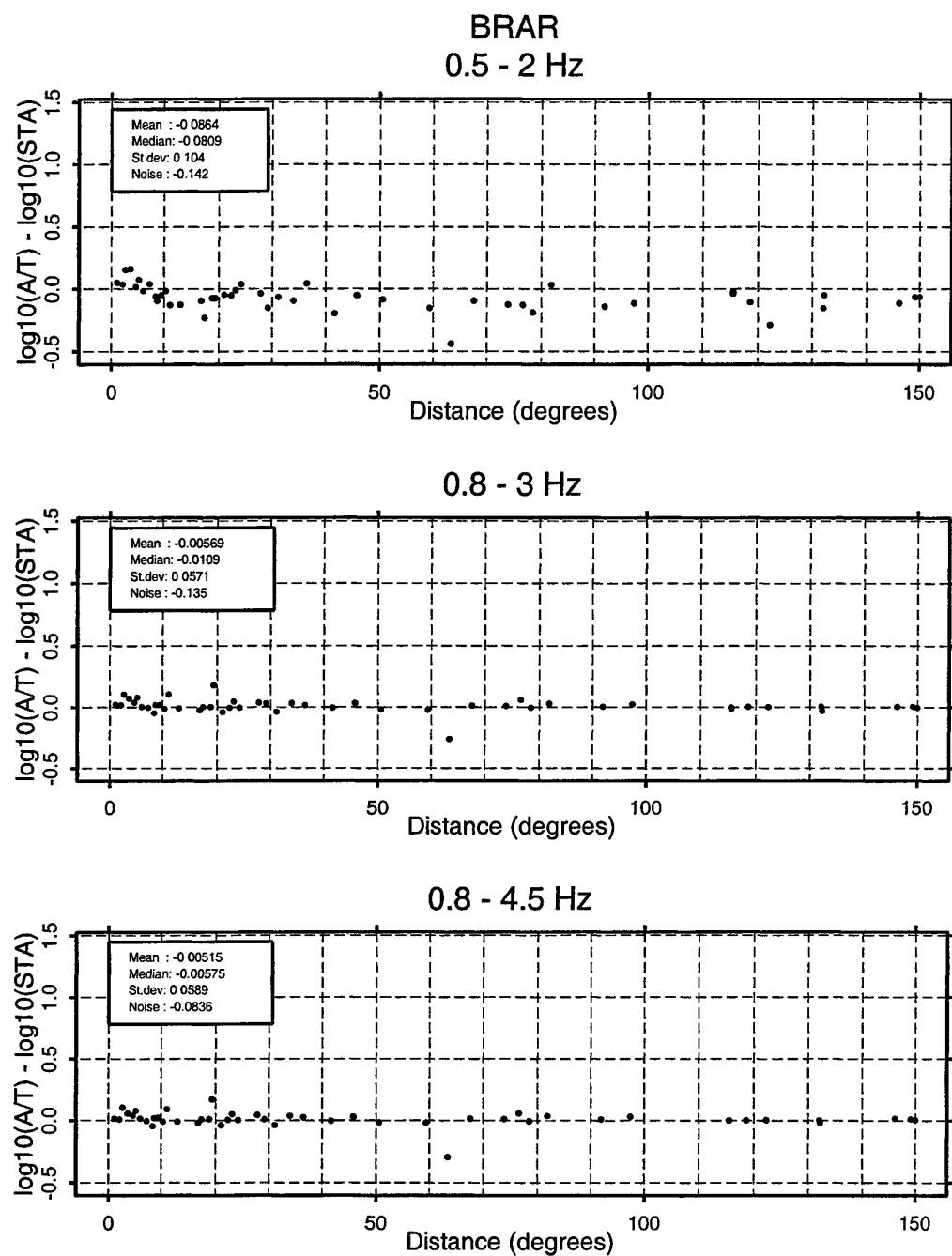
BRAR
0.5 - 2 Hz

Mean : -0 0864
Median: -0 0809
St dev: 0 104
Noise : -0.142

0.8 - 3 Hz

Mean : -0.00569
Median: -0.0109
St.dev: 0 0571
Noise : -0.135

0.8 - 4.5 Hz

Mean : -0 00515
Median: -0.00575
St.dev: 0 0589
Noise : -0.0836

Fig. 6.3.5. *Panels showing the differences between the reference* $\log(A/T)$ *measurements (0.8-4.5 Hz) and* $\log((\pi/2) \cdot STA \times calib)$ *measured in three different filter bands. All tuning events at BRAR have been considered. The mean and median differences and standard deviations are shown for the events along with the average STA level of the preceding noise.*
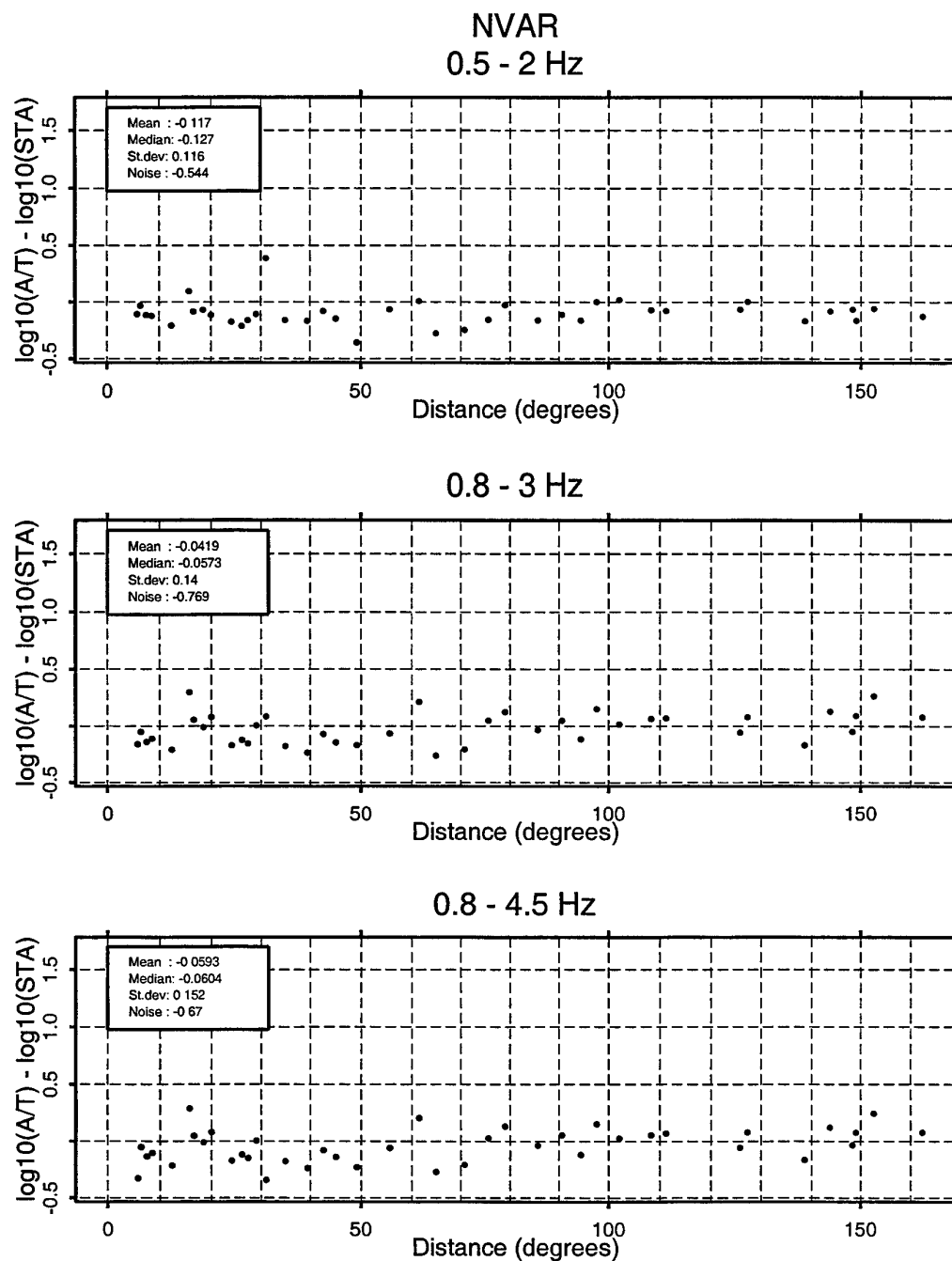
NVAR
0.5 - 2 Hz

Mean : -0.117
Median: -0.127
St.dev: 0.116
Noise : -0.544

0.8 - 3 Hz

Mean : -0.0419
Median: -0.0573
St.dev: 0.14
Noise : -0.769

0.8 - 4.5 Hz

Mean : -0.0593
Median: -0.0604
St.dev: 0.152
Noise : -0.67

Fig. 6.3.6. *Panels showing the differences between the reference* $\log(A/T)$ *measurements (0.8-4.5 Hz) and* $\log((\pi/2) \cdot STA \times calib)$ *measured in three different filter bands. All tuning events at NVAR have been considered. The mean and median differences and standard deviations are shown for the events along with the average STA level of the preceding noise.*

Signal Loss and Mis-steering

As outlined in the Threshold Monitoring Operations Manual (Taylor et. al., 1998), we need to have available estimates of the expected beamforming signal loss as a function of the mis-steering of the beams for each array. This is done by measuring the signal loss as a function of the mis-steering of the filtered beams, according to the relation:

sloss=(beam STA)/(Average STA of individual sensors)

where STA is taken to be the maximum within 8 seconds of the first arrival.

In Figure 6.3.7 we show the signal loss as a function of mis-steering for all BRAR events. As discussed in the preceding section, the prefilter passband 0.8-3.0 Hz was applied to the data. We see from the figure that the average signal loss for correct beam steering is 0.43 dB, and that additional 3 dB signal loss is expected to be found at a mis-steering of 0.148 s/km.
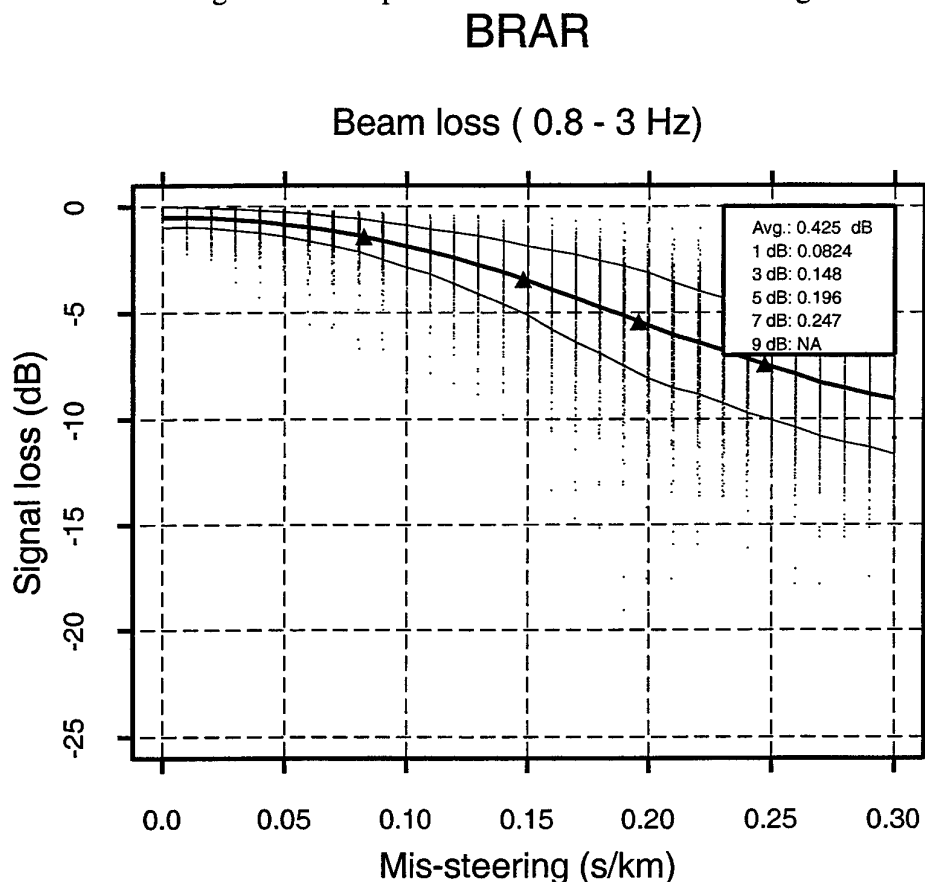
BRAR

Beam loss (0.8 - 3 Hz)

Avg.: 0.425 dB
1 dB: 0.0824
3 dB: 0.148
5 dB: 0.196
7 dB: 0.247
9 dB: NA

Fig. 6.3.7. *Signal loss for BRAR events prefiltered in the passband 0.8-3.0 Hz. The three lines show the average and the 1 σ levels of the signal loss. For no mis-steering the average signal loss is 0.43 dB. An additional 3 dB signal loss is expected at a mis-steering of 0.148 s/km.*

In Figure 6.3.8 we show the signal loss as a function of mis-steering for all NVAR events, again for beams filtered in the passband 0.8-3.0 Hz. The average signal loss for correct beam steering

is 1.05 dB, and that additional 3 dB signal loss is expected to be found at a mis-steering of 0.086 s/km.

NVAR

Beam loss (0.8 - 3 Hz)
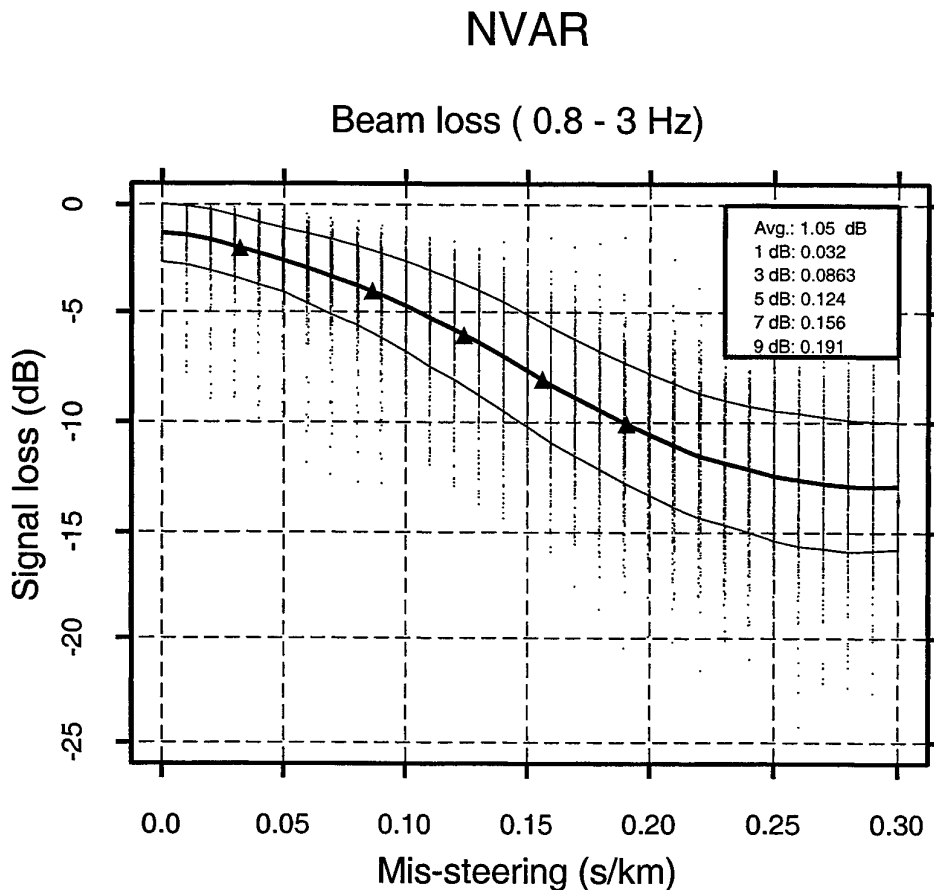
Fig. 6.3.8. *Signal loss for NVAR events prefiltered in the passband 0.8-3.0 Hz. The three lines show the average and the 1 σ levels of the signal loss. For no mis-steering the average signal loss is 1.05 dB. An additional 3 dB signal loss is expected at a mis-steering of 0.086 s/km.*

Beam Deployment

According to the IASP91 travel-time tables, the P phases used for estimation of network detection thresholds span the slowness range 0.0-0.124 s/km. According to Figure 6.3.7, the BRAR beams in this distance range have an expected 3 dB signal loss at a mis-steering of 0.148 s/km, such that only **one** beam with zero slowness is sufficient for covering the slowness area of interest (i.e., 0.0-0.124 s/km). The BRAR array has currently only six elements covering an aperture of about 2 km. Because of the relatively few sensors involved, beamforming require little computer resources. We have therefore decided to add four additional beams to the one required for complete coverage. In this way, signal loss due to mis-steering of the beams should be within 1 dB. The steering parameters of the BRAR beams are given in Table 6.3.5.

For NVAR beams we expect the 3 dB signal loss at a mis-steering of 0.086 s/km (see Figure 6.3.8). The procedure for deploying the beams is illustrated in Figure 6.3.9, where the dashed circles with radii of 0.086 s/km (3 dB level) are fitted within the slowness range 0.0-0.124 s/km. The center points of the small circles correspond to the steering parameters of the beams.
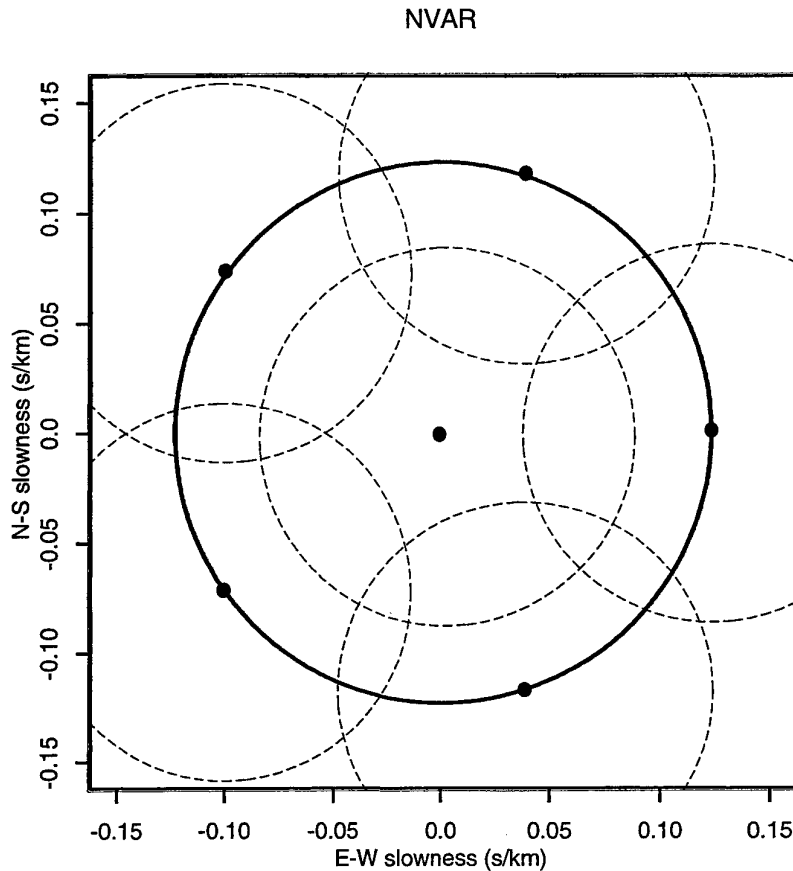
NVAR

Fig. 6.3.9. *NVAR beam deployment used in the TM system for assessing the detection capability in the distance range 0-180 degrees. The area within the large circle corresponds to the expected slowness range of P-phases from surface events in this distance range. In order to ensure complete coverage within the 3 dB level, it was necessary to deploy 6 beams, represented by the centers of the dashed circles. The radius of each small circle is 0.086 s/km, corresponding to the expected mis-steering associated with the 3 dB signal loss.*

Details on the tuned processing parameters for BRAR and NVAR are given in Tables 6.3.3-6.3.5 below.

Table 6.3.3: Definitions of Array Configurations

Array	Configuration	sta_chan
BRAR	vertical	BR01_sz BR02_sz BR03_sz BR04_sz BR05_sz BR06_sz
NVAR	vertical	NV01_sz NV02_sz NV03_sz NV04_sz NV05_sz NV06_sz NV07_sz NV08_sz NV09_sz NV10_sz

Table 6.3.4: TM Tuning Parameters

Array	Distance interval (deg)	Config.	Frequency band (Hz)	A/T correction (m_b units)	Signal loss (dB)	3 dB level (s/km)	Number of beams
BRAR	0-180	vertical	0.8 - 3.0	−0.011±0.057	0.425	0.148	5
NVAR	0-180	vertical	0.8 - 3.0	−0.057±0.140	1.050	0.086	6

Table 6.3.5: Beam Steering Parameters

Array	Distance interval (deg)	Azimuth (deg) and slowness (s/km) of beams					
BRAR	0-180	0.0, 0.0	0.0, 0.123	90.0, 0.123	180.0, 0.123	270.0, 0.123	
NVAR	0-180	0.0, 0.0	0.0, 0.123	72.0, 0.123	144.0, 0.123	216.0, 0.123	288.0, 0.123

References

Taylor, L., T. Kværna, and F. Ringdal (1998). Threshold Monitoring Operations Manual. NORSAR Contribution No. 639.

T. Kværna
L. Taylor

6.4   The MASI-1999 field experiment

Introduction

In northern Norway, the seismicity is relatively low (e.g. Bungum et al. (1991)). However, the Stuoragurra fault near Masi in Finnmark came in focus, after Olesen (1988) discovered that this fault shows a vertical offset of at least 8 m since the glaciation of the last ice age. Some of the open questions in connection with this fault are: How active is this fault today? Can the recent seismicity be connected to the observed faultgauge and are observed source mechanisms compatible with the orientation of the fault? How deeply can this fault be traced into the crust?

To investigate these questions, NORSAR was interested in installing a temporary network of seismic stations in Finnmark. NORSAR got the information that the University of Potsdam, Germany, owns a set of 13 mobile seismic stations, which were available for such an experiment during the summer of 1999. Therefore, NORSAR planned the field experiment MASI-1999 as a cooperative effort between the two institutions.

Because the ARCES array is also located in Finnmark, all investigations of the structure of this area are in also part of the needed calibration of this primary station of the IMS network. Study the wave field from local and regional events using many stations distributed over the whole area, will give a better understanding of the observations of local and regional phases at the ARCES array.

Some time ago, Frank Krüger from the Institute of Geoscience at the University in Potsdam, Germany, was involved in a study about possible source locations of microseisms. He found in the data of the Gräfenberg array in southern Germany indications that one source of microseisms is most likely located north of Scandinavia in the Norwegian and / or Barents Sea (Krüger, 1998). To get a better location for the source region where these microseisms are generated, it is interesting to observe the microseisms in the vicinity of the assumed source region.

So, different interests for installing a temporary seismic network in Finnmark came together, and the project MASI-1999 was carried out.

The field experiment and the data base

In the time period 18 - 27 May 1999, 13 Lennartz MARSlite data loggers equipped with three-component LE-3D/5s seismometers were installed. These instruments have an eigenperiod of 5 seconds. The coordinates of the seismometer sites are given in Table 6.4.1 and Fig. 6.4.1 shows a corresponding map of the Finnmark area. The poles and zeroes of the transfer function are given in Table 6.4.2. During the installation phase, one station was running in parallel at the ARCES array site ARA0 to check the compatibility of data from the mobile stations and the ARCES array. At all sites, continuous data were recorded and written on hard disks. With the chosen sampling rate of 125 samples per second, these hard disks were filled up after about 2 months. Therefore, two disk-change and maintenance trips were necessary during the deployment time of the mobile stations. In the middle of August, during the last disk-change trip, the station MA05 was moved to the ARCES array site ARA0, to have a continuous data stream available also during the ARCES refurbishment and upgrading in September 1999. The field experiment was finished during the last days of September, when all stations were dismantled and sent back to Germany. The last available data records from the mobile stations were from 1

October 1999. The performance of the 13 stations was quite good, only 3 stations had outages (see Table 6.4.1) due to technical problems.

All data from the mobile stations were stored continuously on recordable CDs together with all available data from the permanent stations in and around Finnmark: ARCES, KEV, KTK, and TRO (see Fig. 6.4.1). The data from the Kevo station (KEV) are, except for some minor outages, continuously available. We included in our data base the output of the broad-band 80 Hz sampled Guralp CMG-3T instrument at KEV. The short period data from the stations Kautokeino (KTK) and Tromsø (TRO) are unfortunately triggered data, so that these stations contribute little to the data base. All data from the ARCES array (i.e. all short period array channels and the channels from the ARCES broad-band site ARE0) were copied into the data base. However, due to the ARCES upgrading work, the ARCES array was out of operation for about 3 weeks. The data from both the mobile MASRlite stations and the other stations were reformatted into a common GSE2.0 format (double differences, 6 bit compression).

The whole data base is copied to CDs, to have all data easily available by direct access. One CD usually contains the data for a half day. In addition, all available bulletins were copied to the CDs, i.e. the automatically produced listings of NORSAR's data processing for ARCES and Apatity (detection lists, fk-lists, the single array location bulletins, and the GBF bulletins), the preliminary Scandinavian bulletin produced at the University of Helsinki, and the pIDC-produced REBs. Because the experiment ended only a few weeks ago, the production of these CDs at NORSAR has just been completed. For backup, the contents of all CDs were copied in addition onto EXA-BYTE tapes. As soon as possible, the data base will be copied to a second set of CDs at the University in Potsdam such that both partners can work with the data in their research programs.

Data examples

Although the field experiment and the production process of the recordable CDs ended very recently, some preliminary data examples of this campaign can be shown. Because one main topic of this experiment was the detection of neotectonic movements in northern Scandinavia, a first screening of the data concentrates on local and regional events which cannot be associated to known sources of man-made seismic sources like the northern Swedish iron mines or the mines and quarries on the Kola peninsula, Russia.

Unfortunately, a felt earthquake in the north-east of the Stuoragurra fault system (30 March 1999) occurred just before the mobile stations were installed, and the largest earthquake in recent years offshore of Tromsø (17 October 1999) occurred two weeks after demobilization of the stations. Although we missed these two very interesting events, we recorded some local seismicity. Up to now, the data until the end of June 1999 have been preliminarily searched. During this time at least two smaller, non felt events could be found and located. One on the Stuoragurra fault and one at the end of the Porsanger Fjord, in addition, on 22 August 1999, a M_L 2.6 (GBF) event occurred near Masi on the Stuoragurra fault, which was large enough to be felt by local people.

Fig. 6.4.2 shows vertical-component seismograms of the small event at the end of the Porsanger Fjord on 24 May 1999. All seismograms shown were recorded in 1° to 2° epicentral distance range. This event with $M_L = 1.9$ (GBF) was not observable at all stations and shows a relatively low SNR. However, with the MASI-1999 stations the epicenter could be well located

(see Table 6.4.3). For estimating the depth of this event, which presumably occurred close to the Earth's surface, a better S velocity model of the region is needed.

Fig. 6.4.3 shows a map with unfiltered records at all temporary seismic stations (vertical components) of the felt event from 22 August 1999 south of Masi on the Stuoragurra fault. Fig. 6.4.4 shows the same records as single seismograms, and Fig. 6.4.5 shows the same data high-pass filtered above 40 Hz. Note the low attenuation for the high frequently energy in this region. A preliminary location of the event is listed in Table 6.4.3.

On 17 August 1999 a mining induced event occurred near Lovozero on the Kola peninsula. The event was the strongest earthquake observed during the last years in this area and was well recorded with the MASI-1999 stations. Fig. 6.4.6 shows the raw data and Fig. 6.4.7 the broad-band filtered (8 - 20 s) data, where a dominant Rayleigh wave is visible. Using these Rayleigh observations, one can get a surface wave magnitude estimate of $M_s = 4.3$. The traditional IASPEI formula was applied by measuring amplitudes at shorter dominant periods for the 2° to 5° distance range (e.g. see Willmore, 1979). The measured magnitude is consistent with Kværna et al. (1999), who used NOA and ESDC broad-band data to derive $M_S = 4.2$.

The main set of observed events is related to mining explosions in the Nikel area, Russia and to the Kiruna area of Sweden. Fig. 6.4.8 shows the bandpass filtered (6 - 10 Hz) vertical-component traces of an explosion in the Nikel area.

Further Work

The examples shown indicate that the records of the MASI-1999 experiment are usable to address different scientific issues:

* neotectonic movements on the Stuoragurra fault in Finnmark.

* fault plane solutions for the best observed events in this area.

* better travel-time tables for local/regional P- and S-phases.

* Moho depth measurements in this region with receiver function studies.

* local/regional amplitude attenuation curves by observing the same event at different distances.

* an improved S-phase understanding in northern Scandinavia by analyzing the 3C data.

* crustal structure by inversion of local/regional surface waves.

* source studies of the ocean generated microseisms.

* relative location of seismic events in the different mining areas.

J. Schweitzer

References

Bungum, H., A. Alsaker, L. B. Kvamme, & R. A. Hansen (1991). Seismicity and seismotectonic of Norway and nearby continental shelf areas. *J. Geophys. Res.* **96**, 2249 - 2265.

Friedrich, A., F. Krüger, & K. Klinge (1998). Ocean-generated microseismic noise located with the Gräfenberg array. *J. of Seismology* **2**, 47 - 64.

Kværna, T., L. Taylor, J. Schweitzer & F. Ringdal (1999). Continious assesment of upper limit M_S. *Semiannual Technical Report 1 April - 30 September 1999.* NORSAR Sci. Report 1-1999/2000, Keller, Norway.

Olesen, O. (1988). The Stuoragurra fault, evidence of neotectonics in the Precambrian of Finnmark, northern Norway. *Norsk Geologisk Tidsskrift* **68**, 107 - 118.

Willmore, P. L., editor (1979). Manual of seismological observatory practice. World Data Center A for Solid Earth Geophysics, Report SE-20, reprinted 1982, 165 pp.

Sta-tion	lat [°]	lon [°]	elev. [m]	start time	end time	outages
MA00	69.5346	25.5056	403	18-05-1999 18:16:40	01-10-1999 14:34:59	24-05-1999 13:26:53 - 17-08-1999 10:16:34
MA01	69.3752	24.2122	315	18-05-1999 14:29:01	30-09-1999 11:00:00	-
MA02	69.1875	25.7033	160	19-05-1999 10:19:30	29-09-1999 13:40:38	01-07-1999 21:42:56 - 15-08-1999 17:54:11
MA03	70.0210	27.3962	95	19-05-1999 16:00:59	01-10-1999 09:26:09	-
MA04	69.7127	29.5059	20	19-05-1999 20:41:22	01-10-1999 06:01:02	-
MA05	69.4533	30.0391	30	20-05-1999 09:27:04	16-08-1999 13:05:41	-
MA06	70.4813	25.0610	50	21-05-1999 09:43:37	28-09-1999 12:07:39	-
MA07	69.7050	23.8203	265	21-05-1999 15:44:24	29-09-1999 07:30:27	-
MA08	70.1278	23.3736	15	22-05-1999 09:01:06	29-09-1999 09:38:23	31-07-1999 15:57:28 - 07-08-1999 10:40:41
MA09	69.4566	21.5334	90	22-05-1999 16:01:08	27-09-1999 13:00:00	-
MA10	69.5875	23.5274	375	23-05-1999 16:26:27	30-09-1999 07:00:00	-
MA11	68.6595	23.3219	390	24-05-1999 09:04:58	30-09-1999 09:09:13	-
MA12	69.8349	25.0824	75	24-05-1999 16:35:00	29-09-1999 07:45:51	19-06-1999 17:58:00 - 27-06-1999 08:01:11
MA13	70.3161	25.5156	30	25-09-1999 08:42:10	29-09-1999 05:27:19	-
GP03	69.99	24.94	20	18-05-1999 08:56:17	24-05-1999 19:00:00	-

Table 6.4.1. *Coordinates and recording times of the MASI-1999 mobile station experiment in Finnmark, Norway (the exact end times can be some minutes later). MA00 is the station which recorded at the beginning and at the end of the experiment in parallel with the ARCES array site ARA0. The equipment of the station MA12 was used at MA00 during the first week, and in August the station MA05 was dismantled and the equipment moved to MA00 until the end of the experiment. All dates and times are in the format [dd-mm-yyyy hh:mm:ss]. Station GP03 was used to test some equipment during the first week of the experiment in Lakselv. Although the data are very noisy, they were also stored on the CDs. This station was moved at the end of the installation phase to station MA13.*

	Real	Imagi-nary
Con-stant	6.419832	0.0
Poles	-0.8884425	-0.8887107
	-0.8884425	0.8887107
	-0.4272566	0.0
Zeroes	0.0	0.0
	0.0	0.0
	0.0	0.0
	0.0	0.0

Table 6.4.2. *Parameters of the transfer function (poles and zeroes in the Laplace domain) for the MASI-1999 experiment mobile station. Applying these parameters, the units of the transfer function are [counts/nm].*

DATE	TIME	LATI-DUE	LONGI-TUDE
24 May1999	05:00:12.8	70.91	26.53
22 August 1999	02:08:47.9	69.27	23.70

Table 6.4.3. *Epicentral parameters of two local events, which were observed with the MASI-1999 stations and for which data are shown in Fig. 6.4.2 - 6.4.5.*
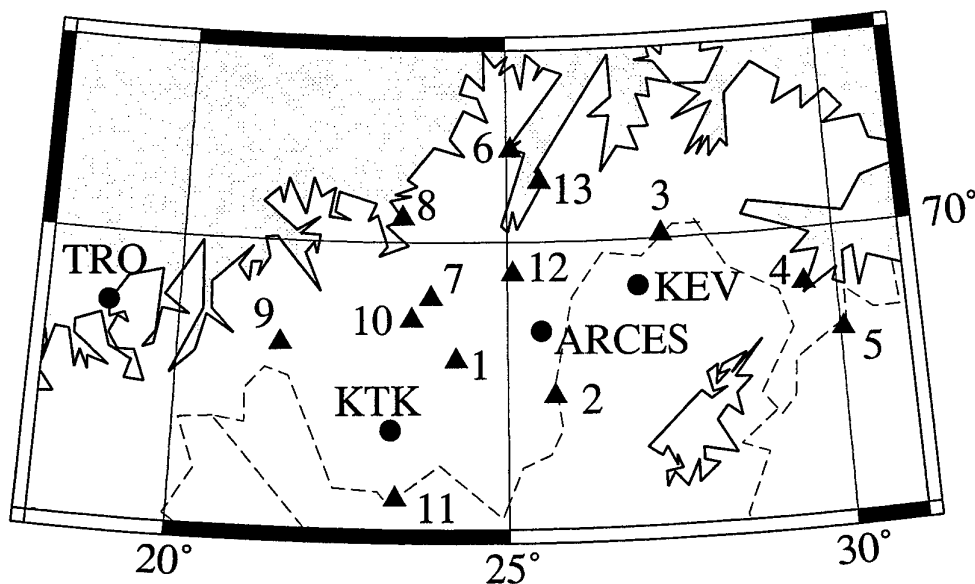
Fig. 6.4.1. *Map of all 13 MASI-1999 stations in Finnmark (triangles). The dots show the positions of the permanent stations ARCES, KEV, KTK, and TRO in the same area. The station MA00 was located at ARCES.*
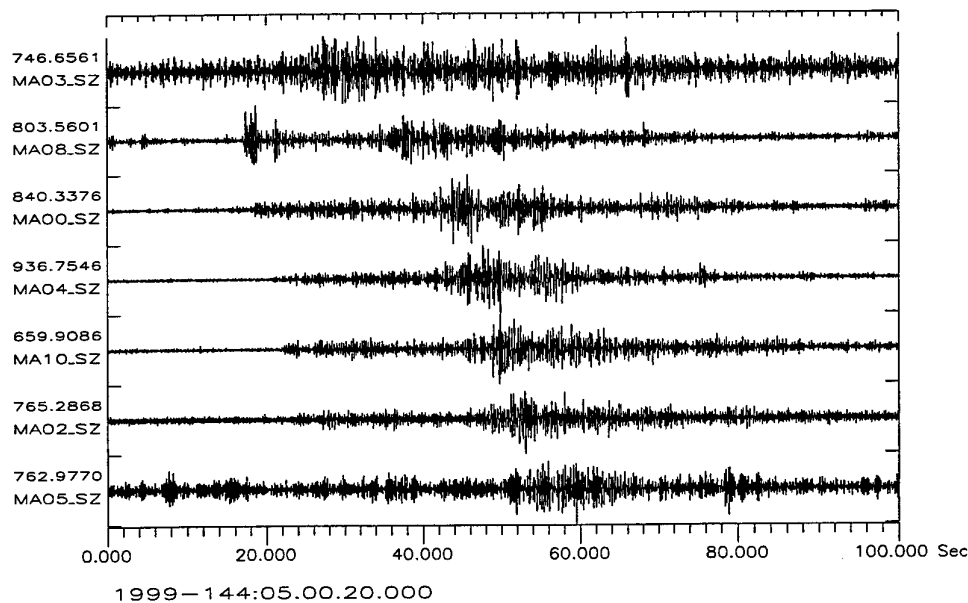
Fig. 6.4.2. *Vertical- component seismograms of the M_L 1.9 event on 24 May 1999 (see Table 6.4.3). The seismograms were band-pass filtered between 3 and 9 Hz, the epicentral distances to the stations are between 1° and 2°.*
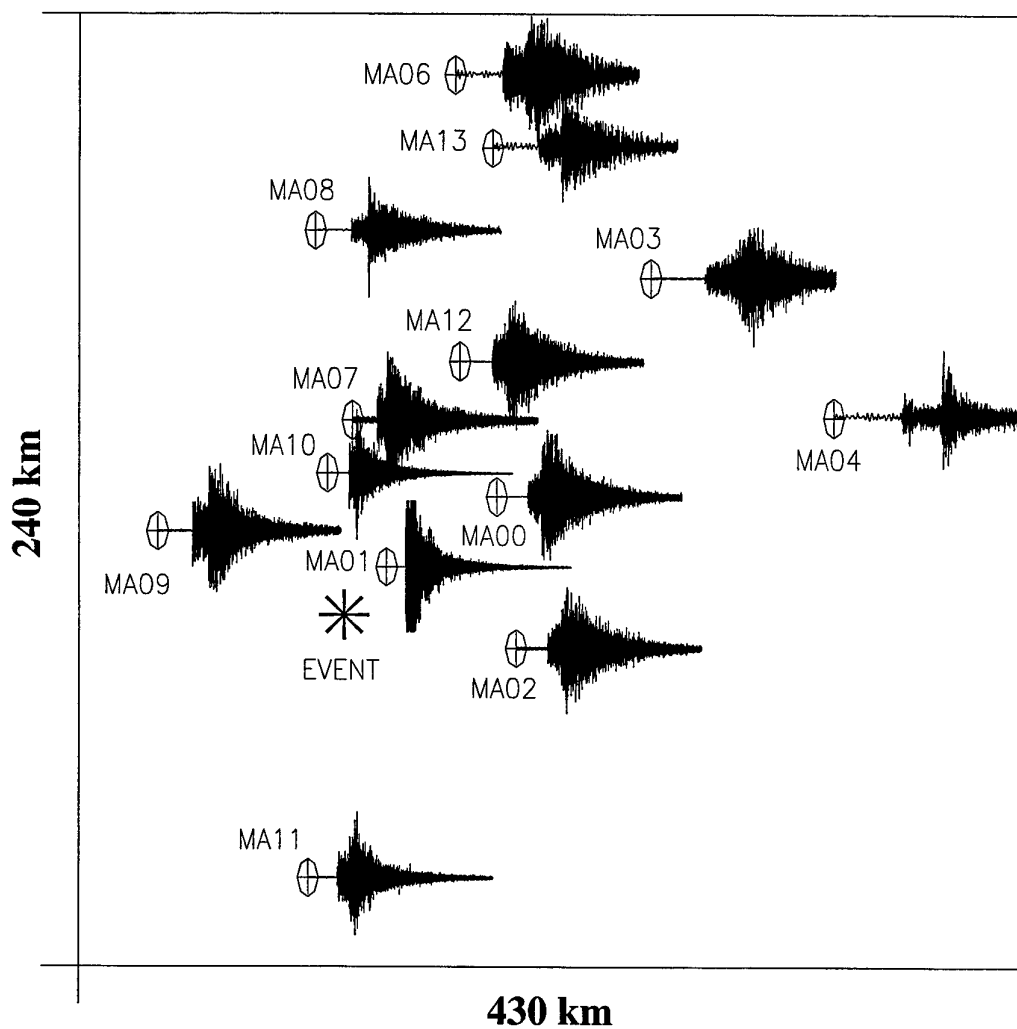
Fig. 6.4.3. *Geographical distribution of observed seismograms with respect to the felt event of 22 August 1999. Shown are unfiltered vertical-component traces. Note that the seismogram at station MA01 is clipped, and the different amplitude ratio between P and S onsets.*
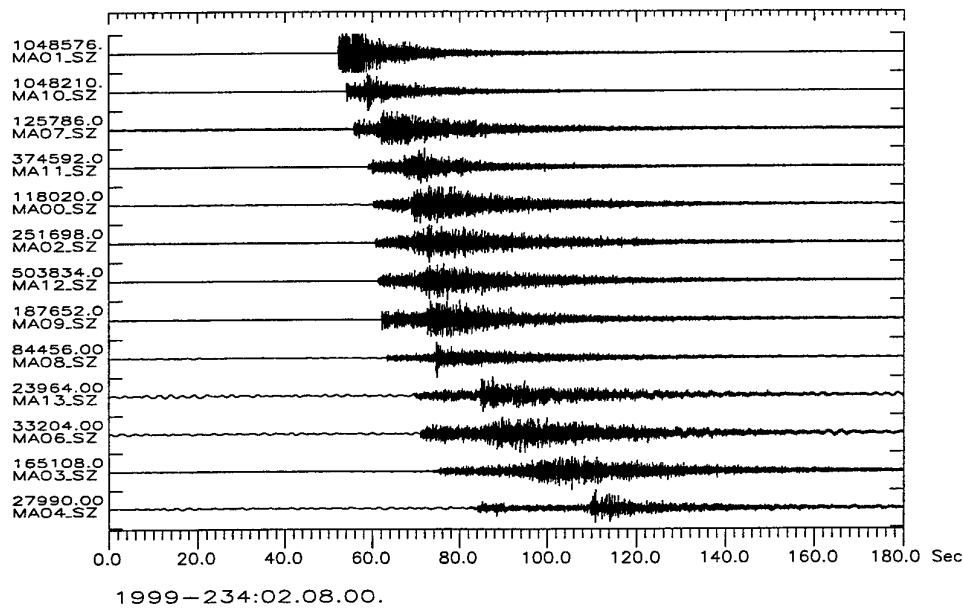
Fig. 6.4.4. *The unfiltered vertical-component records at all MASI-1999 stations of the 22 August 1999 M_L 2.6 event at the Stuoragurra fault. The stations observed the event in epicentral distances between 0.2° and 2°. The closest station MA01 was clipped.*
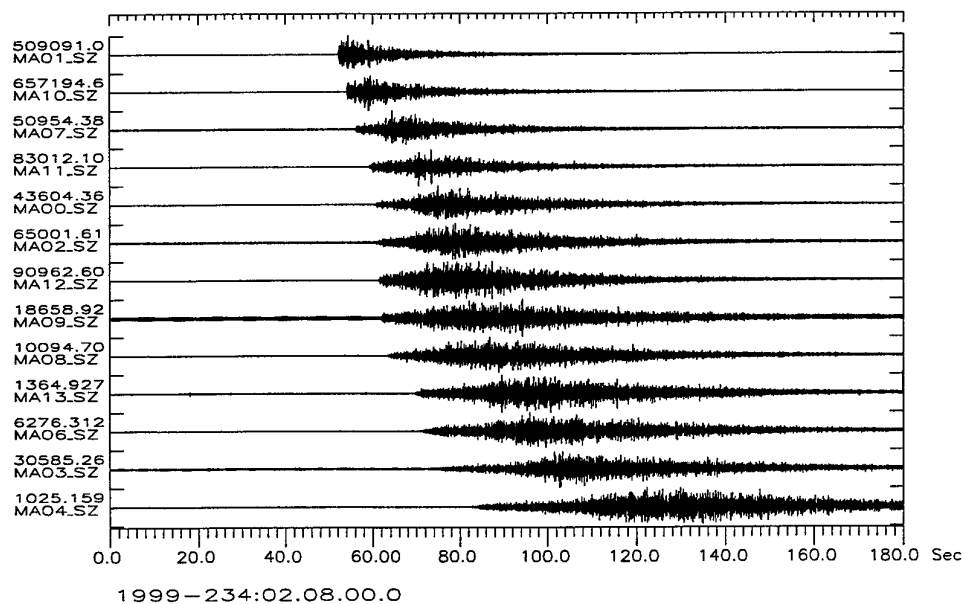
Fig. 6.4.5. *The same data as in Fig. 6.4.4., now filtered with a Butterworth high-pass at 40 Hz. Note the high-frequency scattered energy, which is an indication for a relative high Q structure in the Finnmark area.*
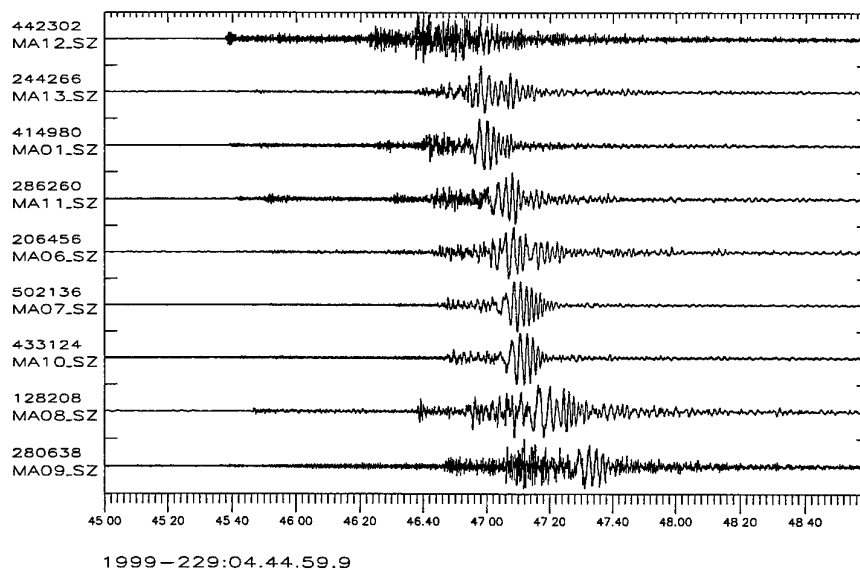
1999−229:04.44.59.9

Fig. 6.4.6. *The raw seismograms of the Lovozero event 17 August 1999 as observed at some of the MASI-1999 stations.*
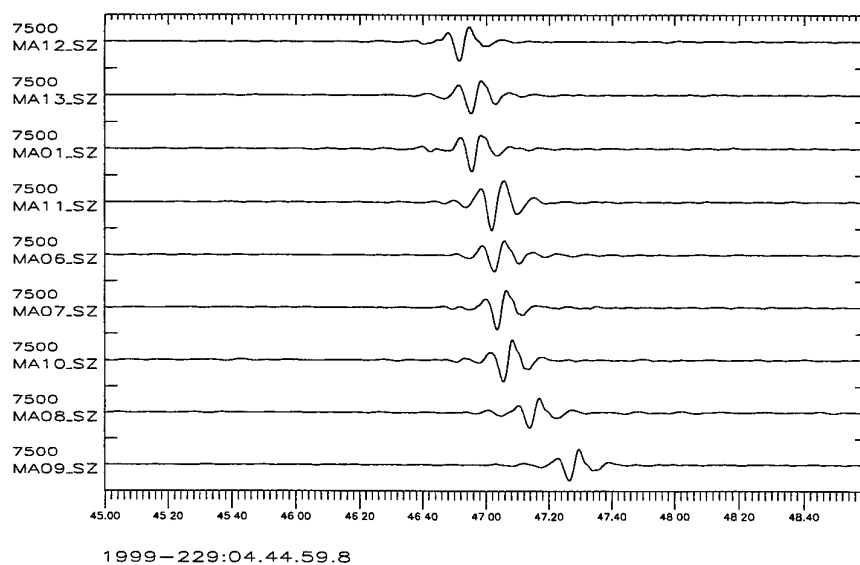

1999−229:04.44.59.8

Fig. 6.4.7. *Seismograms of the Lovozero event 17 August 1999 now filtered with a Butterworth band-pass filter between 8 and 20 seconds. The amplitude scale was normalized to the maximum amplitude. From these data the a M_S value 4.3 was determined.*
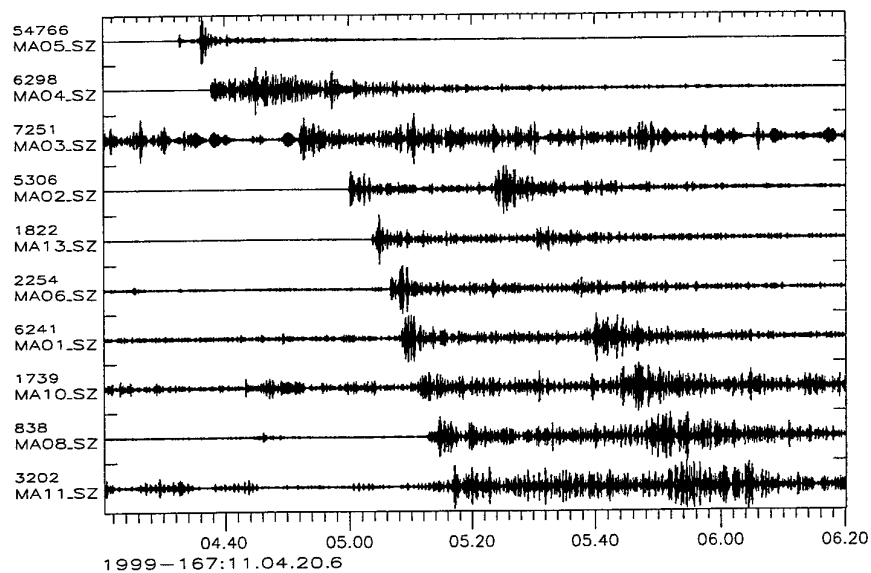
Fig. 6.4.8. *Seismograms of an explosion on 16 June 1999 in the Nikel area (Russia), close to the MASI-1999 station MA01. The seismograms were band-pass filtered between 6 and 10 Hz.*

6.5   Recent developments in connection with the seismic station in Amderma, Russia

Summary

Since 1991, NORSAR and the Kola Regional Seismological Centre (KRSC) have had a cooperative agreement on geophysical research and development. This has led to the establishment in Apatity of an advanced seismic observatory and a data center for geophysical monitoring. A dedicated 64 Kbps connection has been established between Kjeller and Apatity to exchange data on seismic measurements and associated scientific information. This link currently enables both parties to use data from the entire array network in northern Europe in their daily analysis of seismic events in the European Arctic.

The Amderma station (AMD) has been in operation by KRSC for more than 10 years. The location is 69.742N 61.655E, which is just south of Novaya Zemlya (see Fig. 6.5.1). The station is emplaced inside a deserted underground mine. Initially, AMD operated as a standard Russian analog recording station. In 1993, KRSC installed a microarray (with digital recording) at the Amderma site. The hardware comprised short-period S-500 vertical and horizontal seismometers, Nanometric 18 bit digitizer and a Norac array controller. From August 1998, the microarray has been replaced by a broadband 3-component seismometer system of the type RefTek DAS 72A.

Data recorded by AMD is sampled at 100 Hz and registered on a local disk system. Continuous data are transferred to an Exabyte cassette recorder and shipped by mail to Apatity. Typically, these data are available within 1-2 months of the date of recording.

Software to connect the Amderma station to Apatity via an Inmarsat link was developed by KRSC in 1998/99. This software, which is written in Borland Pascal, is documented on KRSC's homepage on the Internwt (http://www.krsc.ru/). The software allows for the retrieval of the following types of data:

• Waveform segments for specified time intervals
• Detection lists
• Compressed STA trace of filtered vertical channel data (filter band 4-12 Hz)
• State-of health indicators.

The Inmarsat link can furthermore be used to remotely controlling the station parameters, and restarting the system in case of occasional failure.

The capability of the Amderma station to detect low-magnitude seismic events in the Barents/ Kara Sea region should by now be well documented. The rapid availability of digital data from this station is therefore expected to contribute significantly to confidence-building and enhanced analysis of future seismic events of monitoring concern in this region.

As examples of the rapid retrieval of waveform segments from AMD, Figure 6.5.2 shows vertical component data for the earthquake in the Kola Peninsula on 17 August 1999. Both long-period surface wave data and short period P and S phases can be clearly seen in appropriate frequency bands. Figure 6.5.3 shows the three components of the Amderma station for the same event, filtered in the band 2-4 Hz. An example of the compressed STA trace at the time of the 17 August 1999 event is shown in Fig. 6.5.4. The two peaks correspond to the P and S phase respectively.

Examples of teleseismic P-wave recordings are shown in Figures 6.5.5 and 6.5.6. These figures show broad-band AMD data, filtered in a suite of frequency bands, for two earthquakes which occurred on 30 May 1999. These time intervals were requested via the Inmarsat link by the KRSC staff in Apatity during the next day, and were subsequently transmitted to NORSAR via the direct link Kjeller-Apatity. As can be seen from the figures, the plots were generated at NORSAR on 1 June 1999.

We plan to continue to use the Inmarsat connection to retrieve detection lists as well as seismic data for events of special interest. Because of the significant cost of the Inmarsat transmission, we currently do not plan to regularly transmit waveform data. However, an interesting possibility is to transmit on a regular basis the STA traces, which can be highly compressed. The STA traces, for appropriately filtered waveforms, form the basis for the Threshold Monitoring technique. Such STA traces, if rapidly available, could therefore make useful contributions to the NORSAR Threshold Monitoring system for the Barents/Kara Sea region.

Vladimir Asming, KRSC
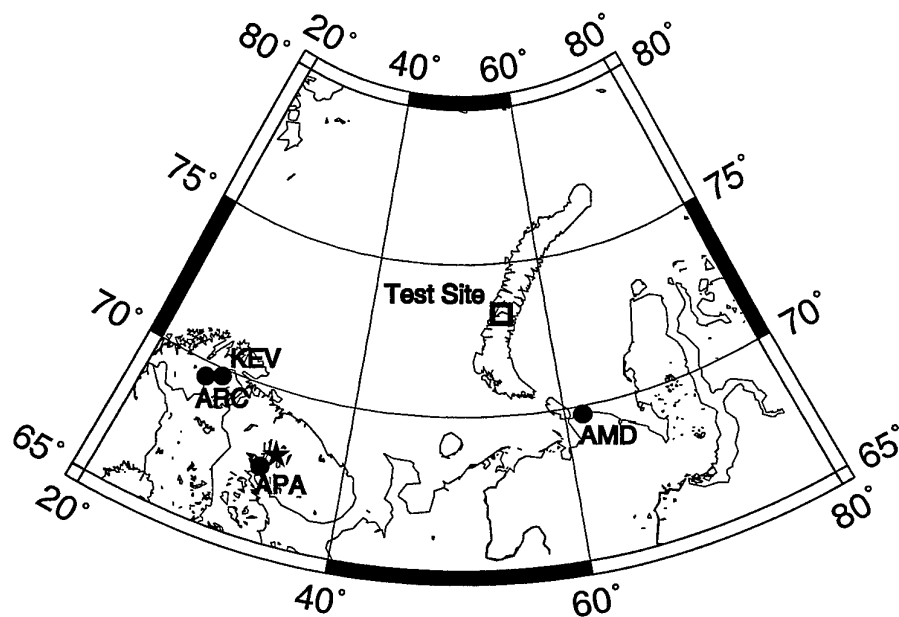**Igor Kuzmin, KRSC**
Frode Ringdal, NORSAR

Fig. 6.5.1. *Map showing the location of the Amderma seismic station (AMD) in relation to others stations in the European Arctic. The Novaya Zemlya nuclear test site is indicated, and the location of the 17 August 1999 Kola earthquake is shown as a filled star.*
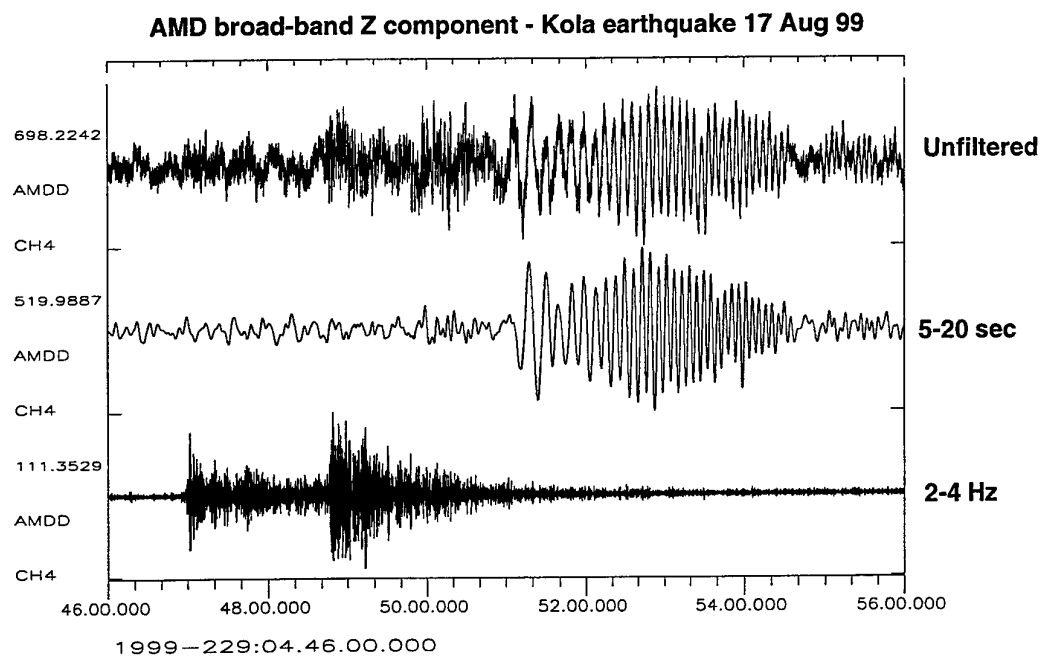
Fig. 6.5.2. *Vertical component broad-band data for the earthquake in the Kola Peninsula on 17 August 1999. Both long-period surface wave data and short period P and S phases can be clearly seen in appropriate frequency bands.*
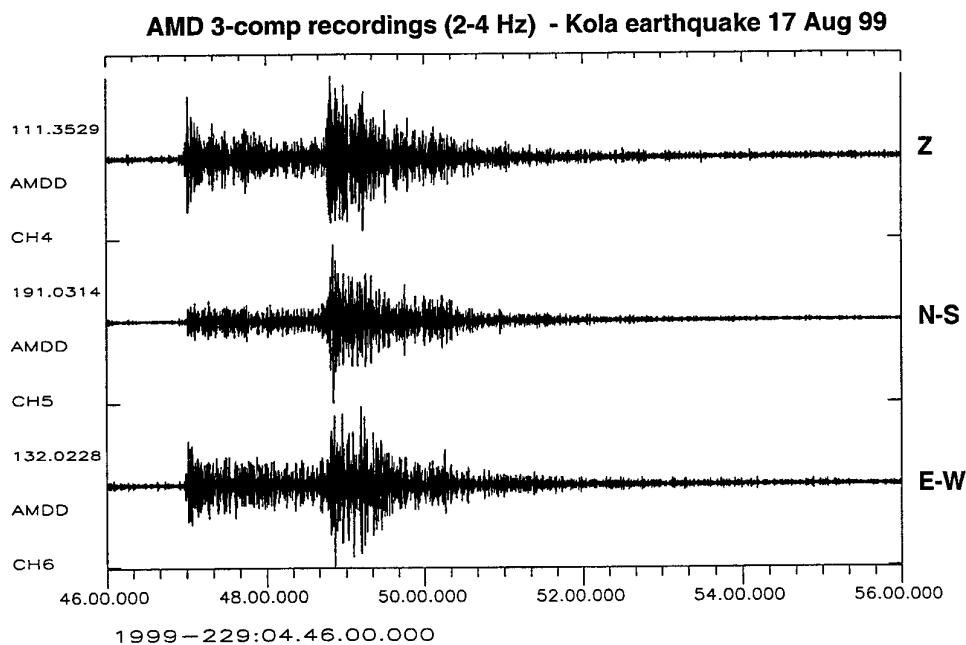

Fig. 6.5.3. *Three-component data of the Amderma station for the 17 August 1999 event, filtered in the band 2-4 Hz.*
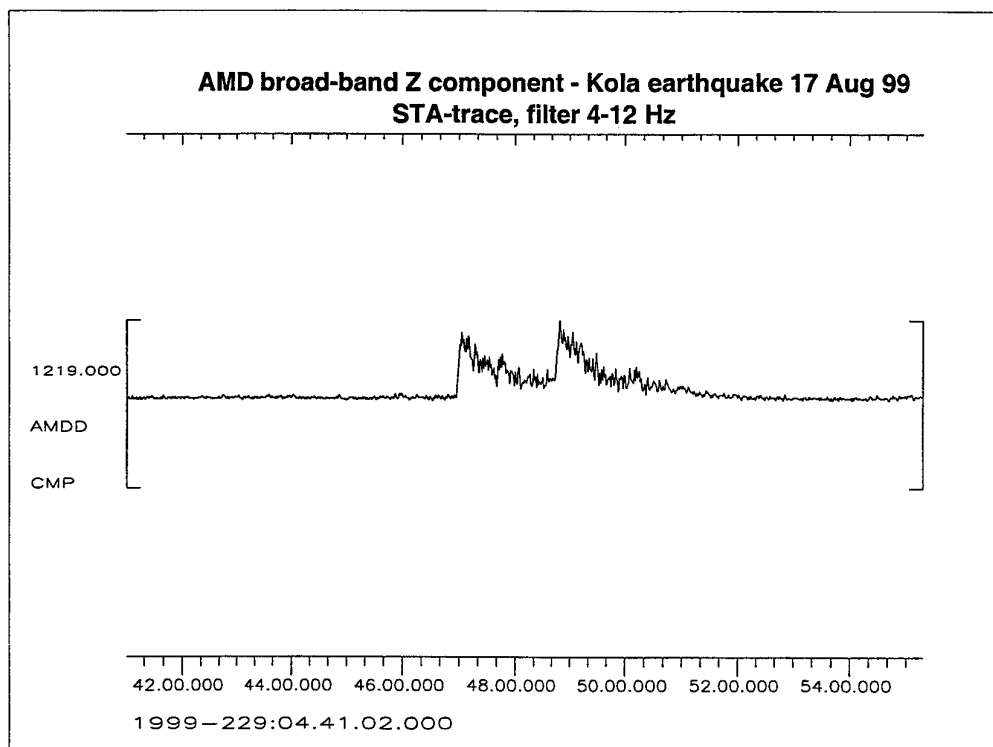
Fig. 6.5.4. *Example of compressed STA trace (filter 4-12 Hz) at the time of the 17 August 1999 event. The two peaks correspond to the P and S phase respectively.*
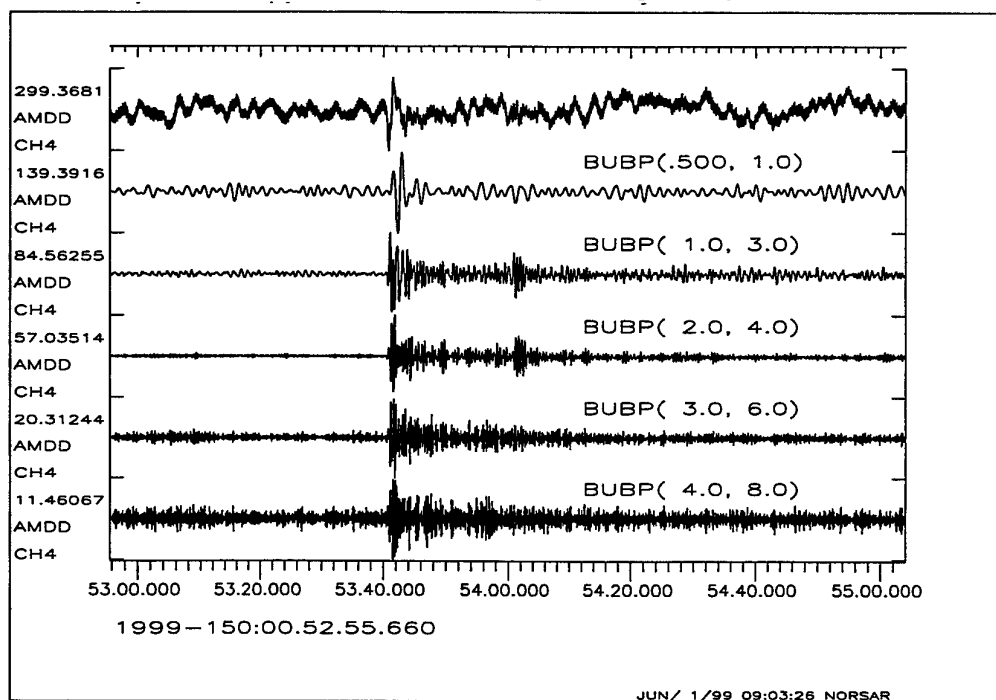

Fig. 6.5.5. *Broad-band AMD data, filtered in a suite of frequency bands, for an earthquake in the Philippine Islands region on 30 May 1999.*

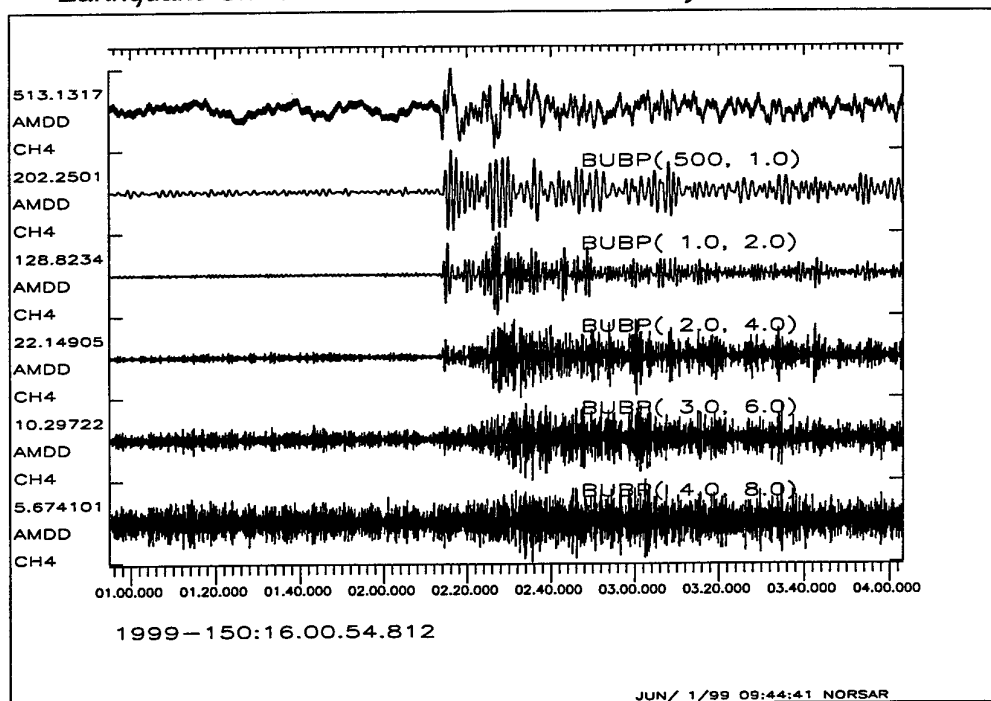*Earthquake China-Russia Border mb=5.6 30 May 1999 O.T.15.56.01*

Fig. 6.5.6. *Broad-band AMD data, filtered in a suite of frequency bands, for an earthquake in the E. Russia, NE. China border region on 30 May 1999.*

6.6   Eurobridge — ground truth observations at the Fennoscandian arrays

Introduction

In order to meet the requirements for event location accuracy of the International Monitoring System (IMS), it has been realized that regionalized travel-time models are needed. Events whose exact origin times and coordinates are known are very important for deriving such models. E.g., NORSAR (NOA) observations of shots used for refraction profiling have previously been investigated by several authors to derive information on travel-time anomalies and the corresponding velocity structure in Fennoscandia (Cassell et al., 1983; Mereu et al., 1983).

A 1130 km seismic refraction profile crossing the Baltic Shield in the northwest and the Ukrainian Shield in the southeast was part of an experiment (Eurobridge) described in the doctoral dissertation of Giese (1998). There were three series of shots, one in 1995 and two in 1996. Observations of these explosions at the Fennoscandian arrays (ARCESS, FINESS, HAGFORS, and NORESS) provide an opportunity to check the accuracy of the travel-time tables in use at NORSAR for Fennoscandia. Figs. 6.6.1 and 6.6.2 show maps of the shot points and the arrays used in this investigation.

Details on origin times, locations and yields of the Eurobridge shots are given in Table 6.6.1, together with information on the SNR of the automatically detected P-arrivals at each array. The term "visual" in Table 6.6.1 indicates cases when no automatic P-detections are found, but where a signal was found by manual analysis. The shots along the main profile had yields varying between 150 and 1100 kg, whereas the largest shot, located off the coast of Gotland, had a yield of 3500 kg.

For each station, 900 seconds of data beginning approximately 60 seconds before the origin time of each shot were retrieved and stored on disk. The main part of the data was requested via AutoDRM from the prototype International Data Center (pIDC) in Arlington, Virginia. In several cases where data were unavailable from the pIDC; we were able to retrieve them from our archive tapes at NORSAR. For some events, data from FINESS and NORESS are missing (see Table 6.6.1).

In the case of Hagfors data requested from the pIDC, it was necessary to correct for a 0.493 second delay introduced by a FIR filter used in the Nanometric data acquisition system. This correction had already been made for data read from the tapes stored at NORSAR.

Automatic event locations provided by the GBF system

Results from NORSARs automatic signal detection system DP/EP, as operated at the time of the Eurobridge experiment in 1995 and 1996, were reprocessed with the Generalized Beam-forming (GBF) method (Kværna et al., 1999) to provide automatic network-based event locations. As described by Kværna et al. (1999), some improvements were recently made to the GBF software. Among others this included an enlarged grid system where the events were located on a grid with a density of 0.2 degrees. Our first experiment was to compare the event locations provided by the GBF method to the ground-truth locations of the Eurobridge shots.

Fig. 6.6.3 shows the locations of the GBF events associated with the Eurobridge experiment (filled squares), where the number of arrays used to locate the events are given together with the shot labels. Table 6.6.2 provides origin times and coordinates of the GBF locations, local

magnitudes, the number of P- and S-phases associated with each event, and the absolute location error.

Except for one case, we find that events located with all four stations had small absolute location errors, 17.8, 14.9, 27.1, 19.9, and 9.1 km, respectively. For shot I1, the location difference is as large as 322.6 km. From analyzing the list of associated phases for shot I1, we find that the Sn arrival at FINES is misinterpreted as Lg by the GBF procedure, resulting in a location too close to the FINES array.

Seven of the shots had no S-phase detections and were located using P-phases only. These shots had location errors varying between 134.6 and 1026.7 km. This relatively poor performance can be explained by configuration of the array network as seen in relation to the Eurobridge profile (see Fig. 6.6.1). With only P detections available, this network will have a relatively low resolution for locating events outside of the network. The GERES array is also included in the network processed by GBF, but due to the blockage of regional seismic waves by the Teisseyre-Tornquist zone (Schweitzer, 1995), none of the Eurobridge shots are observed at GERES.

From Table 6.6.2 we also see that all events located with two or more S-phases had location errors less than 27.1 km. The importance of having S-phase detections available for the GBF processing were taken into account in a recent upgrade of the processing recipes for the signal detection system (Schweitzer, 1994; Kværna et al. 1999). New beams with S-type velocities, combined with rotations of the horizontal components into both radial and transverse directions were introduced for all arrays. However, in 1995 and 1996, when the original data were processed by the DP/EP system, these features were not yet implemented.

Array observations of P-phases from the Eurobridge shots

One task in this study is to analyze the travel-times of the ground-truth Eurobridge events, and compare these to the travel-times calculated from the Fennoscandian crustal and upper mantle velocity model. This model, illustrated in Fig. 6.6.4 (Mykkeltveit and Ringdal, 1981), is currently used at NORSAR for locating events in Fennoscandia and adjacent areas. At the pIDC, a similar travel-time model is used for locating events in the same region.

As seen from Table 6.6.1, P-phases from most of the Eurobridge shots are observed at FINESS, HAGFORS and NORESS arrays. At the more distant ARCESS array, located between 1400 and 2000 km from the profile line, 12 out of 29 events are seen. For each array, seismic sections were plotted with a reduction velocity of 8 km/s (13.9 s/deg), see Figs. 6.6.5 - 6.6.8. The travel-time curves of the Fennoscandian model are also shown on each section. For each shot, the array data were beamformed using the estimated slowness and azimuth of the arriving P-phase. The traces shown on the seismic sections are the beams filtered in the passband providing the highest SNR.

On the seismic sections (Figs. 6.6.5 - 6.6.8) we observe significant differences between the model predictions and the P-onsets, and it is our plan to investigate these in more detail. A striking feature is the difference between the Hagfors and NORESS sections shown in Figs. 6.6.5 and 6.6.6. At Hagfors, the P-onsets are consistently late as compared to the model predictions, whereas the consistency at NORES is much better. Details on the time differences between the manual time picks and the model predictions are given in Table 6.6.3. In view of the fact that Hagfors and NORES are located only 135 km apart along the direction of the

Eurobridge profile line (see Fig. 6.6.1), it is difficult to interpret these differences in terms of anomalous velocity structures below these two arrays. This means that we also have to look into alternative explanations like timing problems at the two arrays.

In the extension of this study we plan to include data form the large-aperture NORSAR array (NOA), and also to analyze the S-arrivals. Our ultimate goal will be to derive station-specific travel-time corrections (SSSCs) for the region of the Eurobridge shots such that we can obtain more accurate event locations in the Lithuania-Belarus region.

L. Taylor
J. Schweitzer
T. Kværna

References

Cassell, B.R., S. Mykkeltveit, R. Kanestrøm and E.S. Husebye (1983): A North Sea-Southern Norway seismic crustal profile. *Geophys. J. R. Astron. Soc.* **72**, 733-753.

Giese, Rüdiger (1998). Eine zweidimensionale Interpretation der Geschwindigkeitsstruktur der Erdkruste des südwestlichen Teils der Osteuropäischen Plattform (Projekt EURO-BRIDGE). PhD thesis Freie Universität Berlin. GeoForschungsZentrum Potsdam, Scientific Technical Report STR98/16, 190 pp.

Kværna, T., J. Schweitzer, L. Taylor and F. Ringdal (1999): Monitoring of the European Arctic Using Regional Generalized Beamforming. In: NORSAR Semiannual Tech. Summ. 1 October 1998 - 31 March 1999, *NORSAR Sci. Rep. 2-98/99*, Kjeller, Norway, 78-94.

Mereu, R.F., S. Mykkeltveit and E.S. Husebye (1983): FENNOLORA Recordings at NORSAR (NORSAR Contribution No. 322). *J. Geophys.* **52**, 119-130.

Mykkeltveit, S. and F. Ringdal (1981): Phase identification and event location at regional distance using small-aperture array data. In: Husebye, E.S. and S. Mykkeltveit (eds.), 1981: *Identification of seismic sources - earthquake or underground explosion.* D. Reidel Publishing Company, 467-481.

Schweitzer, J. (1994): Some improvements of the detector / SigPro - system at NORSAR. In: NORSAR Semiannual Tech. Summ. 1 October 1993 - 31 March 1994, *NORSAR Sci. Rep. 2-93-94*, Kjeller, Norway, 128-139.

Schweitzer (1995): Blockage of regional seismic waves by the Teisseyre-Tornquist zone. *Geophys. J. Int.* **123**, 260-276.

Table 6.6.1: EUROBRIDGE Shots

Origin Time (GMT)	Lat (deg)	Lon (deg)	Yield (kg)	Shot Point	Shot Label	SNR of automatic P_n detection			
						ARC	FIN	HFS	NRS
1995-147:21.00.02.400	55.1792	22.9417	600.00	6	G0	visual	39.5	11.0	13.0
1995-147:21.20.01.290	54.4321	24.4526	1000.00	10	K0	12.8	61.9	23.7	15.0
1995-147:21.40.01.187	55.5133	22.2094	800.00	4	E0	visual	42.8	10.5	10.5
1995-147:22.00.01.375[a]	54.8254	23.6588	800.00	8	I0	visual	33.4	6.2	12.2
1995-147:22.19.59.616	55.8599	21.4519	1000.00	2	C0	6.1	81.8	44.5	26.2
1995-148:21.00.05.230	55.3447	22.5173	200.00	5	F0	no det.	12.2	visual	no det.
1995-148:21.20.01.960	54.6089	24.0969	200.00	9	J0	no det.	no det.	6.6	visual
1995-148:21.40.00.807	55.7066	21.8052	200.00	3	D0	no det.	21.6	15.7	6.1
1995-148:22.00.01.255	55.0024	23.3008	200.00	7	H0	no det.	visual	visual	visual
1995-148:22.20.01.187	56.0105	21.1390	200.00	1	B0	4.2	37.7	17.9	16.4
1995-150:02.00.00.000[b]	57.1710	18.0760	3500.00	0	A0	88.7	103.9	187.9	77.3
1996-189:21.00.01.172	54.6089	24.0972	300.00	10	J1	visual	no data	11.7	5.6
1996-189:21.30.01.944	54.0644	25.1653	679.20	12	M1	no det.	no data	23.3	10.8
1996-189:22.30.00.339	53.7111	25.8383	508.80	14	O1	no det.	no data	13.4	5.7
1996-189:23.00.04.146	52.9389	27.0944	339.20	18	S1	no det.	no data	visual	visual
1996-190:00.00.03.025	54.2528	24.8258	150.00	11	L1	no det.	no data	8.7	5.2
1996-190:21.00.03.630	54.8258	23.6617	800.00	8	I1	visual	17.6	12.2	13.1
1996-190:22.00.01.012	53.5244	26.1500	212.40	15	P1	no det.	no det.	no det.	no det.
1996-190:22.30.00.726	53.3322	26.4944	679.20	16	Q1	no det.	no det.	visual	no det.
1996-190:23.00.00.701	52.5600	27.6425	1102.40	20	U1	no det.	6.3	5.7	6.3
1996-191:00.00.00.214	53.8922	25.4983	212.00	13	N1	no det.	5.0	visual	visual
1996-194:21.00.00.591	53.7111	25.8383	848.00	14	O2	visual	9.4	27.5	9.8
1996-194:22.30.03.260	52.1436	28.2553	848.00	22	W2	no det.	visual	8.1	no data
1996-194:22.59.59.982	51.7170	28.8300	1102.40	24	Y2	no det.	4.8	no det.	no data
1996-195:01.00.01.066	53.1311	26.8344	848.00	17	R2	6.3	visual	7.6	no data
1996-195:21.00.00.775	52.5600	27.6425	460.80	20	U2	no det.	no det.	no det.	no data
1996-195:22.00.00.249	51.9233	28.5569	212.00	23	X2	no det.	no det.	no det.	no data
1996-195:22.30.02.695	52.3164	27.9810	212.00	21	V2	visual	5.4	7.8	no data
1996-195:23.00.00.361	52.7439	27.3810	212.00	19	T2	no det.	4.8	visual	no data

a. Shot time originally listed as 1995-147:21.20.01.375 by Giese (1998)
b. Shot time originally listed as 1995-149:22.20.01.187 by Giese (1998)

Table 6.6.2: GBF events associated with the Eurobridge experiment

Shot Label	GBF Origin Time (GMT)	Lat (deg)	Lon (deg)	Mag	Number of defining Arrays	P	S[a]	Error (deg)	Error (km)
G0	1995-147:21.00.37.0	57.48	25.02	1.38	1	1	1	2.8782	320.4067
K0	1995-147:21.20.00.0	54.48	24.64	2.56	4	4	3	0.1598	17.7920
E0	1995-147:21.40.02.0	55.49	22.05	2.39	4	4	4	0.1334	14.8522
I0	1995-147:22.00.01.0	54.67	23.43	2.22	4	4	2	0.2430	27.0532
C0	1995-147:22.19.57.0	55.69	21.52	2.34	4	4	3	0.1790	19.9250
F0	1995-148:20.59.57.0	54.57	23.10	1.93	1	1	1	0.9098	101.2797
J0	1995-148:21.19.41.0	52.93	24.82	-	2	2	0	1.7773	197.8511
D0	1995-148:21.39.52.0	54.97	22.09	2.02	3	3	1	0.7729	86.0448
H0	1995-148:21.59.54.0	54.28	25.16	1.93	1	1	1	1.6795	186.9633
B0	1995-148:22.20.02.0	56.09	21.16	1.56	4	4	1	0.0814	9.0599
A0	1995-150:02.00.03.0	57.37	17.95	2.33	4	3	7	0.2255	25.0990
J1	1996-189:21.00.33.0	56.42	22.39	-	3	3	0	2.2934	255.3047
M1	1996-189:21.28.05.0	46.56	32.15	-	2	2	0	9.2231	1026.7120
O1	1996-189:22.30.42.0	54.94	20.00	-	2	2	0	4.8984	545.2934
I1	1996-190:21.00.35.0	57.45	22.18	1.38	4	4	1	2.8982	322.6284
O2	1996-194:20.58.57.0	49.07	28.35	-	3	3	0	5.0384	560.8758
R2	1996-195:01.00.18.0	54.34	26.79	-	2	2	0	1.2094	134.6338
V2	1996-195:22.29.45.0	51.16	28.78	-	2	2	0	1.3156	146.4529

a. Includes S, Lg, and Rg

Table 6.6.3: Observed - predicted arrival times for Pn (seconds)

Shot	ARC	FIN	HFS	NRS
G0	-	0.976	0.831	-0.759
K0	-1.799	0.037	0.753	-0.743
E0	1.827	2.000	-0.866	0.342
I0	-1.145	0.724	0.486	-0.594
C0	-0.737	0.954	1.582	0.283
F0	-	1.551	2.916	-
J0	-	-0.115	1.062	0.093
D0	-	1.269	1.357	-0.180
H0	-	0.832	1.525	1.655
B0	-0.957	1.362	2.338	0.536
A0	-2.893	1.592	1.757	0.116
J1	1.270	-	4.689	3.554
M1	-	-	0.727	-0.226
O1	-	-	1.559	0.079
S1	-	-	1.135	0.458
L1	-	-	1.087	0.135
I1	-4.852	0.509	0.376	-0.587
P1	-	-	-	-
Q1	-	-	1.527	-
U1	-0.093	-0.525	-0.584	-0.649
N1	-	-0.324	1.127	-0.570
O2	-1.233	0.303	0.670	-0.302
W2	-	-0.682	1.156	-
Y2	-	-	-	-
R2	2.292	1.122	1.056	-
U2	-	-	-	-
X2	-	-	-	-
V2	0.605	-1.420	-0.017	-
T2	-	-0.878	0.707	-
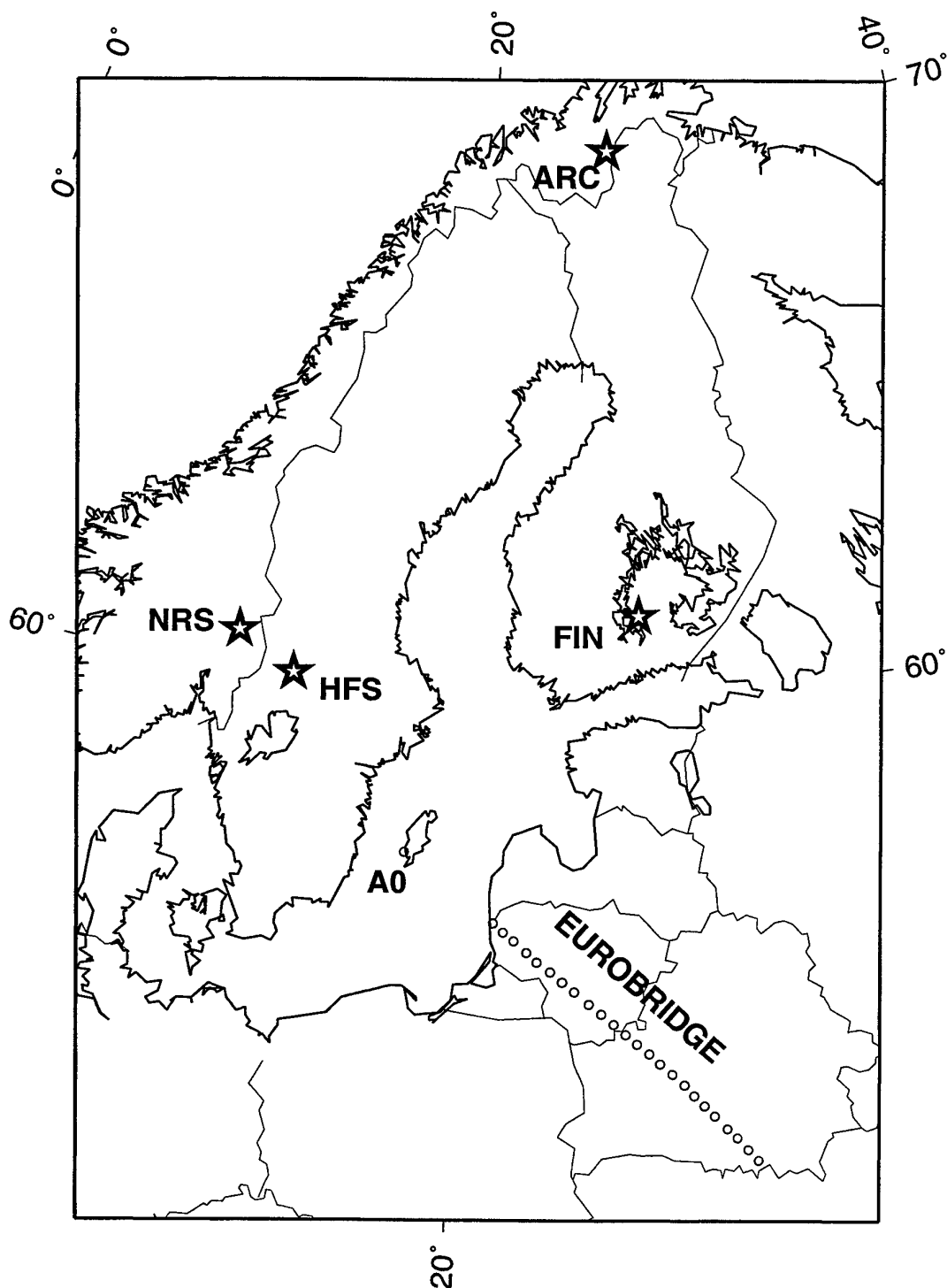
Fig. 6.6.1. *Map showing the locations of the Eurobridge shots and the four arrays included in this study (ARCESS, FINESS, HAGFORS, and NORESS). A0, located off the southern coast of Gotland, was part of the Eurobridge experiment. See Fig. 6.6.2 for a more detailed map of the remaining shot points.*
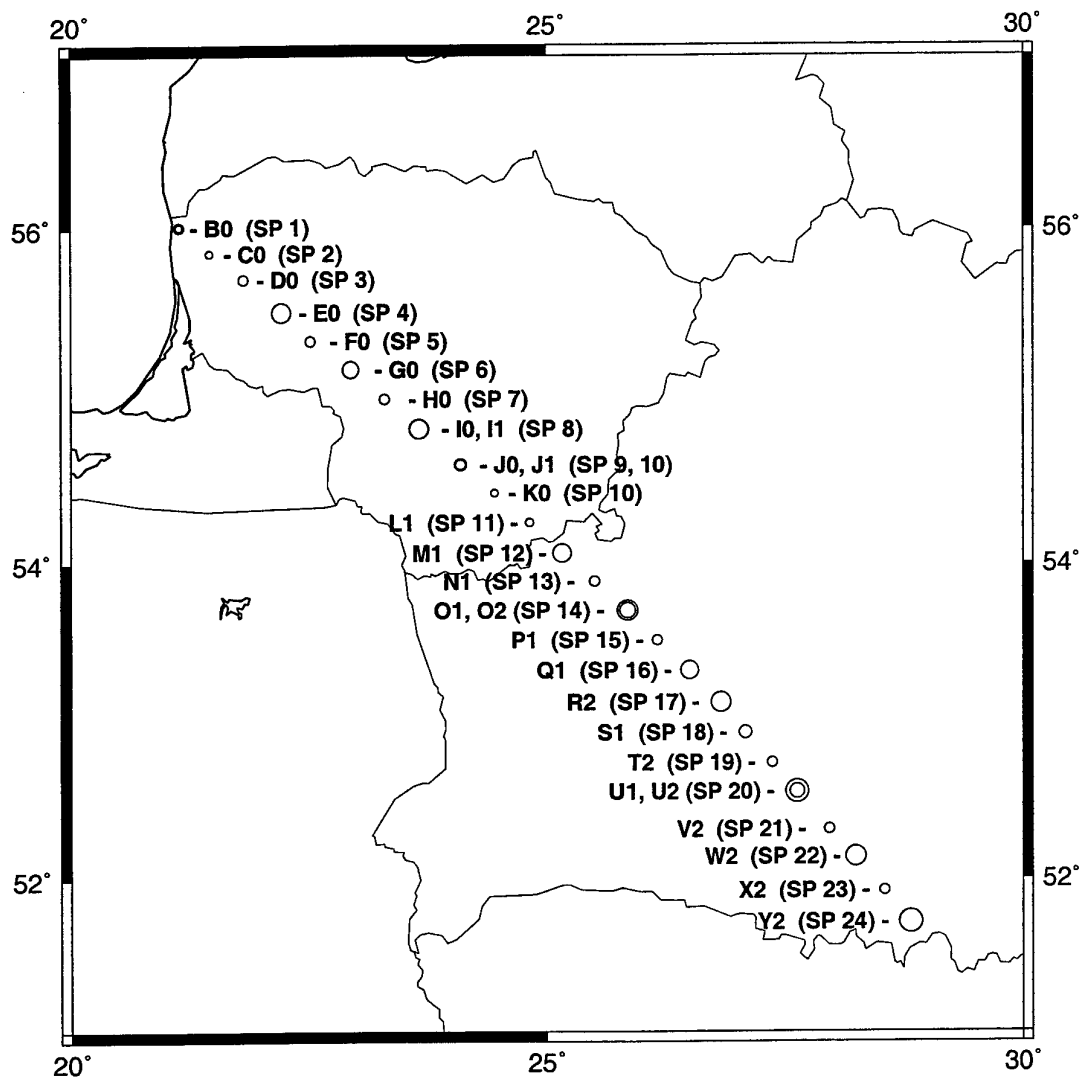
Fig. 6.6.2. *Map showing the Eurobridge shot points represented by circles with areas proportional to the yields. The labels that we have adopted are shown along with the original shot point numbers. See Fig. 6.6.1 for shot A0, which was located off the southern coast of Gotland. Detailed information on each shot is given in Table 6.6.1.*
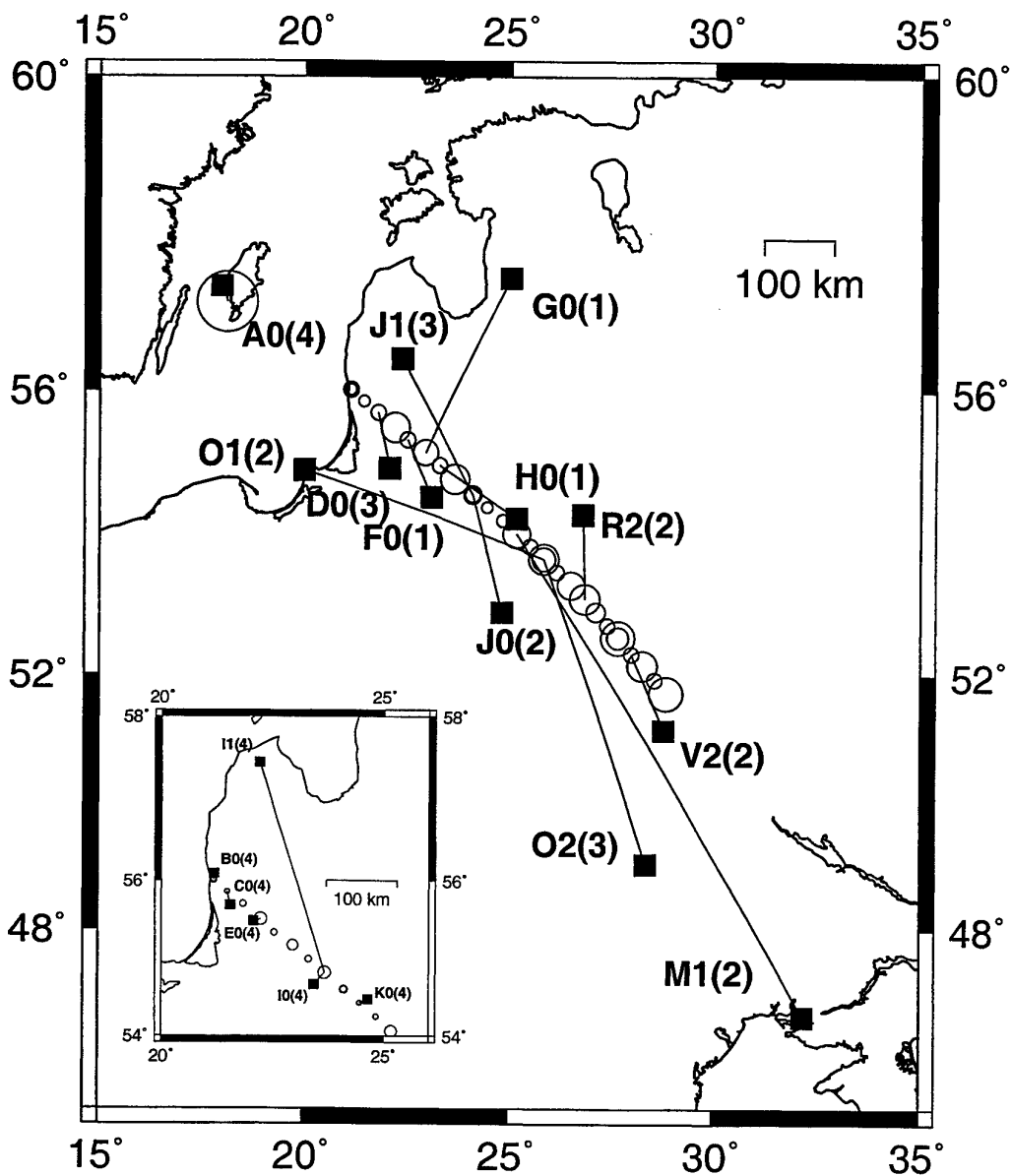
Fig. 6.6.3. *GBF events associated with Eurobridge experiment. A line is drawn between each GBF location (black squares) and the corresponding Eurobridge shot (circles). The shot label is given with the number of arrays used to locate the event. All mainland locations, where four arrays were used, are shown in the inset; the remaining locations are shown on the main map.*

FENNOSCANDIA P-VELOCITY MODEL
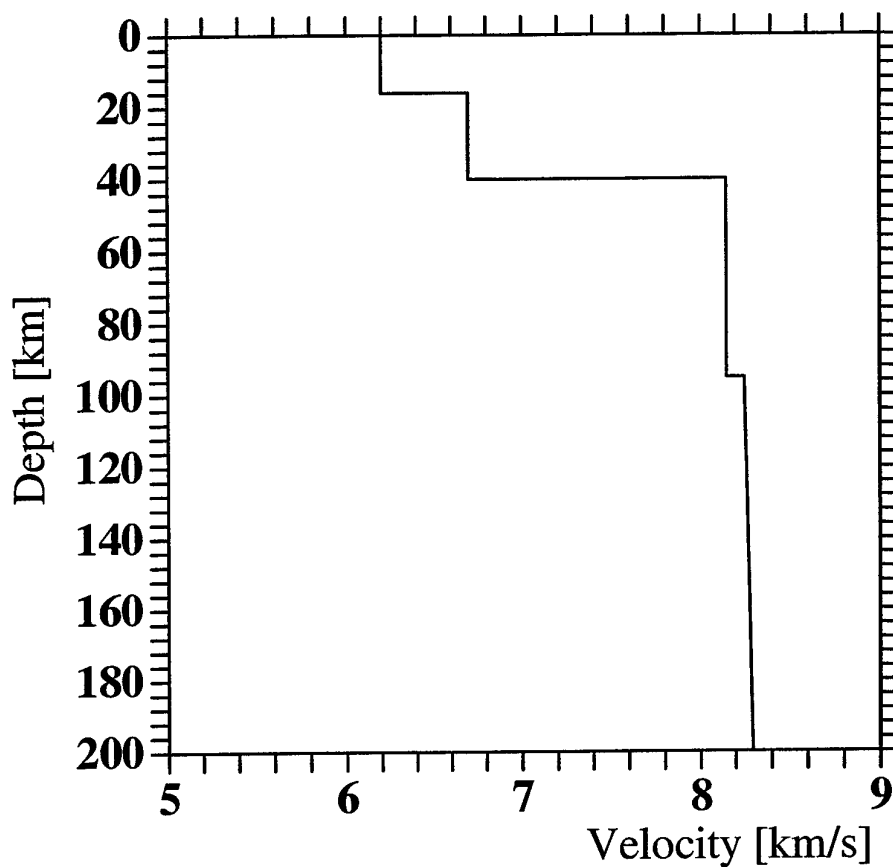
Fig. 6.6.4. *One-dimensional P-velocity model used for locating events in the Fennoscandian region and for calculating the theoretical travel-time curves shown in Figs. 6.6.5 - 6.6.8.*
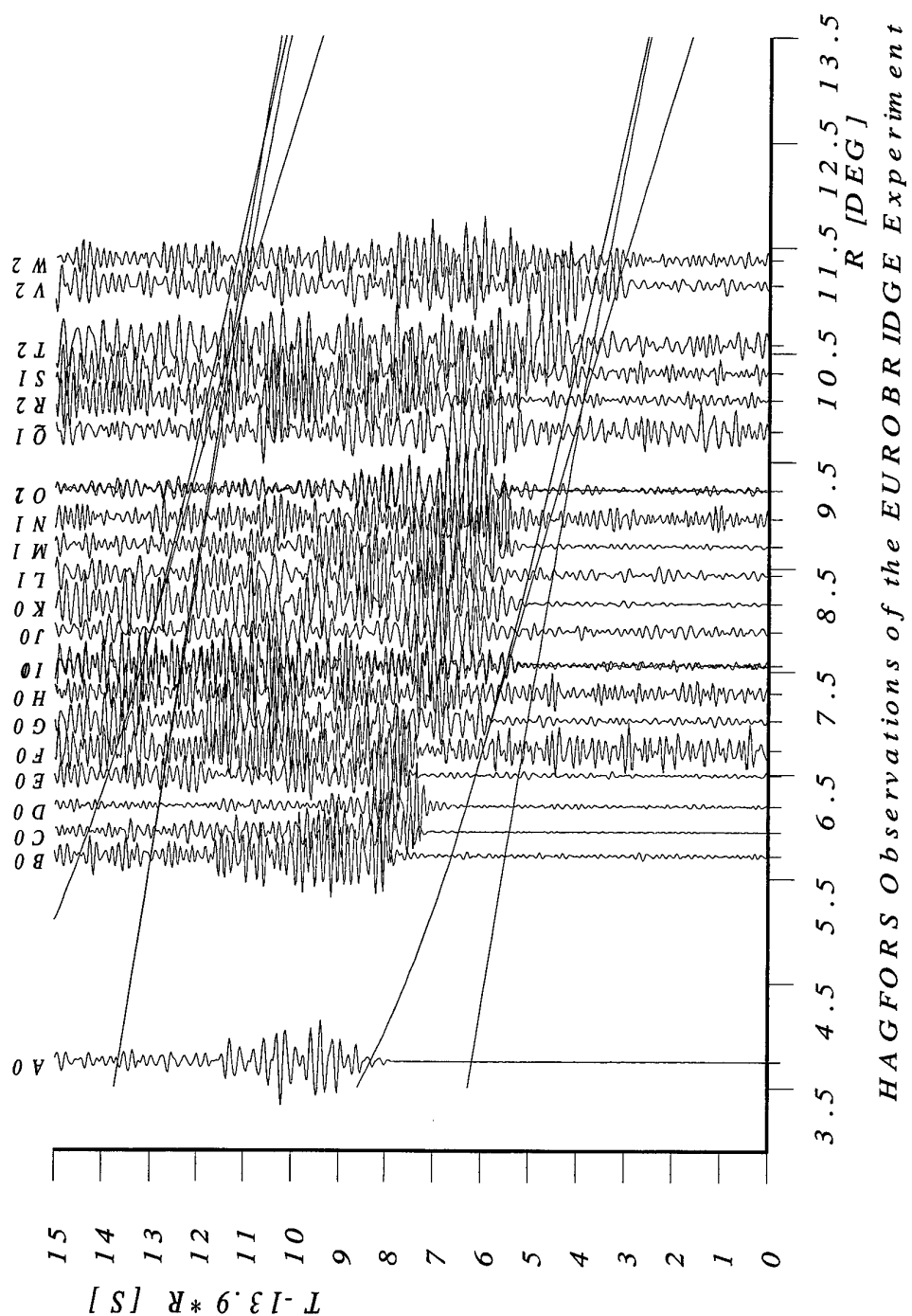
Fig. 6.6.5. *Section of Eurobridge shots recorded at Hagfors with travel-time curves of the Fennos-candian model superimposed. The shot labels (see Table 6.6.1) are shown above each trace.*
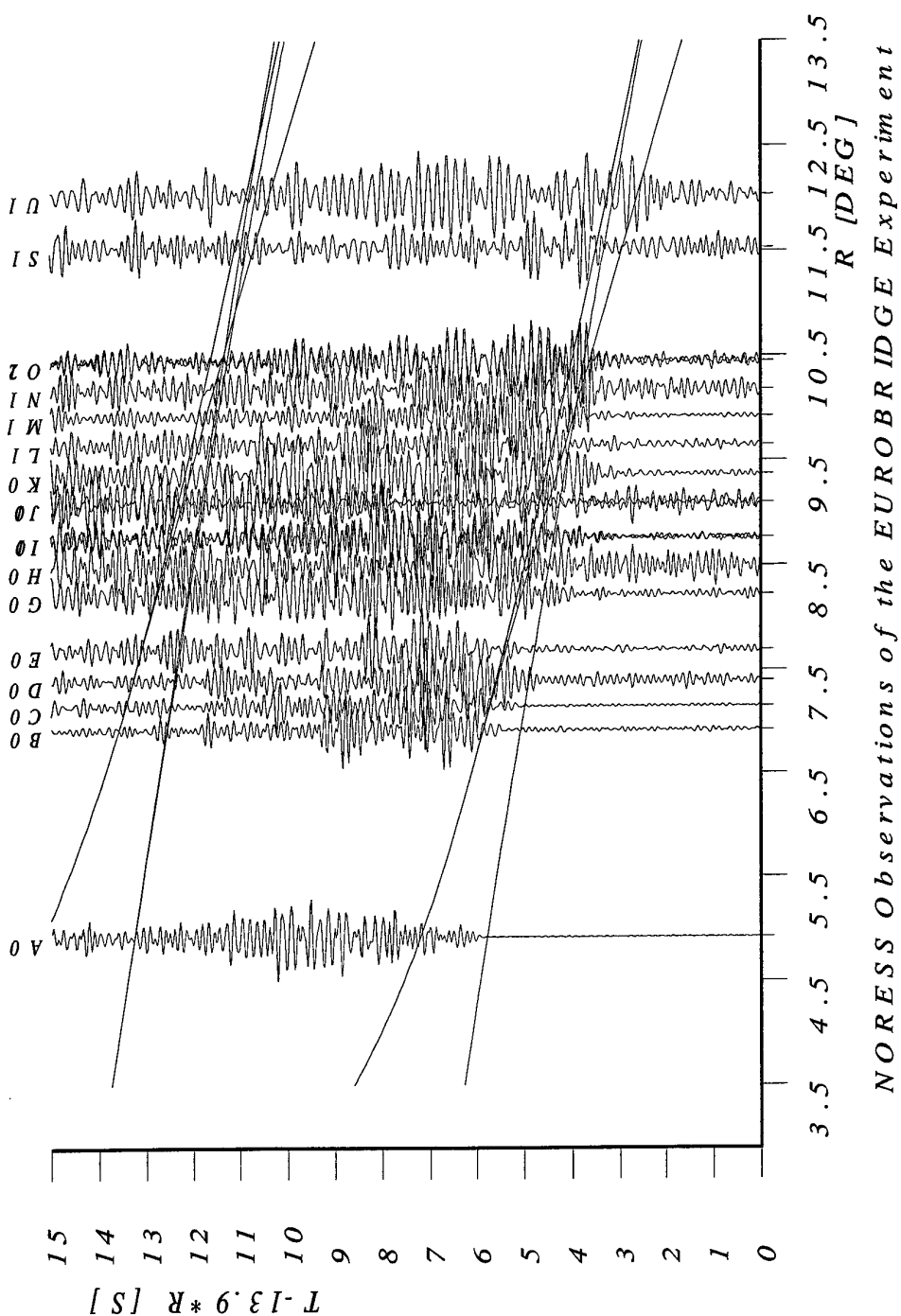
Fig. 6.6.6. *Section of Eurobridge shots recorded at NORESS with travel-time curves of the Fennoscandian model superimposed. The shot labels (see Table 6.6.1) are shown above each trace.*
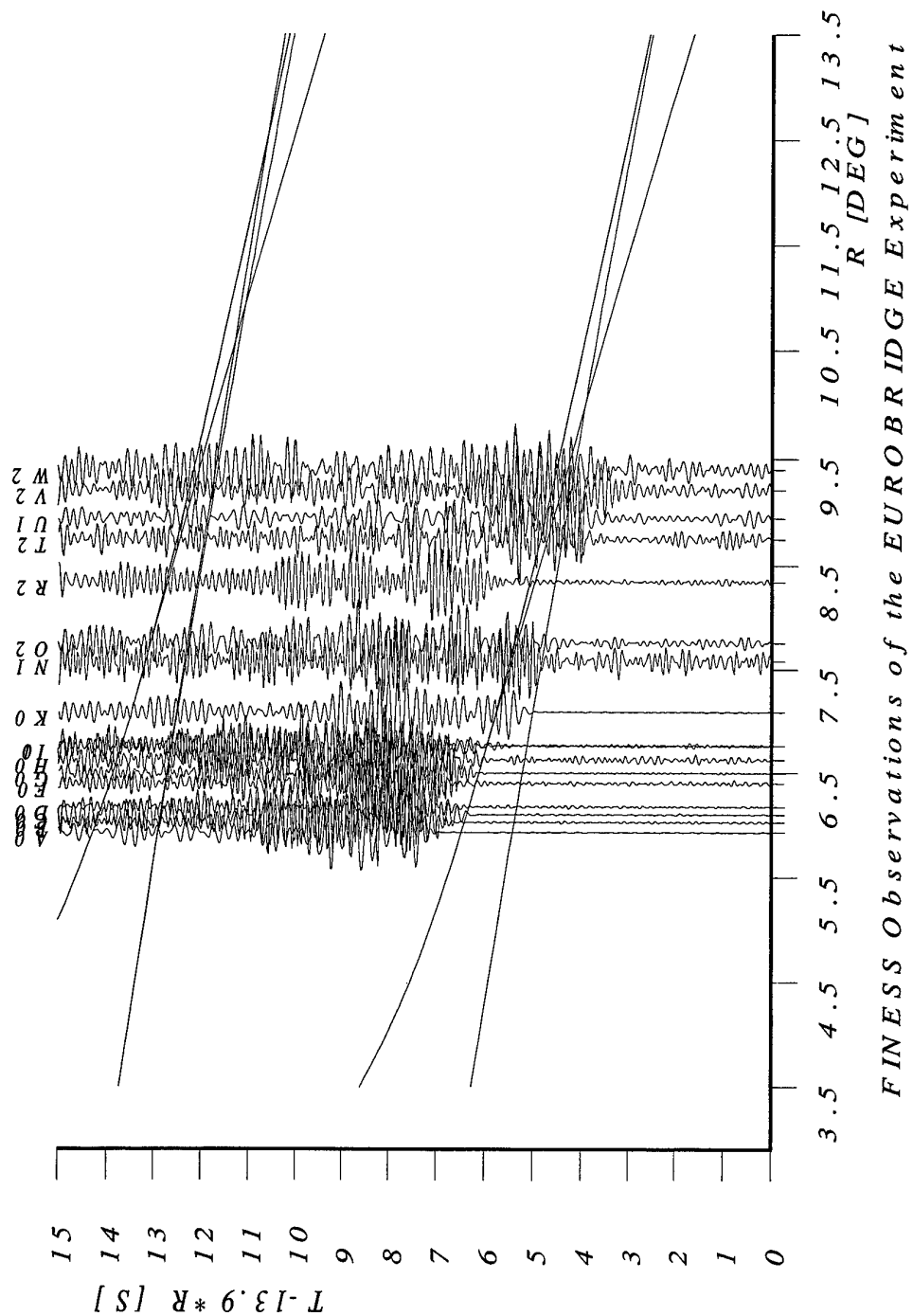
Fig. 6.6.7. *Section of Eurobridge shots recorded at FINESS with travel-time curves of the Fennos-candian model superimposed. The shot labels (see Table 6.6.1) are shown above each trace.*
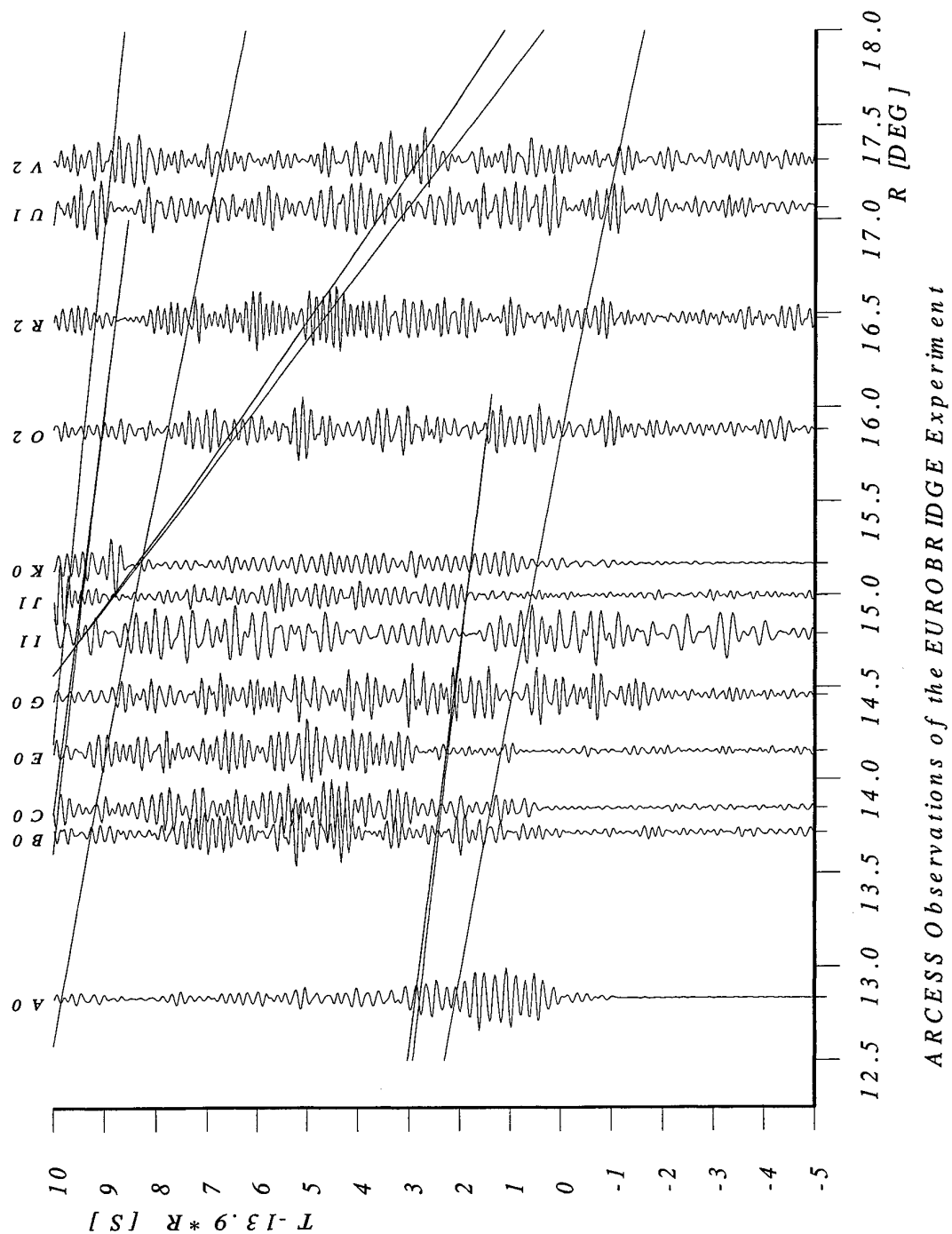
Fig. 6.6.8. *Section of Eurobridge shots recorded at ARCESS with travel-time curves of the Fennos-candian model superimposed. The shot labels (see Table 6.6.1) are shown above each trace.*